The Mixed Mode Fracture of Functionally Graded Materials

by

Xiang Long

A dissertation submitted to the Graduate Faculty in Engineering in partial fulfillment of the requirements for the degree of Doctor of Philosophy, The City University of New York

2003

UMI Number: 3103135

ProQuest Information and Learning Company
300 North Zeeb Road
P.O. Box 1346
Ann Arbor, MI 48106-1346

This manuscript has been read and accepted for the Graduate Faculty in Engineering in satisfaction of the dissertation requirement for the degree of Doctor of Philosophy.

9/11/03
Date

Feridun Delale
Professor Feridun Delale
Chair of Examining Committee (Mentor)

9-11-2003
Date

Mumtaz K. Kassir
Professor Mumtaz K. Kassir
Executive Officer

Professor Benjamin Liaw
Department of Mechanical Engineering, CCNY

Professor Stephen C. Cowin
Department of Mechanical Engineering, CCNY

Professor Ali M. Sadegh
Department of Mechanical Engineering, CCNY

Professor Alan Lau
Mechanical Engineering & Mechanics,
Drexel University

The City University of New York

ABSTRACT

THE MIXED MODE FRACTURE OF FUNCTIONALLY GRADED MATERIALS

by

Xiang Long

Adviser: Professor Feridun Delale

The newly developed functionally graded materials (FGMs) may have wide technological applications. These materials are designed in a way that combines beneficial mechanical and strength properties of different materials to create some new materials useful in practice. The composition and hence the properties of FGMs vary spatially, which make them suitable for specific requirements encountered in engineering applications.

Some crack problems in FGMs have been solved during the past decade, but most of these studies are limited to semi-infinite or infinite domains and symmetric problems. In this thesis, the more general problem of an arbitrarily oriented crack in a FGM layer is investigated. Specifically the stress intensity factors and crack opening displacements for a functionally graded layer bonded to a substrate are studied analytically. Variable mechanical loads are applied to make it more general.

The problem will be formulated in terms of a system of singular integral equations, which can be solved numerically. The stress intensity factors at the crack tips are

computed. A complete parametric study, by varying both the geometric and material parameters, is conducted. When possible, results are compared to existing experimental data and other numerical results.

It is believed that the information obtained through this study will provide a solid foundation for further theoretical studies using the singular integral equation approach to fracture problems in advanced composites.

Acknowledgements

I would like to take this opportunity to express my sincere gratitude to my mentor, Professor Feridun Delale, for his guidance, understanding and great patience throughout the course of this study. His help is not limited to academic matters, but also to my whole career.

Special thanks to Prof. Benjamin Liaw, for his invaluable guidance and advice on my research and life.

I would like to thank Thomas Cheung, Jianjun Liu, Peng Guo, Yanxiong Liu, Xiaobing Zhang, Wei Yuan and all my other fellow graduate students who helped me enormously.

I also have to mention my friend Jian Deng, Yangqing Xu and Huaqing Zhao for their great help on my dissertation study.

Finally, I would like to express my profound appreciation to Ms. Lidan You. Without her, I would never have even thought of working on my Ph. D. study. I would like to dedicate this thesis to her.

Table of Contents

CHAPTER 1 INTRODUCTION.....1

1.1 FUNCTIONALLY GRADED MATERIALS AND THERMAL BARRIER COATINGS.....2

1.2 MACROMECHANICAL ANALYSIS OF FGMS.....5

1.3 REVIEW OF PREVIOUS WORK.....7

1.3.1 Analytical Studies of a Single Crack in Single Phase Media.....7

1.3.2 Analytical Studies of Cracks in Bonded Plates.....11

1.3.3 Experimental Investigations on Fracture of FGMs.....16

1.3.4 Numerical Studies of Fracture Problems in FGMs.....17

1.4 THE SINGULAR INTEGRAL EQUATION METHOD USED IN THIS STUDY.....18

CHAPTER 2 PRELIMINARY RESEARCH ON INTERNAL OR EDGE CRACK IN A FGM STRIP.....22

2.1 THE FORMULATION.....23

2.2 THE SINGULAR INTEGRAL EQUATION.....26

2.3 THE NUMERICAL SOLUTION AND THE RESULTS.....34

CHAPTER 3 MIXED MODE CRACK PROBLEM IN FGM STRIP 38

3.1 THE FORMULATION 39

3.2 THE INTEGRAL EQUATIONS 50

3.3 THE NUMERICAL SOLUTION 54

3.4 RESULTS AND DISCUSSION 57

CHAPTER 4 THE MIXED MODE CRACK PROBLEM IN A FGM STRIP BONDED TO A HOMOGENEOUS HALF PLANE 74

4.1 THE FORMULATION 75

4.2 THE INTEGRAL EQUATIONS 85

4.3 THE NUMERICAL SOLUTION 93

4.4 RESULTS AND DISCUSSION 96

CHAPTER 5 PROPOSED ADDITIONAL STUDIES 106

REFERENCES 109

List of Tables

1. Comparison of stress intensity factors from current study with those from Ref. [59] for an inclined crack in an infinite FGM plate under uniform crack surface traction 58

2. Comparison of stress intensity factors from current study with results from chapter 2 for a FGM strip with an internal center crack under uniform strain loadings 60

List of Figures

1. Geometry of problem in Ref. [21] 8

2. Geometry of problem in Ref. [59] 10

3. Geometry of problem in Ref. [39] 11

4. Geometry of problem in Ref. [28] 11

5. Geometry of problems in Ref. [19] and [22] 12

6. Geometry of problems in Ref. [93] and [13] 13

7. Geometry of problem in Ref. [30] 14

8. Geometry of problem in Ref. [23] 15

9. Geometry of problem in Ref. [36] 15

10. Geometry of problems in Ref. [15] and [95] 16

11. Variation of the normalized stress intensity factors $K_1/\sigma_0\sqrt{a'}$ with a'/h for an internal crack under fixed grip loading 36

12. Variation of the normalized stress intensity factors $K_1/\sigma_0\sqrt{b}$ with b/h for an edge crack under fixed grip loading 37

13. Geometry of the mixed mode crack problem in a FGM strip 39

14. Variation of the normalized stress intensity factors K/K_0 with θ/π for an internal inclined crack in a FGM strip under uniform strain, $a'/h = 0.05$ 62

15. Variation of the normalized stress intensity factors K/K_0 with θ/π for an internal inclined crack in a FGM strip under uniform strain, $a'/h = 0.10$ 63

16. Variation of the normalized stress intensity factors K/K_0 with θ/π for an internal inclined crack in a FGM strip under uniform strain, $a'/h = 0.15$ 64

17. Variation of the normalized stress intensity factors K/K_0 with θ/π for an internal inclined crack in a FGM strip under uniform strain, $a'/h = 0.20$ 65

18. Variation of the normalized stress intensity factors K/K_0 with θ/π for an internal inclined crack in a FGM strip under uniform strain, $a'/h = 0.25$ 66

19. Variation of the normalized stress intensity factors K/K_0 with θ/π for an internal inclined crack in a FGM strip under uniform strain, $a'/h = 0.30$ 67

20. Variation of the normalized stress intensity factors K/K_0 with θ/π for an internal inclined crack in a FGM strip under uniform strain, $a'/h = 0.35$ 68

21. Variation of the normalized stress intensity factors $K_1(b)/K_0$ with θ/π for an internal inclined crack in a FGM strip under uniform strain, for various a'/h ratios 69

22. Variation of the normalized stress intensity factors K/K_0 with a'/h for an internal inclined crack in a FGM strip under uniform strain, $\theta = \pi/4$ 70

23. Crack surface openings in the y_1 direction for $a'/h = 0.35$, $\theta = 0^0$, 45^0 and 67.5^0 71

24. Crack surface openings in the x_1 direction for $a'/h = 0.35$, $\theta = 4.5^0$, 45^0 and 67.5^0 72

25. Variation of the normalized stress intensity factors $K_1(b)/K_0$ with θ/π for an internal inclined eccentric crack in a FGM strip under uniform strain 73

26. Geometry of the crack in a bonded strip 75

27. Variation of the normalized stress intensity factors K/K_0 with θ/π for an internal inclined crack in a FGM strip and a FGM strip bounded to a homogeneous half-plane under uniform strain, $a'/h = 0.05$ 98

28. Variation of the normalized stress intensity factors K/K_0 with θ/π for an internal inclined crack in a FGM strip and a FGM strip bounded to a homogeneous half-plane under uniform strain, $a'/h = 0.10$ 100

29. Variation of the normalized stress intensity factors K/K_0 with θ/π for an internal inclined crack in a FGM strip and a FGM strip bounded to a homogeneous half-plane under uniform strain, $a'/h = 0.15$ 101

30. Variation of the normalized stress intensity factors K/K_0 with θ/π for an internal inclined crack in a FGM strip and a FGM strip bounded to a homogeneous half-plane under uniform strain, $a'/h = 0.20$ 102

31. Variation of the normalized stress intensity factors K/K_0 with θ/π for an internal inclined crack in a FGM strip and a FGM strip bounded to a homogeneous half-plane under uniform strain, $a'/h = 0.25$ 103

32. Crack surface openings in the y_1 direction for $a'/h = 0.20$, $\theta = 0^0$, 45^0 and 67.5^0 104

33. Crack surface openings in the x_1 direction for $a'/h = 0.20$, $\theta = 4.5^0$, 45^0 and 67.5^0 105

34. Geometry of the problem for an arbitrarily oriented crack in a FGM layer bonded to a homogeneous substrate, with another crack along the interface. 107

Chapter 1 Introduction

In the recent past, there has been a strong increase in interest in Functionally Graded Materials (FGMs). FGMs are multiphase composite materials whose composition, microstructure and properties vary gradually. They can be tailored to meet the rigorous requirements encountered in practice through the design of their constituents. The materials are synthesized in a way that combines the desirable characteristics of each of the constituents. FGMs have great potential for applications in safety-critical structures such as nuclear fusion, aircraft fuselages, microelectronic devices and biomaterials, but the greatest area of focus and initial emphasis appear to be in thermal barrier protection for turbines engines, etc. in high temperature environments.

FGMs are unique, from the viewpoint of mechanics, because their mechanical properties vary spatially. This distinctive feature that makes FGMs such promising candidates for advanced technological applications, happens to create enormous difficulties for those who want to analytically study the fracture behavior of FGMs. It is well known that if the mechanical properties of the material are not constant, the governing elasticity equations become partial differential equations with variable coefficients, which complicate the analysis significantly. Except for a few idealized cases, most crack problems for FGMs are not amenable to analytical treatments because of their intrinsic complexities. Some crack problems in FGMs have been solved in the past decade, but most of them are limited to semi-infinite or infinite domains, simple load cases and certain assumed crack orientations, notably cracks perpendicular or parallel to the direction along which material property varies. The more general problem of crack propagation of an arbitrarily oriented

crack in a FGM layer does not appear to have been studied. In this thesis, a series of theoretical studies are carried out to determine the stress intensity factors and crack opening displacements for cracks in FGMs, leading to fracture studies under various loading conditions. Here, analytical expressions for stress intensity factors of mixed-mode cracks in a strip have been derived for the first time. A parametric study, by varying both the geometric and material parameters, is conducted based on these analytical expressions.

It is believed that the fracture analysis proposed in this study will lead to a better design of FGMs and lay a solid foundation for further theoretical studies of crack problems in FGMs and other advanced composite materials.

1.1 Functionally Graded Materials and Thermal Barrier Coatings

The idea of Functionally Graded Materials initially came from the need of more efficient combustion process in many high temperature aerospace applications such as turbines, compressors and combustion chambers. Temperatures in these structures can go extremely high (up to 1800^0C in the combustion chamber [11]). It seems that no simple metal or alloy material can withstand these temperatures and at the same time have enough strength and toughness to meet the design requirements. Thus, the use of structural ceramics to protect the hot sections becomes almost a necessity. Conventional thermal barrier coatings (TBCs) consist of a ceramic layer bonded to a metal substrate. Ceramics can withstand higher temperatures than metals, and consequently, a higher temperature achieved inside the engine chamber leads to a more efficient combustion process. However, conventional thermal barrier coatings are prone to fracture because of the brittle nature of ceramics and the thermal stresses generated due to the mismatch in thermal expansion

coefficients between the ceramic coating and the metal substrate. The fracture modes may vary depending on the thermal and mechanical loads, and also the manufacturing process, but thermo-mechanical stresses and mismatch in thermal-mechanical properties always play important roles in the failure of TBCs. An effective thermal barrier coating that can sustain very high temperatures, must be chemically compatible with the metallic substrate so that bonding can be achieved to have enough toughness to resist cracking and crack propagation. Obviously, pure ceramic coatings cannot satisfy all these demands simultaneously, thus comes the need for thermal barrier coatings made of Functionally Graded Materials.

The name of Functionally Graded Materials (FGMs) was first coined by Japanese materials scientists in the Sendai area in 1984 as a means of manufacturing thermal barrier coating materials. Unlike conventional composite materials, which are macroscopically homogeneous while microscopically inhomogeneous because of the coexistence of two different phases, FGMs are essentially two-phase particulate composites that are inhomogeneous macroscopically and microscopically. Most FGMs are made from ceramics and metals. Ceramics provide thermal and corrosion resistance of the final materials while metals provide the necessary mechanical toughness and heat conductivity. The volume fractions of the constituents in a FGM usually vary continuously from 100% ceramic at the surface to 0% near the interface continuously. The conditions for both high temperature and high toughness can then be met simultaneously.

Though the concept of FGMs is relatively new, these kinds of materials have existed in nature for a long time and used widely in engineering practice. For example,

many of the structures of living organisms, such as tree stems or human and animal bones are all some sort of FGMs in nature [79]. Another interesting example is the interfacial regions created from the bonding process, such as cladding or welding of dissimilar materials. Regardless of the mechanism of the binding process, there always exists an interfacial zone between two bonded materials. In an interfacial region, the volume concentration of different materials changes gradually because of interdiffusion, thus making this region a perfect example of FGM. The existence of the interfacial areas was the initial driving force of the earlier fracture studies in nonhomogeneous materials before the idea of FGMs came into being. Those earlier works which will be discussed in the latter part of this chapter contribute significantly to the study of FGMs [19,21,22,23,30,35,36,37,68,78].

Recent advances in the analysis, design and fabrication of FGMs have marked the beginning of a revolution in materials science, as they have opened the door to tailor a material at the microstructural level for the specific performance requirements of an intended environment. Although the development of FGMs is still at a rather early stage, gradation in many materials may be achieved through the addition of particles or fibers during the manufacturing process. The methods most often used to fabricate FGMs include thermal spraying, powdered metal sintering, chemical vapor deposition (CVD), physical vapor deposition, combustion synthesis, thermo-chemical diffusion treatments, sedimentation and self-propagating high-temperature synthesis [65,70,71,87,90]. More manufacturing methods are currently being developed.

1.2 Macromechanical Analysis of FGMs

One of the main reasons of developing FGMs is to avoid the problems associated with the low toughness of many ceramics. Thus, the fracture behavior of FGMs is extremely important. The mechanical analysis in functionally graded thermal barrier coatings can be done at the microstructural or macroscopic level.

At the microstructural level, the main task is to propose efficient models to determine effective thermal-mechanical properties based on constituent material volume fractions, properties and microstructures. On this subject, one may cite the excellent work of Aboudi, Arnold and Pindera [1,2,3,4,5,6,7,81,82,83,84,85]. In a series of papers, they have dealt with the microstructural theory for the analysis of functionally graded materials, and have developed a higher-order theory that explicitly couples the microstructure of the material with structural global analysis.

At the macromechanical level, the microstructural details are expressed by assuming that the material is nonhomogeneous and that the properties have a spatial variation. In one of the early papers on nonhomogeneous materials [21], it was shown that if the elastic constants vary exponentially, then the governing elasticity equation can be reduced to a partial differential equation with constant coefficients. The basic equations for plane mechanical fracture problems in FGMs will be given below.

From the theory of elasticity, the two-dimensional field equations of FGMs can be expressed by the Navier's equations:

$$(\kappa+1)\frac{\partial^2 u}{\partial x^2}+(\kappa-1)\frac{\partial^2 u}{\partial y^2}+2\frac{\partial^2 v}{\partial x\partial y}+\beta(\kappa+1)\frac{\partial u}{\partial x}+\beta(3-\kappa)\frac{\partial v}{\partial y}=0$$
$$(\kappa-1)\frac{\partial^2 v}{\partial x^2}+(\kappa+1)\frac{\partial^2 v}{\partial y^2}+2\frac{\partial^2 u}{\partial x\partial y}+\beta(\kappa-1)(\frac{\partial v}{\partial x}+\frac{\partial u}{\partial y})=0 \qquad (1)$$

where u and v are the displacement components in the x and y directions respectively. We assume an exponential variation in x for the Young's modulus as:

$$E = E_0 e^{\beta x} \qquad (2)$$

where β is a material constant describing the nonhomogeneity of the material.

The Poisson's ratio ν, has little effect on the stress intensity factors near the crack tips [21], thus, it is assumed as constant.

In equation (1)

$$\kappa = \begin{cases} 3-4\nu & \textit{for plane strain problems} \\ (3-\nu)/(1+\nu) & \textit{for plane stress problems} \end{cases} \qquad (3)$$

Based on these basic equations, many fracture problems with different geometries and loadings in functionally graded materials have been studied. To make the problem mathematically tractable, most problems considered are either plane stress, plane strain, or axisymmetric. The loadings are in-plane mechanical, anti-plane shear or in some cases thermal. The crack orientation may be parallel or perpendicular to the free surfaces or along the interfaces. The geometry of most problems is limited to infinite or semi-infinite domains. In this thesis, the general problem of an arbitrarily oriented crack in a FGM strip on a homogeneous substrate is studied.

1.3 Review of Previous Work

Many researchers have been concerned with solving crack problems in FGM media. Erdogan and his coworkers pioneered in theoretical analysis of fracture mechanics of FGMs. They have solved some basic problems for cracks in FGMs under different mechanical and thermal loadings. An excellent review was given by Erdogan in 1995 [31], which summarized the most important fracture results of FGMs until that time. As more analytical and experimental results are being reported, it is almost impossible to give an exhaustive review of all the related studies. A short review will be given here, with its focus limited on important studies and results directly relevant to the present research.

1.3.1 Analytical Studies of a Single Crack in Single Phase Media

Before the concept of FGM was introduced, several researchers had investigated crack problems in nonhomogeneous media in which mechanical properties vary continuously with the spatial coordinates. From the viewpoint of fracture mechanics, FGMs are materials with inhomogeneous mechanical properties, thus these analytical works on modeling such materials laid important bases for studying the fracture behavior of FGMs.

Among the many mixed boundary value problems in nonhomogeneous materials, problems dealing with a single crack in an infinite plate under antiplane share are relatively simple. Not surprisingly, these problems were solved first. In two papers published in 1978 (Clements et al [18] and Dhaliwal and Singh [24]), antiplane shear crack problems were considered in a nonhomogeneous media. In [18], the Young's moduli were restricted to those enabling the displacements and stresses to be written in terms of a harmonic function.

In [24], the Young's modulus of the material was assumed in the form of $E(x,y) = E_0 e^{(\alpha|x|+\beta|y|)}$ with the crack at $y = 0$.

In practice, mode *III* crack problems are not of great interest in themselves. Mode *I* cracks are far more common. Mode *I* problems were first considered by Rogers and Clements using Bergman's integral operator in [88], under a rather restrictive if not unrealistic assumption that the Poisson's ratio for the material was $\nu = 0.5$, i.e., the material was incompressible. Gerasoulis and Srivastav [41] studied a Griffith crack problem for a nonhomogeneous medium, with the Young's modulus assumed as $E = \frac{E_0}{1+c|y|}, c \geq 0$.

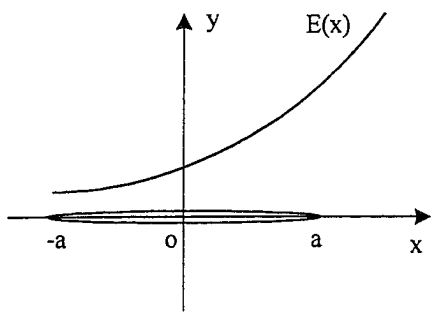

Fig. 1. Geometry of problem in Ref. [21]

In perhaps one of the most important papers in this area (Delale and Erdogan [21]), the relatively more complicated mode *I* crack problem was studied. The Young's modulus varied exponentially in the direction parallel to the crack as $E(x) = E_0 e^{\beta x}$ in an infinite plate, with the crack located on the $y = 0$ plane (Fig. 1). Like most of the studies mentioned in the foregoing and latter, the Poisson's ratio was assumed to be constant and the material was isotropic. The mixed boundary value problem was reduced to a singular

integral equation with a Cauchy type kernel, and the stress intensity factors and crack surface displacements were determined for a variety of loading cases. It was shown that as for homogeneous materials, the crack-tip stresses have the conventional square-root singularity, making the stress intensity factor concept well defined. One of the most important conclusions in this paper is that the effect of the Poisson's ratio on the stress intensity factors is negligible, and thus, it was invariably assumed to be a constant in subsequent studies [21].

The same geometry was investigated again by Schovanec [91], with the Young's modulus varying perpendicular to the crack. Symmetry was imposed by assuming the Young's modulus as $E(y) = E_0 e^{\beta|y|}$. In both studies, stress intensity factors were found to be affected significantly by the nonhomogeneity of the material.

The aforementioned analyses of crack problems concluded that the standard square root singularity at the crack tips is maintained if the material parameters are continuous and differentiable. In a brief note published in 1994 [53], Jin and Noda studied singular stress and heat flux fields at the tip of the crack in a general nonhomogeneous material. It was found that the crack-tip field singularities and angular distributions are identical to those in the homogeneous material provided that the properties of the material are continuous and piecewise differentiable [53]. Hence, the stress intensity factor concept is still valid in these cases.

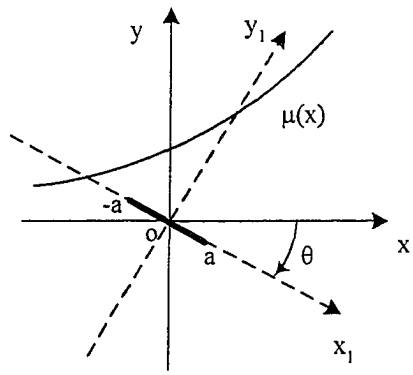

Fig. 2. Geometry of problem in Ref. [59]

Most studies in the foregoing dealt with Mode *I* or Mode *III* problems only. Konda and Erdogan first tried to solve a more general case of mixed mode crack problem in FGMs [59]. The problem studied was an arbitrarily oriented crack in an infinite nonhomogeneous medium (Fig. 2). Again, the Young's modulus was assumed to be varying exponentially and the Poisson's ratio was constant. Although the solution was given only for infinite domains, which greatly limited its practical importance, it is still unique in that it was the first time that a mixed-mode crack problem for FGMs had been solved analytically.

Konda and Erdogan's work [59] somehow completed the research of single crack problems in infinite domain under plane strain or generalized plan stress conditions. Wu and Erdogan took another step in [39], by solving the mode *I* crack problem in a FGM strip. Unlike previous studies that deal mostly with unbounded media, the geometry of this problem was an internal or surface crack in a strip with finite width (Fig. 3). The crack was perpendicular to the boundaries of the plate, and the Young's modulus was given by $E(x) = E_0 e^{\beta x}$.

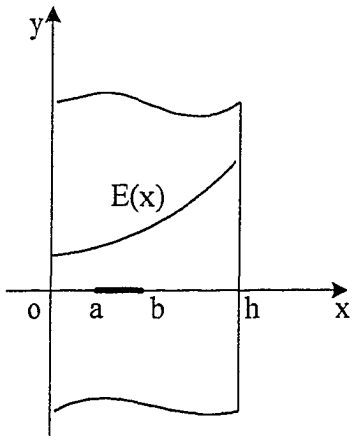

Fig. 3. Geometry of problem in Ref. [39]

The mode *I* crack parallel to the boundary of an infinite strip was solved by El-Borgi et al. [28] , with the Young's modulus varying exponentially in an arbitrary direction (Fig. 4).

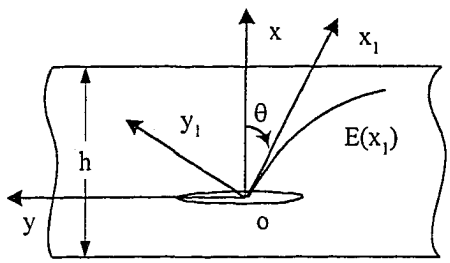

Fig. 4. Geometry of problem in Ref. [28]

1.3.2 Analytical Studies of Cracks in Bonded Plates

While some researchers focused on single crack problems in single-phase media, others solved crack problems in bonded plates. These problems first arose in investigating the interfacial zone between two dissimilar materials.

It appears that the problem of a crack between two bonded plates of nonhomogeneous materials was first studied by Delale [19]. The problem dealt with a

crack between two dissimilar nonhomogeneous half planes subjected to anti-plane shear loadings. The crack was located along the interface of these two half-planes (Fig. 5). The shear moduli were assumed to vary exponentially with the spatial coordinates. That geometry with different loading (plane stress or plane strain) was reconsidered in [22] by Delale and Erdogan, with particular interest on the singular nature and the angular distribution of the stress state around the crack tips. It was concluded that "if the material parameters are continuous functions with continuous derivatives", "the asymptotic behavior of the stress state around a crack tip is identical to that of a homogeneous medium" [22].

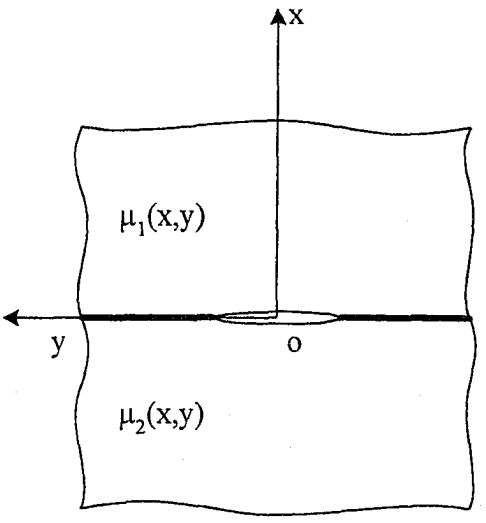

Fig. 5. Geometry of problems in Ref. [19] and [22]

Chen and Erdogan studied the Mode *I* crack along the interface of a nonhomogeneous coating and a homogeneous strip [13]. In their study, the thickness of coating and the homogeneous substrate were finite (with only layer 1 and layer 2 in Fig. 6). The shear modulus of the nonhomogeneous layer was assumed as an exponential function of x (perpendicular to the crack surface). This problem was further considered later by

Shbeeb and Binienda [93] with one more homogeneous layer added on top of the FGM layer (Fig. 6).

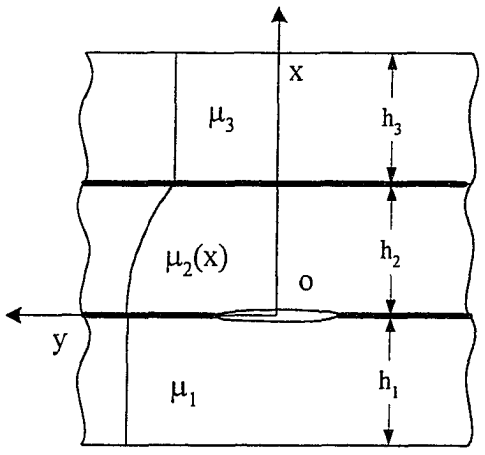

Fig. 6. Geometry of problems in Ref. [93] and [13]

Erdogan also investigated a crack in a nonhomogeneous half-plane bonded to another half-plane under anti-plane shear loading [30]. The crack was located in one half-plane, perpendicular to the interface (Fig. 7). The shear moduli of both planes were assumed as exponential functions of x (parallel to the crack line). As in [19], the loading was also antiplane shear, which greatly simplified the analysis, but reduced the practical importance of the problem.

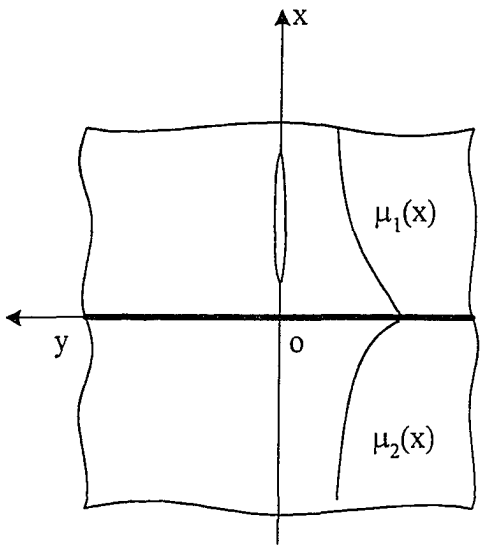

Fig. 7. Geometry of problem in Ref. [30]

In [23], Delale and Erdogan studied a crack in the interfacial region of two bonded half-planes. The interfacial region of the bonded homogeneous half-planes was modeled as a nonhomogeneous layer of constant thickness. The crack was located parallel to the interface at an arbitrary position in the layer (Fig. 8). The shear modulus in the layer was assumed to vary exponentially in the direction perpendicular to the crack.

From these studies on bonded dissimilar materials through a nonhomogeneous layer, it can be observed that if the crack is along the material interface, the square-root behavior of the stress singularity remains unaffected. In a short note by Schovanec and Walton [92], it was further demonstrated that when the crack tip terminates at the interfacial line, the normal square-root behavior will also be maintained, despite the discontinuity of the derivatives of elastic moduli along such zones. This result validates the definition of stress intensity factors in these cases.

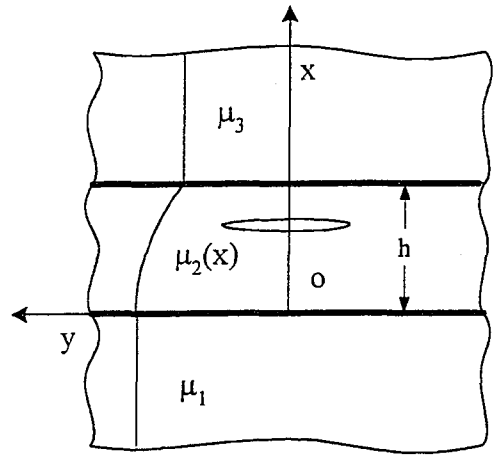

Fig. 8. Geometry of problem in Ref. [23]

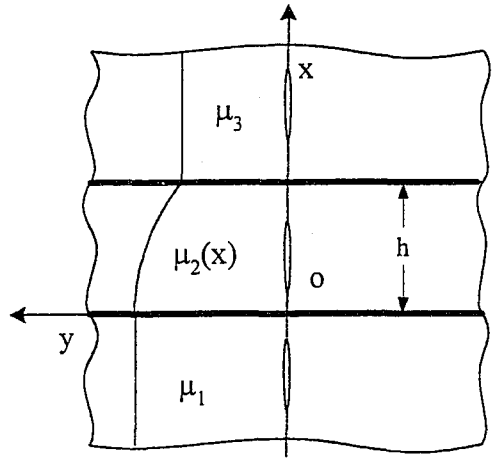

Fig. 9. Geometry of problem in Ref. [36]

Erdogan et al tried to solve the crack problem in [30] under mode *I* loading conditions [35] (see Fig. 7). To make the problem more tractable, the half plane containing the crack was assumed as homogeneous, and its shear modulus was given by $\mu_1 = \mu_0$. The second half-plane was nonhomogeneous with the shear modulus given as $\mu_2(x) = \mu_0 e^{\beta x}$. In another paper published the same year by the same researchers [36], the mode *III* crack problem in two bonded homogeneous half planes with a nonhomogeneous interfacial zone was studied. The cracks were located in both the homogeneous half-planes and the

interfacial zone (Fig. 9), and were all perpendicular to the interface. Again, the assumption that the cracks were under mode *III* deformations made this problem easier to solve, yet greatly diminished its applicability. It should be noted that in both papers, the stress states were found to have the standard square root singularity.

The mode *I* problem for a more complicated geometry of bonded layers was studied by Choi in [15]. The crack was located in a homogeneous semi-infinite substrate that was bonded to a surface layer through a nonhomogeneous interfacial layer. The crack was perpendicular to the nominal interface (Fig. 10). In another paper published in 2001 [17], Choi investigated the mode *I* crack in the same geometry but at an arbitrary angle to the graded interfacial zone, instead of perpendicular to it. Ueda studied a similar problem, by restricting the substrate to a finite thickness (layer 3 in Fig. 10) [95].

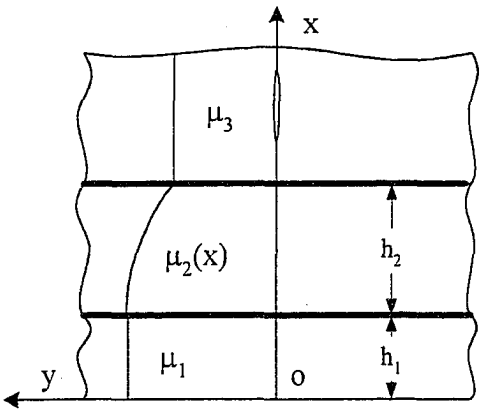

Fig. 10. Geometry of problems in Ref. [15] and [95]

1.3.3 Experimental Investigations on Fracture of FGMs

In contrast to a growing body of analytical work on the fracture mechanics of FGMs, there is a relative scarcity of experimental research on this topic. This is primarily due to the difficulties of fabricating FGM specimens suitable for laboratory testing and the

paucity of efficient methods to measure the fracture parameters of FGMs. Optical measurements of crack tip deformation in FGMs which were done by Tippur, Rousseau, Marur and Butcher were reported in a series of papers [12,69,89]. Hill and Carpenter constructed the K R-curve for a layered ceramic-metallic FGM [46]. Li and Lambros [67] studied Mode *I* edge crack problems in a strip. The results were compared with Erdogan and Wu's theoretical work [39], and satisfactory agreement was noted. From this short survey it is clear that far more experimental data are needed to ascertain the usefulness of the theoretical studies.

1.3.4 Numerical Studies of Fracture Problems in FGMs

Another method to tackle the fracture problems of FGM is to study the near-tip fields for a crack numerically. Most of these studies relied on the Finite Element Method (FEM) [8,9,10,25,26,27,43,44,47,56,58,66,69]. For example, Dolbow and Gosz [26] computed mixed-mode stress intensity factors at the tips of arbitrarily oriented cracks in FGM, and the results were compared with the analytical solutions presented by Konda and Erdogan in [59]. Good agreement was reported. In [58], Kim and Paulino gave a rather general finite element modeling of fracture in FGMs, with many interesting numerical results reported in papers. Some of these results are used for comparison with the results obtained in this study.

From all of the studies mentioned above, we can conclude the following:

1. Most problems considered in the literature dealt with infinite or semi-infinite planes, studies on FGM strip problems are rather limited.

2. The crack is usually parallel or perpendicular to the boundary of the plate. The material properties are also assumed to vary in the direction perpendicular or parallel to the crack line.
3. No arbitrarily oriented crack in a FGM strip has been systematically studied. The only problem that has been investigated is a crack in a strip perpendicular to the boundary, which was done by Erdogan and Wu [39]. The rather general mixed-mode crack problem was considered by Konda and Erdogan [59], but in an infinite domain. El-Borgi et al. solved the mode *I* crack problem for a crack in a FGM strip with the material properties varying in an arbitrary direction [28], but the crack was assumed parallel to the boundary, which greatly limited its technical importance.
4. For bonded layers, in most problems, the cracks are located in the homogeneous layer. For the problem of an arbitrarily oriented crack in a FGM coating bonded to a substrate, which is of great technical interest, no solution exists in the literature.

It is worthwhile to point out that in a Ph.D. thesis by Zhao [96], the crack problem in a FGM strip and a FGM strip bonded to a homogeneous substrate has been studied. Again, the crack was assumed to be perpendicular to the boundary.

1.4 The Singular Integral Equation Method Used in this Study

Most crack problems in FGMs are mixed boundary value problems. Mathematically, a linear elliptic partial differential equation (PDE) with suitable boundary conditions, such as Dirichlet, Neumann, or mixed type boundary condition can usually be

recast into a system of singular integral equations, by inverting the elliptic operator properly.

This is usually done by either using Fourier transform, calculating the wave numbers as the function of the eigenvalues, and then using the inverse Fourier transform, or by using a Green's function corresponding to the chosen boundary condition, and using Galerkin's approximation. Either way, the formulation leads to a system of singular integral equations such as:

$$v = F(v) = \int_{y \in \partial\Omega} k(x,y)v(y)dy \qquad (4)$$

where the kernel $k(x,y)$ is a symmetric function with a singularity in the form of $|x-y|^r$, with $r < 0$. Here, Ω is the domain under investigation.

Then the singular integral equation (4) can be solved using one of the well-developed algorithms (such as FFT, the spectral method, quadrature method or Galerkin's method).

Erdogan [29] has written an excellent article on mixed boundary value problems. The article describes the most general mixed boundary value problems in fracture mechanics and explains the methods to reduce them to singular integral equations. Particular interest is given to the numerical methods to solve the resulting singular integral equations. Another intriguing review on integral equations in crack problems was written by Chen [14]. In it, the integral equation methods for crack problems in plane elasticity are discussed, with special emphasis on how to formulate Fredholm integral equations. Here a

brief discussion of the singular integral equation method used to study the crack problems in this project is summarized below.

In this study, the crack surface displacements are defined as density functions. The Fourier transform method is used to convert the Navier's equations into a system of Integral Equations with Cauchy type singularity in the form:

$$\frac{1}{\pi}\int_{-1}^{1}\frac{1}{t-x}g(t)dt+\int_{-1}^{1}k(x,t)g(t)dt=p(x) \qquad -1<x<1 \qquad (5)$$

where $g(t)$ is the density function, $k(x,t)$ is a known regular Fredholm kernel and $p(x)$ is a prescribed function. Equation (5) is usually described as the generalized airfoil equation (GAE), since when $k(x,t)=0$, it reduces to the generalized airfoil equation modeling the flow around a slender airfoil [42,86]. One feature of this equation that needs to be pointed out is that the solution of this equation will always have singularities at $x=\pm 1$ [42,80].

Since closed form solutions to most Cauchy-type Singular Integral Equations (CSIEs) are generally not available, intense research efforts were spent to develop numerical solutions. Over the past thirty years, substantial progress has been made in developing numerical solutions to CSIEs. The most developed methods to numerically solve equation (5) are quadrature and polynomial collocation methods [42].

Quadrature methods approximate both singular and regular integrals by numerical integration, and thus reducing them to a system of linear algebraic equations. The Gauss-Chebyshev quadrature method was first developed by Erdogan and Gupta [33], and then

further refined in a series of papers by Erdogan and his associates [29,33,34]. The method was used to solve crack problems in half-planes or strips [21,32,45]. Ioakimidis and his co-workers refined these methods by introducing the Lobato-Chebyshev method, to achieve higher accuracy with less computation [48,49,50,51,94]. Krenk also contributed to the same methods and used them to solve a variety of crack problems [60,61,62,63,64].

Polynomial collocation methods, or polynomial expansion methods, are closely related to quadrature methods. Most theories about quadrature methods are also useful for collocation methods. Collocation methods are based on the expansion of the solution in terms of certain orthogonal polynomials, usually Jacobi polynomials. The singular integral equations are then reduced to an infinite system of linear algebraic equations. In this study, due to the nature of the integral equations, we used the Lobatto-Chebyshev collocation technique in solving the singular integral equations.

Chapter 2 Preliminary Research on Internal or Edge Crack in a FGM Strip

In this chapter, the mode *I* crack problem solved by Erdogan and Wu [39] will be reinvestigated as preparation for the mixed-mode crack problem in a FGM strip that will be studied in the next chapter.

The problem studied here is a FGM strip containing an internal or edge crack perpendicular to the boundary of the strip. To make the problem mathematically tractable, it is treated as a plane strain or generalized plane stress problem. All loadings are perpendicular to the plane of the crack. The shear modulus of the material varies in exponential form along the direction of the crack line (Fig. 3). As it was pointed out in chapter 1, the effect of the Poisson's ratio on the stress intensity factors is rather negligible [21], thus, it is assumed to be constant (taken as 0.3 in the numerical calculations) .

This same problem was also studied by Zhao in his Ph. D. thesis [96] and different results were obtained. Since this problem is a special case of the problem studied in the next chapter, it will serve as a benchmark test for the results to be obtained later, and thus, it is necessary to resolve the discrepancy between the two solutions.

The methods used by the authors are identical. To compare the results the same procedure will be followed here. That is, the Navier's equation will be reduced to a CSIE using Fourier Transform, and solved numerically using the Lobatto-Chebyshev collocation method. The stress intensity factors will then be calculated numerically.

As this problem is only studied for the sake of comparison, thorough parametric studies will not be carried out here. Yet, from results obtained in this study, we conclude that the results given by Erdogan and Wu are more reliable and will be used as benchmark in the next chapter.

2.1 The Formulation

Consider the plane elastostatic problem whose geometry was described in Fig 3. The FGM strip has a thickness of h. The external loads are assumed symmetrical with respect to the plane of the crack. The Young's modulus is given by

$$E = E_0 e^{\beta x} \tag{6}$$

where β is a material constant. The governing equations for the medium are:

$$\begin{aligned}
&(\kappa+1)\frac{\partial^2 u}{\partial x^2}+(\kappa-1)\frac{\partial^2 u}{\partial y^2}+2\frac{\partial^2 v}{\partial x\partial y}+\beta(\kappa+1)\frac{\partial u}{\partial x}+\beta(3-\kappa)\frac{\partial v}{\partial y}=0\\
&(\kappa-1)\frac{\partial^2 v}{\partial x^2}+(\kappa+1)\frac{\partial^2 v}{\partial y^2}+2\frac{\partial^2 u}{\partial x\partial y}+\beta(\kappa-1)(\frac{\partial v}{\partial x}+\frac{\partial u}{\partial y})=0
\end{aligned} \tag{7}$$

where u and v are the displacements in x and y directions. For plane strain problems, $\kappa = 3-4\nu$ and for plane stress problems, $\kappa = (3-\nu)/(1+\nu)$.

Considering the symmetry and regularity conditions, the solution of equation 7 may be expressed in the form of:

$$\begin{aligned}
u(x,y) &= \frac{1}{2\pi}\int_{-\infty}^{\infty} f_1(y,\alpha)e^{-i\alpha x}d\alpha + \frac{2}{\pi}\int_0^{\infty} f_2(x,\alpha)\cos\alpha y d\alpha\\
v(x,y) &= \frac{1}{2\pi}\int_{-\infty}^{\infty} g_1(y,\alpha)e^{-i\alpha x}d\alpha + \frac{2}{\pi}\int_0^{\infty} g_2(x,\alpha)\sin\alpha y d\alpha
\end{aligned} \tag{8}$$

Substituting equations (8) into equations (7), and assuming $g_1(y,\alpha) = D(\alpha)e^{ny}$ and $f_1(y,\alpha) = F(\alpha)e^{ny}$, we obtain the following relationship between $F(\alpha)$ and $D(\alpha)$:

$$F(\alpha) = \frac{(\kappa-1)(\alpha^2 + i\alpha\beta) - (\kappa+1)n^2}{[\beta(\kappa-1) - 2i\alpha]n} D(\alpha) \tag{9}$$

leading to the following characteristic equation:

$$n^4 - (\gamma^2 + 2i\alpha\beta + 2\alpha^2)n^2 + (\alpha + i\beta)^2\alpha^2 = 0 \tag{10}$$

The roots of equation (10) are:

$$\begin{aligned} n_1 &= -n_4 = -\frac{\gamma}{2} - \frac{1}{2}\sqrt{\gamma^2 + 4(\alpha^2 + i\beta\alpha)} \\ n_2 &= -n_3 = \frac{\gamma}{2} - \frac{1}{2}\sqrt{\gamma^2 + 4(\alpha^2 + i\beta\alpha)} \end{aligned} \tag{11}$$

where $\gamma = \beta\sqrt{(3-\kappa)/(1+\kappa)}$. Thus, we can rewrite $g_1(y,\alpha)$ and $f_1(y,\alpha)$ as:

$$\begin{aligned} g_1(y,\alpha) &= \sum_j^4 D_j(\alpha)e^{n_j y} \\ f_1(y,\alpha) &= \sum_j^4 m_j D_j(\alpha)e^{n_j y} \end{aligned} \tag{12}$$

where

$$m_j = \frac{(\kappa-1)(\alpha^2 + i\alpha\beta) - (\kappa+1)n_j^2}{[\beta(\kappa-1) - 2i\alpha]n_j}, \quad j = 1,...,4 \tag{13}$$

Similarly, we have:

$$g_2(x,\alpha)=\sum_j^4 A_j(\alpha)e^{p_j x}$$
$$f_2(x,\alpha)=\sum_j^4 q_j A_j(\alpha)e^{p_j x} \tag{14}$$

$$q_j=\frac{(\kappa-1)(p_j+\beta)p_j-(\kappa+1)\alpha^2}{\alpha[2p_j+\beta(\kappa-1)]},\quad j=1,\ldots,4 \tag{15}$$

$$p_1=-\frac{\beta}{2}-\frac{1}{2}\sqrt{\beta^2+4\alpha^2+4i\gamma\alpha}$$
$$p_2=-\frac{\beta}{2}-\frac{1}{2}\sqrt{\beta^2+4\alpha^2-4i\gamma\alpha}$$
$$p_3=-\frac{\beta}{2}+\frac{1}{2}\sqrt{\beta^2+4\alpha^2+4i\gamma\alpha} \tag{16}$$
$$p_4=-\frac{\beta}{2}+\frac{1}{2}\sqrt{\beta^2+4\alpha^2-4i\gamma\alpha}$$

Using Hooke's law, the stresses can be written as:

$$\sigma_x=\frac{G}{\kappa-1}[(1+k)\frac{\partial u}{\partial x}+(3-\kappa)\frac{\partial v}{\partial y}]$$
$$\sigma_y=\frac{G}{\kappa-1}[(1+k)\frac{\partial v}{\partial y}+(3-\kappa)\frac{\partial u}{\partial x}] \tag{17}$$
$$\tau_{xy}=G(\frac{\partial v}{\partial x}+\frac{\partial u}{\partial y})$$

where G is the shear modulus of the material.

The boundary conditions of the problems can be expressed as:

$$
\begin{aligned}
&\sigma_x(0,y)=0,\tau_{xy}(0,y)=0, && 0<y<\infty && (a)\\
&\sigma_x(h,y)=0,\tau_{xy}(h,y)=0, && 0<y<\infty && (b)\\
&\tau_{xy}(x,0)=0, && 0<x<h && (c)\\
&\sigma_y(x,0)=p(x), && a<x<b && (d)\\
&v(x,0)=0, && 0<x<a, b<x<h && (e)
\end{aligned}
\tag{18}
$$

where $p(x)$ is a known surface traction.

For the stresses to vanish as $y \to \infty$, one must have:

$$D_3(\alpha)=0, \qquad D_4(\alpha)=0 \tag{19}$$

Thus equations (12) become:

$$
\begin{aligned}
g_1(y,\alpha) &= \sum_j^2 D_j(\alpha) e^{n_j y}\\
f_1(y,\alpha) &= \sum_j^2 m_j D_j(\alpha) e^{n_j y}
\end{aligned}
\tag{20}
$$

2.2 The Singular Integral Equation

We now introduce the following auxiliary function:

$$g(x)=\frac{\partial}{\partial x} v(x,0) \tag{21}$$

consequently, all 6 unknown functions above ($D_1(\alpha)$, $D_2(\alpha)$ and $A_k(\alpha)$ $(k=1,...,4)$) can be determined in terms of $g(x)$. After some lengthy algebra, $D_1(\alpha)$ and $D_2(\alpha)$ can be expressed as:

$$D_1(\alpha) = \frac{(m_2 n_2 - i\alpha)i}{(m_2 n_2 - m_1 n_1)\alpha} \int_a^b g(t) e^{i\alpha t} dt$$
$$D_2(\alpha) = -\frac{(m_1 n_1 - i\alpha)i}{(m_2 n_2 - m_1 n_1)\alpha} \int_a^b g(t) e^{i\alpha t} dt \tag{22}$$

Using the boundary conditions, the unknowns $A_k(\alpha)$ $(k = 1,...,4)$ can be determined from:

$$\sum_j^4 [(1+k)p_j q_j + \alpha(3-\kappa)] A_j(\alpha) = \int_a^b F_1(\alpha, t) g(t) dt \tag{23}$$

$$\sum_j^4 [p_j - \alpha q_j] A_j(\alpha) = \int_a^b F_2(\alpha, t) g(t) dt \tag{24}$$

$$\sum_j^4 [(1+k)p_j q_j + \alpha(3-\kappa)] e^{p_j h} A_j(\alpha) = \int_a^b F_3(\alpha, t) g(t) dt \tag{25}$$

$$\sum_j^4 [p_j - \alpha q_j] e^{p_j h} A_j(\alpha) = \int_a^b F_4(\alpha, t) g(t) dt \tag{26}$$

where

$$F_1(\alpha, t) = \frac{i}{2\pi} \int_{-\infty}^{\infty} \frac{1}{\rho} \{ [(3-\kappa)n_1 - (1+k)i\rho m_1] \frac{n_1(m_2 n_2 - i\rho)}{(\alpha^2 + n_1^2)(m_2 n_2 - m_1 n_1)}$$
$$- [(3-\kappa)n_2 - (1+k)i\rho m_2] \frac{n_2(m_1 n_1 - i\rho)}{(\alpha^2 + n_2^2)(m_2 n_2 - m_1 n_1)} \} e^{i\rho t} d\rho \tag{27}$$

$$F_2(\alpha, t) = -\frac{i}{2\pi} \int_{-\infty}^{\infty} \frac{1}{\rho} \{ \frac{\alpha(m_2 n_2 - i\rho)(m_1 n_1 - i\rho)}{(\alpha^2 + n_1^2)(m_2 n_2 - m_1 n_1)}$$
$$- \frac{\alpha(m_1 n_1 - i\rho)(m_2 n_2 - i\rho)}{(\alpha^2 + n_2^2)(m_2 n_2 - m_1 n_1)} \} e^{i\rho t} d\rho \tag{28}$$

$$F_3(\alpha,t)=\frac{i}{2\pi}\int_{-\infty}^{\infty}\frac{1}{\rho}\{[(3-\kappa)n_1-(1+k)i\rho m_1]\frac{n_1(m_2n_2-i\rho)}{(\alpha^2+n_1^{\,2})(m_2n_2-m_1n_1)}$$
$$-[(3-\kappa)n_2-(1+k)i\rho m_2]\frac{n_2(m_1n_1-i\rho)}{(\alpha^2+n_2^{\,2})(m_2n_2-m_1n_1)}\}e^{i\rho(t-h)}d\rho \tag{29}$$

$$F_4(\alpha,t)=-\frac{i}{2\pi}\int_{-\infty}^{\infty}\frac{1}{\rho}\{\frac{\alpha(m_2n_2-i\rho)(m_1n_1-i\rho)}{(\alpha^2+n_1^{\,2})(m_2n_2-m_1n_1)}$$
$$-\frac{\alpha(m_1n_1-i\rho)(m_2n_2-i\rho)}{(\alpha^2+n_2^{\,2})(m_2n_2-m_1n_1)}\}e^{i\rho(t-h)}d\rho \tag{30}$$

Using the theory of residues, and after some lengthy manipulations, $F_k(\alpha,t)$ $(k=1,...,4)$ may be evaluated as:

$$F_1(\alpha,t)=-\frac{(\kappa-1)\alpha^2e^{-t(\lambda_1-\beta/2)}}{\lambda_1\lambda_2(\kappa+1)(\lambda_1^{\,2}+\lambda_2^{\,2})}[(2\lambda_1^{\,2}+2\lambda_2^{\,2}-\lambda_1\beta)\sin(\lambda_2t)-\beta\lambda_2\cos(\lambda_2t)] \tag{31}$$

$$F_2(\alpha,t)$$
$$=\frac{2\alpha e^{-t(\lambda_1-\beta/2)}}{\lambda_1\lambda_2(\kappa+1)(\lambda_1^{\,2}+\lambda_2^{\,2})}[\lambda_1(\lambda_1^{\,2}+\lambda_2^{\,2}-\frac{\beta^2}{4})\sin(\lambda_2t)-\lambda_2(\lambda_1^{\,2}+\lambda_2^{\,2}+\frac{\beta^2}{4})\cos(\lambda_2t)] \tag{32}$$

$$F_3(\alpha,t)=\frac{\alpha^2(\kappa-1)e^{-(h-t)(\lambda_1+\beta/2)}}{\lambda_1\lambda_2(\kappa+1)(\lambda_1^{\,2}+\lambda_2^{\,2})}[(2\lambda_1^{\,2}+2\lambda_2^{\,2}+\lambda_1\beta)\sin(\lambda_2h-\lambda_2t)$$
$$+\beta\lambda_2\cos(\lambda_2h-\lambda_2t)] \tag{33}$$

$$F_4(\alpha,t)=\frac{2\alpha^2e^{-(h-t)(\lambda_1+\beta/2)}}{\lambda_1\lambda_2(\kappa+1)(\lambda_1^{\,2}+\lambda_2^{\,2})}[\lambda_1(\lambda_1^{\,2}+\lambda_2^{\,2}-\frac{\beta^2}{4})\sin(\lambda_2h-\lambda_2t)$$
$$-\lambda_2(\lambda_1^{\,2}+\lambda_2^{\,2}+\frac{\beta^2}{4})\cos(\lambda_2h-\lambda_2t)] \tag{34}$$

where

$$\lambda_1 = \sqrt{\frac{R_1 + R_2}{2}}, \qquad \lambda_2 = \sqrt{\frac{R_1 - R_2}{2}} \tag{35}$$

$$R_1 = \sqrt{(\alpha^2 + \frac{\beta^2}{4})^2 + \frac{3-\kappa}{1+\kappa}\alpha^2\beta^2}, \qquad R_2 = \alpha^2 + \frac{\beta^2}{4} \tag{36}$$

From the above equations, we can solve $A_j(\alpha)$ to give:

$$A_j(\alpha) = \int_a^b C_j(\alpha,t)g(t)dt, \qquad (j = 1,...,4) \tag{37}$$

where

$$C_j(\alpha,t) = \sum_{i=1}^{4} b_{ij}(\alpha)F_j(\alpha,t) \tag{38}$$

and the matrix (b_{ij}) is the inverse of (a_{ij}):

$$\begin{aligned}
a_{1j}(\alpha) &= (1+\kappa)q_j p_j + (3-\kappa)\alpha \\
a_{2j}(\alpha) &= p_j - \alpha q_j \\
a_{3j}(\alpha) &= [(1+\kappa)q_j p_j + (3-\kappa)\alpha]e^{p_j h} \\
a_{4j}(\alpha) &= (p_j - \alpha q_j)e^{p_j h}
\end{aligned} \tag{39}$$

The stress component σ_y can be written in terms of unknown functions $D_j(\alpha)(j = 1,2)$ and $A_j(\alpha)(j = 1,..,4)$ as:

$$\begin{aligned}
\sigma_y = \frac{G(x)}{\kappa - 1}\{&\frac{1}{2\pi}\int_{-\infty}^{\infty}\sum_{j}^{2}[(1+k)n_j - (3-\kappa)i\alpha m_j]D_j(\alpha)e^{n_j y}e^{-i\alpha x}d\alpha \\
&+ \frac{2}{\pi}\int_0^{\infty}\sum_{j}^{4}[(1+k)\alpha + (3-\kappa)p_j q_j]A_j(\alpha)e^{p_j x}\cos\alpha y d\alpha\}
\end{aligned} \tag{40}$$

Using boundary condition (18.d) and rewriting equation (40) in terms of the auxiliary function $g(x)$, we obtain following equation

$$\int_a^b [h_1(x,t)+h_2(x,t)]g(t)dt = \frac{\kappa-1}{G(x)}p(x) \tag{41}$$

where

$$h_1(x,t) = \lim_{y\to+0}\frac{1}{2\pi}\int_{-\infty}^{\infty} K_1(y,\alpha)e^{i\alpha(t-x)}d\alpha \tag{42}$$

$$K_1(y,\alpha) = \frac{i}{(m_2n_2-m_1n_1)\alpha}\{[(1+\kappa)n_1-(3-\kappa)i\alpha m_1](m_2n_2-i\alpha)e^{n_1y} + [(1+\kappa)n_2-(3-\kappa)i\alpha m_2](i\alpha-m_1n_1)e^{n_2y}\} \tag{43}$$

$$h_2(x,t) = \lim_{y\to+0}\frac{2}{\pi}\int_0^{\infty} K_2(x,t,\alpha)\cos\alpha y d\alpha \tag{44}$$

$$K_2(x,t,\alpha) = \sum_j^4 [(1+k)\alpha+(3-\kappa)p_jq_j]C_j(\alpha)e^{p_jx} \tag{45}$$

let $\alpha\to\infty$, then the asymptotic value of K_1 becomes:

$$K_{1\infty}(y,\alpha) = -Sign(\alpha)4i\frac{(\kappa-1)}{\kappa+1}e^{-|\alpha|y} \tag{46}$$

Then equation (42) can be written as:

$$h_1(x,t) = \lim_{y\to+0}\frac{1}{2\pi}\int_{-\infty}^{\infty}[K_1(y,\alpha)-K_{1\infty}(0,\alpha)]e^{i\alpha(t-x)}d\alpha + \lim_{y\to+0}\frac{1}{2\pi}\int_{-\infty}^{\infty}K_{1\infty}e^{i\alpha(t-x)}d\alpha \tag{47}$$

with

$$\lim_{y\to+0}\frac{1}{2\pi}\int_{-\infty}^{\infty}K_{1\infty}e^{i\alpha(t-x)}d\alpha=\frac{4(\kappa-1)}{\pi(\kappa+1)(t-x)} \tag{48}$$

we have:

$$h_1(x,t)=\frac{4(\kappa-1)}{\pi(\kappa+1)}\frac{1}{t-x}+\frac{1}{2\pi}\int_0^{\infty}[M(\alpha)+M(-\alpha)-8\frac{(\kappa-1)}{\kappa+1}\sin\alpha(t-x)]d\alpha \tag{49}$$

where

$$M(\alpha)=K_1(0,\alpha)e^{i\alpha(t-x)} \tag{50}$$

We here define the kernel as:

$$k_a(x,t)=[M(\alpha)+M(-\alpha)-8\frac{(\kappa-1)}{\kappa+1}\sin\alpha(t-x)] \tag{51}$$

After some lengthy analysis, the asymptotic value of K_2 for $\alpha\to\infty$ is found to be:

$$K_{2\infty}(x,t,\alpha)=[A_1\alpha^2+A_2\alpha+A_3]e^{-(x+t)\alpha+\frac{\beta}{2}(t-x)}+[B_1\alpha^2+B_2\alpha+B_3]e^{-(2h-x-t)\alpha+\frac{\beta}{2}(t-x)} \tag{52}$$

The values of $A_i(i=1,..3)$ and $B_i(i=1,..3)$ are giving below:

$$A_1=\frac{16(\kappa-1)\alpha^2}{\gamma^2(\kappa+1)}\sin(\frac{1}{2}\gamma x)\sin(\frac{1}{2}\gamma t) \tag{53}$$

$$\begin{aligned}A_2=&-\frac{2\alpha}{\gamma^2(\kappa+1)}\{[(-4\kappa^2\beta+t\gamma^2\kappa+t\beta^2\kappa+16\beta\kappa-t\gamma^2-4\beta-t\beta^2)\sin(\frac{1}{2}\gamma x)\\&+6\gamma(\kappa-1)\cos(\frac{1}{2}\gamma x)]\sin(\frac{1}{2}\gamma t)+2\gamma(\kappa-1)\cos(\frac{1}{2}\gamma t)\sin(\frac{1}{2}\gamma x)\}\end{aligned} \tag{54}$$

$$A_3 = \frac{1}{8(\kappa+1)\gamma^2}\{[32\gamma^2(\kappa-1)\cos(\frac{1}{2}\gamma x)$$
$$+4\gamma(\gamma^2 t+4\beta-4\kappa^2\beta-t\beta^2\kappa+t\beta^2-\gamma^2 t\kappa+8\beta\kappa)\sin(\frac{1}{2}\gamma x)]\cos(\frac{1}{2}\gamma t)$$
$$+[4\gamma(\kappa-1)(3t\beta^2+3t\gamma^2+20\beta)\cos(\frac{1}{2}\gamma x) \qquad (55)$$
$$+(-t^2\beta^4+t^2\gamma^4\kappa+t^2\beta^4\kappa-8t\beta^3+64\gamma^2\kappa+48\beta^2\kappa-8\gamma^2\kappa^2-24\beta^2\kappa^2+56\beta^2$$
$$-72\gamma^2-8t\beta^3\kappa^2-8t\beta\gamma^2-t^2\gamma^4+2t^2\beta^2\gamma^2\kappa-2t^2\beta^2\gamma^2-8t\beta\gamma^2\kappa^2+32t\beta^3\kappa$$
$$+32t\beta\gamma^2\kappa]\sin(\frac{1}{2}\gamma t)\}$$

$$B_1 = \frac{8(\kappa-1)\alpha^2}{\gamma^2(\kappa+1)}[\cos\frac{\gamma(x+t-2h)}{2}-\cos\frac{\gamma(x-t)}{2}] \qquad (56)$$

$$B_2 = \frac{\alpha}{\gamma^2(\kappa+1)}\{(-\kappa h\gamma^2+16\kappa\beta+t\gamma^2\kappa-t\beta^2-4\kappa^2\beta+t\beta^2\kappa-t\gamma^2$$
$$-\kappa h\beta^2+h\beta^2+h\gamma^2-4\beta)[\cos\frac{\gamma(x+t-2h)}{2}-\cos\frac{\gamma(x-t)}{2}] \qquad (57)$$
$$+2\gamma(\kappa-1)[\sin\frac{\gamma(x-t)}{2}-2\sin\frac{\gamma(x+t-2h)}{2}]\}$$

$$B_3 = -\frac{1}{16(\kappa+1)\gamma^2}\{[(-4th\beta^2\gamma^2 - 32t\beta\gamma^2\kappa - 2t^2\beta^2\gamma^2\kappa - 8\kappa^2\beta h\gamma^2$$
$$+ 8\beta\kappa^2 t\gamma^2 - 2\kappa h^2\beta^2\gamma^2 + 2\kappa th\gamma^4 + 2h^2\beta^2\gamma^2 + 32\kappa\beta^3 h - 2th\gamma^4 - 8\beta h\gamma^2$$
$$- 2th\beta^4 - 8\kappa^2\beta^3 h + 8\beta^3\kappa^2 t - 32t\beta^3\kappa + 2t^2\beta^2\gamma^2 + 8t\beta\gamma^2 - \kappa h^2\gamma^4$$
$$- t^2\gamma^4\kappa - t^2\beta^4\kappa - \kappa h^2\beta^4 - 56\beta^2 + 40\gamma^2 + h^2\beta^4 + t^2\gamma^4 + h^2\gamma^4 + t^2\beta^4$$
$$+ 32\kappa\beta h\gamma^2 + 2\kappa th\beta^4 + 24\kappa^2\beta^2 - 48\beta^2\kappa - 32\gamma^2\kappa - 8\beta^3 h + 8t\beta^3 + 8\kappa^2\gamma^2$$
$$4\kappa th\beta^2\gamma^2)\cos\frac{\gamma(x+t-2h)}{2}$$
$$-(-4th\beta^2\gamma^2 - 32t\beta\gamma^2\kappa - 2t^2\beta^2\gamma^2\kappa - 8\kappa^2\beta h\gamma^2$$
$$+ 8\beta\kappa^2 t\gamma^2 - 2\kappa h^2\beta^2\gamma^2 + 2\kappa th\gamma^4 + 2h^2\beta^2\gamma^2 + 32\kappa\beta^3 h - 2th\gamma^4 - 8\beta h\gamma^2$$
$$- 2th\beta^4 - 8\kappa^2\beta^3 h + 8\beta^3\kappa^2 t - 32t\beta^3\kappa + 2t^2\beta^2\gamma^2 + 8t\beta\gamma^2 - \kappa h^2\gamma^4$$
$$- t^2\gamma^4\kappa - t^2\beta^4\kappa - \kappa h^2\beta^4 - 56\beta^2 + 104\gamma^2 + h^2\beta^4 + t^2\gamma^4 + h^2\gamma^4 + t^2\beta^4$$
$$+ 32\kappa\beta h\gamma^2 + 2\kappa th\beta^4 + 24\kappa^2\beta^2 - 48\beta^2\kappa - 96\gamma^2\kappa - 8\beta^3 h + 8t\beta^3 + 8\kappa^2\gamma^2$$
$$4\kappa th\beta^2\gamma^2)\cos\frac{\gamma(x-t)}{2}$$
$$+ 16\gamma(t\gamma^2 - h\beta^2 - 3\beta\kappa - t\beta^2\kappa - \gamma^2 t\kappa + \kappa\gamma^2 h + \kappa h\beta^2 + 6\beta$$
$$- \kappa^2\beta + t\beta^2 - \gamma^2 h)\sin\frac{\gamma(x-t)}{2} \qquad (58)$$
$$- 8\gamma(2\kappa^2\beta + \kappa\gamma^2 h + t\gamma^2 + t\beta^2 - 14\beta\kappa - t\beta^2\kappa - \gamma^2 h$$
$$- \gamma^2 t\kappa + \kappa h\beta^2 + 8\beta - h\beta^2)\sin\frac{\gamma(x+t-2h)}{2}\}$$

Repeating the same procedure, h_2 can be rewritten as:

$$h_2(x,t) = k_s(x,t) + k_b(x,t) \qquad (59)$$

$$k_s(x,t)$$
$$= \frac{2e^{\frac{\beta}{2}(t-x)}}{\pi}\left[\frac{2A_1}{(t+x)^3} + \frac{A_2}{(t+x)^2} + \frac{A_3}{t+x} + \frac{2B_1}{(2h-x-t)^3} + \frac{B_2}{(2h-x-t)^2} + \frac{B_3}{2h-x-t}\right] \qquad (60)$$

$$k_b(x,t) = \frac{2}{\pi}\int_0^\infty [K_2(x,t,\alpha) - K_{2\infty}(x,t,\alpha)]d\alpha$$

Thus, the following integral equation is obtained:

$$\int_a^b \{\frac{1}{t-x}+\frac{\pi(\kappa+1)}{4(\kappa-1)}[k_a(x,t)+k_s(x,t)+k_b(x,t)]\}g(t)dt=\frac{\pi(\kappa+1)}{4G(x)}p(x) \tag{61}$$

The single-valuedness condition completes the formulation:

$$\int_a^b g(x)dx=0 \tag{62}$$

The stress intensity factors may then be evaluated from following equations:

$$\begin{aligned} k_1(a)&=\lim_{x\to a}\frac{4\mu(x)}{1+\kappa}\sqrt{2(x-a)}g(x)\\ k_1(b)&=-\lim_{x\to b}\frac{4\mu(x)}{1+\kappa}\sqrt{2(b-x)}g(x) \end{aligned} \tag{63}$$

It should be noted that the kernel in equation (61) is different from those obtained in Erdogan and Wu's paper [39] and Zhao's thesis [96]. The discrepancy comes from the generalized singular part $k_s(x,t)$, which becomes unbounded in edge crack problems. Erdogan and Wu's result is the same as the one for a homogeneous material [45,61]. It can be shown that when $\beta\to 0$, equation (60) will reduce to the same result in [39]. Zhao's result looks closer to the one we got here, but his result is not compatible with the homogeneous result. The numerical solution further confirms that the kernel in equation (61) yields the same results as Erdogan and Wu's kernel, while they are totally different from those in Zhao's thesis.

2.3 The Numerical Solution and the Results

Solving equations (61) and (62) using one of the quadrature technique described previously, the stress intensity factors are calculated for a variety of geometry and loadings.

Fig. 11 shows the normalized stress intensity factors at the crack-tips a and b for an internal crack in a FGM strip under fixed grip loadings $\varepsilon_y(x,\pm\infty)=\varepsilon_0$. The crack was assumed at the center of the strip, that is, $(b+a)/2=h/2$. $a'=(b-a)/2$ is the half-length of the crack. $\sigma_0=\frac{E_1}{1-\nu^2}\varepsilon_0$ is the normalizing stress, where E_1 is the Young's modulus at the line of $x=0$ (Fig. 3). The nonhomogeneity factor β is given by:

$$\beta h=\ln(E_2/E_1)=\ln 10 \tag{64}$$

where $E_1=E(0)$ and $E_2=E(h)$.

The curve shown in Fig. 11 fits exactly the corresponding curve obtained in [39].

Fig. 12 shows the variation of the normalized stress intensity factors K_1 for an edge crack in a FGM strip under fixed grip loading with b/h, for various E_2/E_1 ratios. The loads are the same as above. Again, the results agree perfectly with Erdogan and Wu's results.

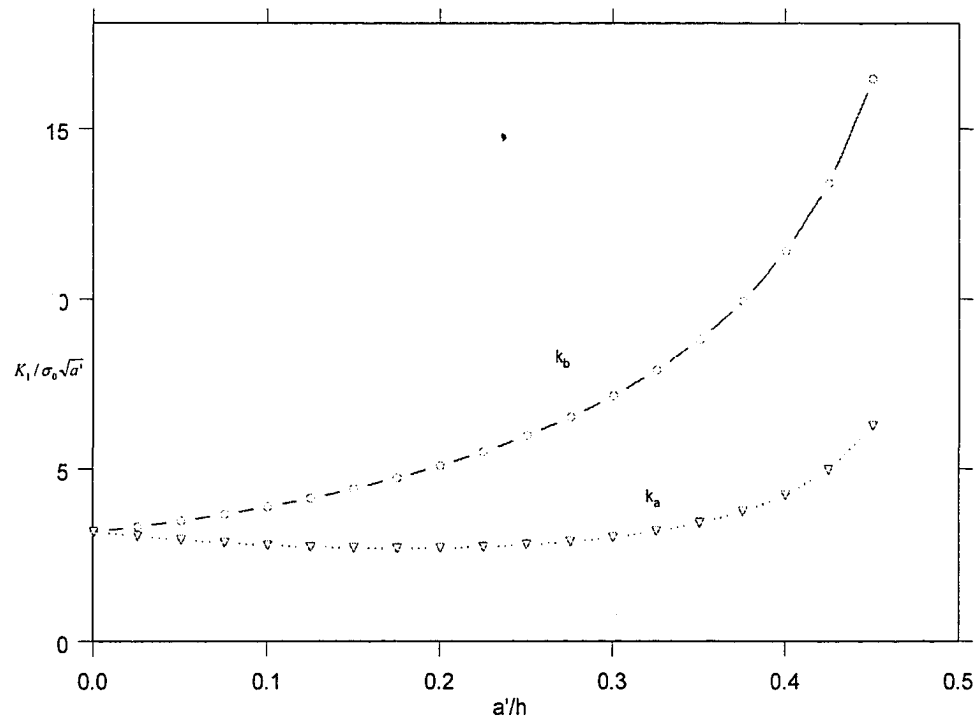

Fig. 11. Variation of the normalized stress intensity factors $K_1/\sigma_0\sqrt{a'}$ with a'/h for an internal crack under fixed grip loading

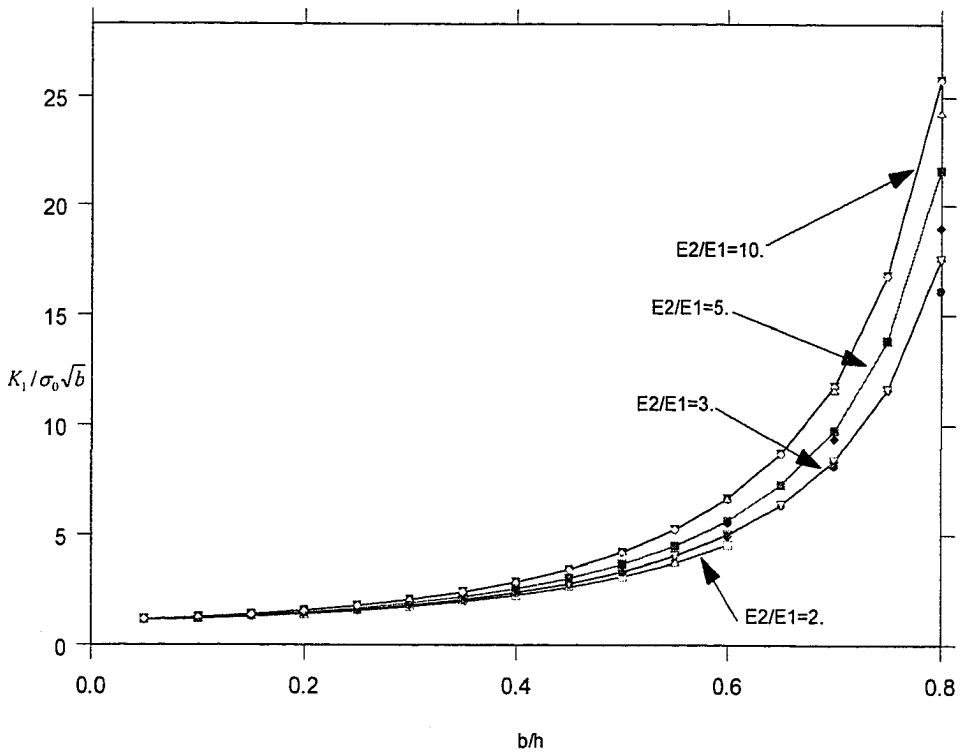

Fig. 12. Variation of the normalized stress intensity factors $K_1/\sigma_0\sqrt{b}$ with b/h for an edge crack under fixed grip loading

Chapter 3 Mixed Mode Crack Problem in FGM Strip

In this chapter, the general in-plane mixed mode problem for an arbitrarily oriented crack in a FGM strip is considered (Fig. 13). This problem is of great technical importance, as most cracks in FGMs are of the mixed-mode variety due to the variation of mechanical properties. Yet, the problem has not been solved before. The primary reason behind this is the extraordinary complexities and difficulties involved in trying to solve it analytically. The problem lacks the symmetry used in most previous studies to simplify the field equations, due to the mismatch between the orientation of the crack and the material property gradients. The loss of symmetry and the mixed-mode nature of the loading complicate the problem significantly.

Some related problems have been solved before, such as the mixed mode problem for an infinite nonhomogeneous medium studied by Konda and Erdogan [59]. El-Borgi et al. investigated an internal crack parallel to the boundary of a nonhomogeneous strip, with the material properties varying in an arbitrary direction [28]. Delale et al. studied an inclined crack in an orthotropic strip [20]. In that problem, the material is orthotropic instead of nonhomogeneous, but the idea behind it is the same as our current problem.

In this chapter, for the first time, we solve this problem analytically. Fourier transforms are used to convert the two partial differential equations into a system of Cauchy-type singular integral equations. These equations are then solved numerically using the Lobatto-Chebyshev collocation method. The effect of the nonhomogeneity parameters and the orientation of the crack line on the stress intensity factors are studied numerically.

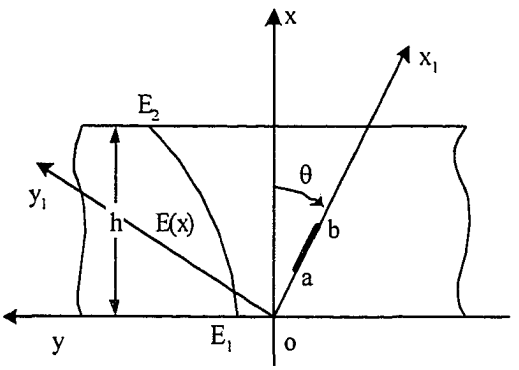

Fig. 13. Geometry of the mixed mode crack problem in a FGM strip

3.1 The Formulation

Here we consider a FGM strip containing an embedded finite crack on the $y_1 = 0$ plane (Fig. 13). The material properties vary in the direction perpendicular to the boundaries. The Poisson's ratio is assumed constant. The Young's modulus E and the shear modulus μ are defined by

$$E(x) = E_1 e^{\delta x} \tag{65}$$

or

$$E(x_1, y_1) = E_1 e^{\beta x_1 + \gamma y_1} \tag{66}$$

with

$$\beta = \delta \cos\theta, \quad \gamma = -\delta \sin\theta, \tag{67}$$

and

$$\mu(x) = \mu_1 e^{\delta x} \tag{68}$$

$$\mu(x_1, y_1) = \mu_1 e^{\beta x_1 + \gamma y_1} \tag{69}$$

The material's elastic Lame constant is:

$$\lambda(x, y) = \frac{3-\kappa}{\kappa-1}\mu_1 e^{\beta x_1 + \gamma y_1} \tag{70}$$

Here, δ is a constant that describes the nonhomogeneity of the material. The relationship between the two coordinates system is as below:

$$\begin{aligned} x_1 &= x\cos\theta + y\sin\theta \\ y_1 &= -x\sin\theta + y\cos\theta \end{aligned} \tag{71}$$

The direction of θ is as shown in Fig. 13 and it is assumed that $|\theta| \le \pi/2$. To simplify the discussion, we assume $\delta \ge 0$.

This problem will be solved under in-plane conditions. The boundary and continuity conditions of the problem are:

$$\begin{aligned} \sigma_{y_1}(x_1,+0) &= \sigma_{y_1}(x_1,-0) \\ \tau_{x_1y_1}(x_1,+0) &= \tau_{x_1y_1}(x_1,-0) \end{aligned} \tag{72}$$

$$\sigma_x(0,y) = \sigma_x(h,y) = \tau_{xy}(0,y) = \tau_{xy}(h,y) = 0 \qquad -\infty < y < \infty \tag{73}$$

$$\begin{aligned} v(x_1,+0) &= v(x_1,-0) \\ u(x_1,+0) &= u(x_1,-0) \end{aligned} \qquad x_1 < a \text{ or } x_1 > b \tag{74}$$

$$\begin{aligned} \sigma_{y_1}(x_1,0) &= p_1(x_1) \\ \tau_{x_1y_1}(x_1,0) &= p_2(x_1) \end{aligned} \qquad a < x_1 < b \tag{75}$$

where $p_1(x_1)$ and $p_2(x_1)$ are known crack surface tractions, which can be found by solving the elasticity problem for the uncracked strip under the given external loads.

The solution is expressed as the sum of two displacement sets in forms of $u_1(x_1, y_1)$, $v_1(x_1, y_1)$ and $u_2(x, y)$ and $v_2(x, y)$ where the coordinates (x_1, y_1) and (x, y) are defined in Fig. 13. The first set of displacements, that is, $u_1(x_1, y_1)$ and $v_1(x_1, y_1)$, are those obtained by Konda and Erdogan [59] for a crack in an infinite domain while the second set is for the strip without the crack and similar to that in [39]. Detailed steps to formulate this problem are shown below.

If we allow $\kappa = 3 - 4\nu$ for plane strain and $\kappa = (3-\nu)/(1+\nu)$ for plane stress, the governing equations in (x_1, y_1) system may be expressed as:

$$(\kappa+1)\frac{\partial^2 u_1}{\partial x_1^2} + (\kappa-1)\frac{\partial^2 u_1}{\partial y_1^2} + 2\frac{\partial^2 v_1}{\partial x_1 \partial y_1} + \beta(\kappa+1)\frac{\partial u_1}{\partial x_1} + \gamma(\kappa-1)\left(\frac{\partial u_1}{\partial y_1} + \frac{\partial v_1}{\partial x_1}\right) + \beta(3-\kappa)\frac{\partial v_1}{\partial y_1} = 0$$

$$(\kappa-1)\frac{\partial^2 v_1}{\partial x_1^2} + (\kappa+1)\frac{\partial^2 v_1}{\partial y_1^2} + 2\frac{\partial^2 u_1}{\partial x_1 \partial y_1} + \gamma(3-\kappa)\frac{\partial u_1}{\partial x_1} + \beta(\kappa-1)\left(\frac{\partial u_1}{\partial y_1} + \frac{\partial v_1}{\partial x_1}\right) + \gamma(\kappa+1)\frac{\partial v_1}{\partial y_1} = 0 \tag{76}$$

Assuming $u_1(x_1, y_1)$, $v_1(x_1, y_1)$ as

$$u_1(x_1, y_1) = \frac{1}{2\pi}\int_{-\infty}^{\infty} U(y_1, \alpha) e^{-i\alpha x_1} d\alpha$$
$$v_1(x_1, y_1) = \frac{1}{2\pi}\int_{-\infty}^{\infty} V(y_1, \alpha) e^{-i\alpha x_1} d\alpha \tag{77}$$

and substituting in (76), we get:

$$U(y_1,\alpha)=\sum_{j=1}^{4}m_jF_j(\alpha)e^{n_jy_1},\quad V(y_1,\alpha)=\sum_{j=1}^{4}F_j(\alpha)e^{n_jy_1} \tag{78}$$

where $F_j(\alpha)$ are unknown functions, $m_j(j=1,...,4)$ are given by

$$m_j=\frac{[2\alpha i+\beta(\kappa-3)]n_j+i\alpha\gamma(\kappa-1)}{(\kappa-1)n_j^{\,2}+(\kappa-1)\gamma m_j-(\kappa+1)(\alpha+i\beta)\alpha} \tag{79}$$

and $n_j(j=1,...,4)$ are the roots of the characteristic equation,

$$\begin{aligned}&n^4+2\gamma n^3+[-2\alpha(\alpha+i\beta)+\gamma^2+\beta^2\frac{\kappa-3}{\kappa+1}]n^2+\alpha\gamma(-2\alpha-i\beta\frac{8}{\kappa+1})n\\&+\alpha^2(\alpha^2+2i\alpha\beta-\beta^2+\gamma^2\frac{3-\kappa}{\kappa+1})=0\end{aligned} \tag{80}$$

Equation (80) may be simplified as,

$$[n^2+\gamma n-\alpha(a+i\beta)]^2+\frac{3-\kappa}{\kappa+1}(\alpha\gamma-i\beta n)^2=0 \tag{81}$$

From equation (81), the values of n_j are obtained as:

$$\begin{aligned}&n_1=-\frac{\Delta_1}{2}-\frac{\sqrt{\Delta_1^{\,2}+4(\alpha^2+i\alpha\Delta_2)}}{2} \qquad n_2=-\frac{\Delta_3}{2}-\frac{\sqrt{\Delta_3^{\,2}+4(\alpha^2+i\alpha\Delta_4)}}{2}\\&n_3=-\frac{\Delta_1}{2}+\frac{\sqrt{\Delta_1^{\,2}+4(\alpha^2+i\alpha\Delta_2)}}{2} \qquad n_4=-\frac{\Delta_3}{2}+\frac{\sqrt{\Delta_3^{\,2}+4(\alpha^2+i\alpha\Delta_4)}}{2}\\&\Delta_1=\gamma+\beta\sqrt{\frac{3-\kappa}{\kappa+1}} \qquad \Delta_3=\gamma-\beta\sqrt{\frac{3-\kappa}{\kappa+1}}\\&\Delta_2=\beta-\gamma\sqrt{\frac{3-\kappa}{\kappa+1}} \qquad \Delta_4=\beta+\gamma\sqrt{\frac{3-\kappa}{\kappa+1}}\end{aligned} \tag{82}$$

To satisfy the regularity conditions, u and v must vanish for $x_1^2 + y_1^2 \to \infty$, then the unknown functions $F_j(\alpha)(j = 1,...,4)$ satisfy the relations:

$$\begin{aligned} F_3(\alpha) = F_4(\alpha) = 0, \quad & y > 0 \\ F_1(\alpha) = F_2(\alpha) = 0, \quad & y < 0 \end{aligned} \tag{83}$$

Using Hooke's Law, the stresses are found to be:

$$\begin{aligned} \sigma_{x_t}(x_1, y_1) &= \frac{\mu}{2\pi(\kappa - 1)} \int_{-\infty}^{\infty} \sum_{j=l}^{l+1} [-i\alpha m_j(1+\kappa) + n_j(3-\kappa)] F_j(\alpha) e^{n_j y_1 - i\alpha x_1} d\alpha \\ \sigma_{y_1}(x_1, y_1) &= \frac{\mu}{2\pi(\kappa - 1)} \int_{-\infty}^{\infty} \sum_{j=l}^{l+1} [-i\alpha m_j(3-\kappa) + n_j(1+\kappa)] F_j(\alpha) e^{n_j y_1 - i\alpha x_1} d\alpha \\ \tau_{x_1 y_1}(x_1, y_1) &= \frac{\mu}{2\pi} \int_{-\infty}^{\infty} \sum_{j=l}^{l+1} [n_j m_j - i\alpha] F_j(\alpha) e^{n_j y_1 - i\alpha x_1} d\alpha \end{aligned} \tag{84}$$

where $l = 1$ for $y > 0$ and $l = 3$ for $y < 0$.

Applying the boundary and continuity conditions (72), and the expressions of stresses obtained in (84), we find

$$F_3(\alpha) = R_1(\alpha)F_1(\alpha) + R_2(\alpha)F_2(\alpha), \quad F_4(\alpha) = R_3(\alpha)F_1(\alpha) + R_4(\alpha)F_2(\alpha) \tag{85}$$

where $R_j(\alpha)$ are given by

$$\begin{aligned} R_1(\alpha) &= \{(m_4 - m_1)[(1+\kappa)n_1 n_4 + (3-\kappa)\alpha^2] + i\alpha(n_4 - n_1)[1 + \kappa - (3-\kappa)m_1 m_4]\} / R_0 \\ R_2(\alpha) &= \{(m_4 - m_2)[(1+\kappa)n_2 n_4 + (3-\kappa)\alpha^2] + i\alpha(n_4 - n_2)[1 + \kappa - (3-\kappa)m_2 m_4]\} / R_0 \\ R_3(\alpha) &= -\{(m_3 - m_1)[(1+\kappa)n_1 n_3 + (3-\kappa)\alpha^2] + i\alpha(n_3 - n_1)[1 + \kappa - (3-\kappa)m_1 m_3]\} / R_0 \\ R_4(\alpha) &= -\{(m_3 - m_1)[(1+\kappa)n_1 n_3 + (3-\kappa)\alpha^2] + i\alpha(n_3 - n_1)[1 + \kappa - (3-\kappa)m_1 m_3]\} / R_0 \\ R_0(\alpha) &= (m_4 - m_3)[(1+\kappa)n_3 n_4 + (3-\kappa)\alpha^2] + i\alpha(n_4 - n_3)[1 + \kappa - (3-\kappa)m_3 m_4] \end{aligned} \tag{86}$$

To determine the two remaining unknown functions $F_1(\alpha)$ and $F_2(\alpha)$, we introduce the following new auxiliary functions in terms of the crack surface derivatives:

$$\begin{aligned} g_1(x_1) &= \frac{\partial}{\partial x_1}[u_1(x_1,+0) - u_1(x_1,-0)], \quad a < |x_1| < b \\ g_2(x_1) &= \frac{\partial}{\partial x_1}[v_1(x_1,+0) - v_1(x_1,-0)], \quad a < |x_1| < b \end{aligned} \tag{87}$$

From definitions of $g_1(x_1)$ and $g_2(x_1)$, one can easily conclude that $g_1(x_1) = 0$ and $g_2(x_1) = 0$ when $0 < |x_1| < a$ or $|x_1| > b$ and

$$\int_a^b g_j(t)dt = 0, \quad j = 1,2 \tag{88}$$

Equations (88) are referred to as the single-valuedness conditions.

Substituting u_1 and v_1 into the definition of $g_1(x_1)$ and $g_2(x_1)$, we get

$$\begin{aligned} g_1(x_1) &= \frac{1}{2\pi}\int_{-\infty}^{\infty} \frac{-i\alpha(1+\kappa)[(f_{11} - i\alpha f_{41})F_1 + (f_{12} - i\alpha f_{42})F_2]}{R_0} e^{-i\alpha x_1} d\alpha \\ g_2(x_1) &= \frac{1}{2\pi}\int_{-\infty}^{\infty} \frac{-i\alpha\{[-(1+\kappa)f_{31} + i\alpha(3-\kappa)f_{21}]F_1 + [-(1+\kappa)f_{32} + i\alpha(3-\kappa)f_{22}]F_2\}}{R_0} e^{-i\alpha x_1} d\alpha \end{aligned} \tag{89}$$

where

$$\begin{aligned} f_{1j} &= n_3 m_4 m_j (n_4 - n_j) + n_4 m_3 m_j (n_j - n_3) + n_j m_3 m_4 (n_3 - n_4) \\ f_{2j} &= m_4 m_j (n_4 - n_j) + m_3 m_j (n_j - n_3) + m_3 m_4 (n_3 - n_4) \\ f_{3j} &= n_3 m_3 (n_4 - n_j) + n_4 m_4 (n_j - n_3) + n_j m_j (n_3 - n_4) \\ f_{4j} &= m_3 (n_4 - n_j) + m_4 (n_j - n_3) + m_j (n_3 - n_4) \end{aligned} \qquad j = 1,2 \tag{90}$$

Inverting the Fourier integrals of equation (89), we obtain

$$\int_{-\infty}^{\infty} g_1(t)e^{i\alpha t}dt = \frac{-i\alpha(1+\kappa)[(f_{11}-i\alpha f_{41})F_1+(f_{12}-i\alpha f_{42})F_2]}{R_0}$$
$$\int_{-\infty}^{\infty} g_2(t)e^{i\alpha t}dt = \frac{-i\alpha\{[-(1+\kappa)f_{31}+i\alpha(3-\kappa)f_{21}]F_1+[-(1+\kappa)f_{32}+i\alpha(3-\kappa)f_{32}]F_2\}}{R_0}$$

(91)

Thus, we can solve F_1 and F_2 in terms of g_1 and g_2 as,

$$F_1 = \int_{-\infty}^{\infty} \frac{[\alpha(3-\kappa)f_{22}+i(1+\kappa)f_{32}]g_1+(if_{12}+\alpha f_{42})(1+\kappa)g_2}{(1+\kappa)\alpha\omega_0} e^{i\alpha t}dt$$
$$F_2 = -\int_{-\infty}^{\infty} \frac{[\alpha(3-\kappa)f_{21}+i(1+\kappa)f_{31}]g_1+(if_{11}+\alpha f_{41})(1+\kappa)g_2}{(1+\kappa)\alpha\omega_0} e^{i\alpha t}dt$$

(92)

where

$$\omega_0 = (m_1-m_2)(m_3-m_4)(n_1n_2+n_3n_4)+(m_1-m_4)(m_2-m_3)(n_2n_3+n_1n_4)$$
$$-(m_1-m_3)(m_2-m_4)(n_1n_3+n_2n_4)$$

(93)

Then substituting F_1 and F_2 back into equation (84), we can express σ_{x_1}, σ_{y_1} and $\tau_{x_1y_1}$ in terms of g_1 and g_2, for $y_1 > 0$ as,

$$\sigma_{x_1}^{(1)}(x_1,y_1) = \frac{\mu(x_1,y_1)}{2\pi(1+\kappa)}\int_0^{\phi}\sum_{j=1}^{2} h_{1j}^{(1)}(x_1,y_1,t)g_j(t)dt$$
$$\sigma_{y_1}^{(1)}(x_1,y_1) = \frac{\mu(x_1,y_1)}{2\pi(1+\kappa)}\int_0^{\phi}\sum_{j=1}^{2} h_{2j}^{(1)}(x_1,y_1,t)g_j(t)dt$$
$$\tau_{x_1y_1}^{(1)}(x_1,y_1) = \frac{\mu(x_1,y_1)}{2\pi(1+\kappa)}\int_0^{\phi}\sum_{j=1}^{2} h_{3j}^{(1)}(x_1,y_1,t)g_j(t)dt$$

(94)

where

$$h_{kj}^{(1)}(x_1,y_1,t) = \int_{-\infty}^{\infty} K_{kj}^{(1)}(y_1,\alpha)e^{i\alpha(t-x_1)}d\alpha, \quad k=1,2; \quad j=1,2,$$

(95)

and

$$
\begin{aligned}
K_{11}^{(1)}(y_1,\alpha) &= -\frac{i\alpha m_1(1+\kappa)-n_1(3-\kappa)}{\alpha\omega_0(\kappa-1)}[\alpha(3-\kappa)f_{22}+i(1+\kappa)f_{32}]e^{n_1y_1} \\
&+\frac{i\alpha m_2(1+\kappa)-n_2(3-\kappa)}{\alpha\omega_0(\kappa-1)}[\alpha(3-\kappa)f_{21}+i(1+\kappa)f_{31}]e^{n_2y_1} \\
K_{12}^{(1)}(y_1,\alpha) &= -\frac{i\alpha m_1(1+\kappa)-n_1(3-\kappa)}{\alpha\omega_0(\kappa-1)}(if_{12}+\alpha f_{42})(1+\kappa)e^{n_1y_1} \\
&+\frac{i\alpha m_2(1+\kappa)-n_2(3-\kappa)}{\alpha\omega_0(\kappa-1)}(if_{11}+\alpha f_{41})(1+\kappa)e^{n_2y_1}
\end{aligned}
\tag{96}
$$

$$
\begin{aligned}
K_{21}^{(1)}(y_1,\alpha) &= \frac{i\alpha m_1(\kappa-3)+n_1(1+\kappa)}{\alpha\omega_0(\kappa-1)}[\alpha(3-\kappa)f_{22}+i(1+\kappa)f_{32}]e^{n_1y_1} \\
&-\frac{i\alpha m_2(\kappa-3)+n_2(1+\kappa)}{\alpha\omega_0(\kappa-1)}[\alpha(3-\kappa)f_{21}+i(1+\kappa)f_{31}]e^{n_2y_1} \\
K_{22}^{(1)}(y_1,\alpha) &= \frac{i\alpha m_1(\kappa-3)+n_1(1+\kappa)}{\alpha\omega_0(\kappa-1)}(if_{12}+\alpha f_{42})(1+\kappa)e^{n_1y_1} \\
&-\frac{i\alpha m_2(\kappa-3)+n_2(1+\kappa)}{\alpha\omega_0(\kappa-1)}(if_{11}+\alpha f_{41})(1+\kappa)e^{n_2y_1}
\end{aligned}
\tag{97}
$$

$$
\begin{aligned}
K_{31}^{(1)}(y_1,\alpha) &= \frac{(n_1m_1-i\alpha)}{\alpha\omega_0}[\alpha(3-\kappa)f_{22}+i(1+\kappa)f_{32}]e^{n_1y_1} \\
&-\frac{(n_2m_2-i\alpha)}{\alpha\omega_0}[\alpha(3-\kappa)f_{21}+i(1+\kappa)f_{31}]e^{n_2y_1} \\
K_{32}^{(1)}(y_1,\alpha) &= \frac{(n_1m_1-i\alpha)}{\alpha\omega_0}(if_{12}+\alpha f_{42})(1+\kappa)e^{n_1y_1} \\
&-\frac{(n_2m_2-i\alpha)}{\alpha\omega_0}(if_{11}+\alpha f_{41})(1+\kappa)e^{n_2y_1}
\end{aligned}
\tag{98}
$$

Similarly, after some manipulation, we get σ_{x_1}, σ_{y_1} and $\tau_{x_1y_1}$ when $y_1<0$,

$$\sigma_{x_1}^{(2)}(x_1,y_1)=\frac{\mu(x_1,y_1)}{2\pi(1+\kappa)}\int_0^{\phi}\sum_{j=1}^{2}h_{1j}^{(2)}(x_1,y_1,t)g_j(t)dt$$

$$\sigma_{y_1}^{(2)}(x_1,y_1)=\frac{\mu(x_1,y_1)}{2\pi(1+\kappa)}\int_0^{\phi}\sum_{j=1}^{2}h_{2j}^{(2)}(x_1,y_1,t)g_j(t)dt \qquad (99)$$

$$\tau_{x_1y_1}^{(2)}(x_1,y_1)=\frac{\mu(x_1,y_1)}{2\pi(1+\kappa)}\int_0^{\phi}\sum_{j=1}^{2}h_{3j}^{(2)}(x_1,y_1,t)g_j(t)dt$$

where

$$h_{kj}^{(2)}(x_1,y_1,t)=\int_{-\infty}^{\infty}K_{kj}^{(2)}(y_1,\alpha)e^{i\alpha(t-x_1)}d\alpha,\quad k=1,2;\qquad j=1,2, \qquad (100)$$

$$K_{11}^{(2)}(y_1,\alpha)=-\frac{i\alpha m_3(1+\kappa)-n_3(3-\kappa)}{\alpha\omega_0(\kappa-1)}[\alpha(3-\kappa)f_{24}+i(1+\kappa)f_{34}]e^{n_3y_1}$$
$$+\frac{i\alpha m_4(1+\kappa)-n_4(3-\kappa)}{\alpha\omega_0(\kappa-1)}[\alpha(3-\kappa)f_{23}+i(1+\kappa)f_{33}]e^{n_4y_1}$$
$$K_{12}^{(2)}(y_1,\alpha)=-\frac{i\alpha m_3(1+\kappa)-n_3(3-\kappa)}{\alpha\omega_0(\kappa-1)}(if_{14}+\alpha f_{44})(1+\kappa)e^{n_3y_1} \qquad (101)$$
$$+\frac{i\alpha m_4(1+\kappa)-n_4(3-\kappa)}{\alpha\omega_0(\kappa-1)}(if_{13}+\alpha f_{43})(1+\kappa)e^{n_4y_1}$$

$$K_{21}^{(2)}(y_1,\alpha)=\frac{i\alpha m_3(\kappa-3)+n_3(1+\kappa)}{\alpha\omega_0(\kappa-1)}[\alpha(3-\kappa)f_{24}+i(1+\kappa)f_{34}]e^{n_3y_1}$$
$$-\frac{i\alpha m_4(\kappa-3)+n_4(1+\kappa)}{\alpha\omega_0(\kappa-1)}[\alpha(3-\kappa)f_{23}+i(1+\kappa)f_{33}]e^{n_4y_1}$$
$$K_{22}^{(2)}(y_1,\alpha)=\frac{i\alpha m_3(\kappa-3)+n_3(1+\kappa)}{\alpha\omega_0(\kappa-1)}(if_{14}+\alpha f_{44})(1+\kappa)e^{n_3y_1} \qquad (102)$$
$$-\frac{i\alpha m_4(\kappa-3)+n_4(1+\kappa)}{\alpha\omega_0(\kappa-1)}(if_{13}+\alpha f_{43})(1+\kappa)e^{n_4y_1}$$

$$K_{31}^{(2)}(y_1,\alpha)=\frac{(n_3m_3-i\alpha)}{\alpha\omega_0}[\alpha(3-\kappa)f_{24}+i(1+\kappa)f_{34}]e^{n_3y_1}$$
$$-\frac{(n_4m_4-i\alpha)}{\alpha\omega_0}[\alpha(3-\kappa)f_{23}+i(1+\kappa)f_{33}]e^{n_4y_1}$$
$$K_{32}^{(2)}(y_1,\alpha)=\frac{(n_3m_3-i\alpha)}{\alpha\omega_0}(if_{14}+\alpha f_{44})(1+\kappa)e^{n_3y_1} \qquad (103)$$
$$-\frac{(n_4m_4-i\alpha)}{\alpha\omega_0}(if_{13}+\alpha f_{43})(1+\kappa)e^{n_4y_1}$$

where

$$f_{1j}=-[n_1m_2m_j(n_2-n_j)+n_2m_1m_j(n_j-n_1)+n_jm_1m_2(n_1-n_2)]$$
$$f_{2j}=-[m_2m_j(n_2-n_j)+m_1m_j(n_j-n_1)+m_1m_2(n_1-n_2)]$$
$$f_{3j}=-[n_1m_1(n_2-n_j)+n_2m_2(n_j-n_1)+n_jm_j(n_1-n_2)] \qquad (104)$$
$$f_{4j}=-[m_1(n_2-n_j)+m_2(n_j-n_1)+m_j(n_1-n_2)] \qquad j=3,4$$

In the coordinate system (x,y), the Navier's equations for the elastic medium may be expressed as:

$$(\kappa+1)\frac{\partial^2u}{\partial x^2}+(\kappa-1)\frac{\partial^2u}{\partial y^2}+2\frac{\partial^2v}{\partial x\partial y}+\delta(\kappa+1)\frac{\partial u}{\partial x}+\delta(3-\kappa)\frac{\partial v}{\partial y}=0$$
$$(\kappa-1)\frac{\partial^2v}{\partial x^2}+(\kappa+1)\frac{\partial^2v}{\partial y^2}+2\frac{\partial^2u}{\partial x\partial y}+\delta(\kappa-1)(\frac{\partial v}{\partial x}+\frac{\partial u}{\partial y})=0 \qquad (105)$$

Assuming the solution of $u_2(x,y)$ and $v_2(x,y)$ as

$$u_2(x,y)=\frac{1}{2\pi}\int_{-\infty}^{\infty}qA(\alpha)e^{px}e^{-i\alpha y}d\alpha$$
$$v_2(x,y)=\frac{1}{2\pi}\int_{-\infty}^{\infty}A(\alpha)e^{px}e^{-i\alpha y}d\alpha \qquad (106)$$

the characteristic equations for p and q may be expressed as

$$\begin{aligned}&[(\kappa+1)p^2-(\kappa-1)\alpha^2+\delta(\kappa+1)p]q-i\alpha[2p+\delta(3-\kappa)]=0 \qquad (a)\\&(\kappa-1)p^2+\delta(\kappa-1)p-(\kappa+1)\alpha^2-i\alpha q[2p+\delta(\kappa-1)]=0 \qquad (b)\end{aligned} \tag{107}$$

solving equations (107), we have:

$$q_j=\frac{(\kappa-1)(p_j+\delta)p_j-(\kappa+1)\alpha^2}{\alpha i[2p_j+\delta(\kappa-1)]},\quad j=1,...,4 \tag{108}$$

Define $\omega=\delta\sqrt{(3-\kappa)/(1+\kappa)}$, using equations (108), equations (107) yields the roots p as:

$$\begin{aligned}p_1&=-\frac{\delta}{2}-\frac{1}{2}\sqrt{\delta^2+4\alpha^2+4i\omega\alpha}\\p_2&=-\frac{\delta}{2}-\frac{1}{2}\sqrt{\delta^2+4\alpha^2-4i\omega\alpha}\\p_3&=-\frac{\delta}{2}+\frac{1}{2}\sqrt{\delta^2+4\alpha^2+4i\omega\alpha}\\p_4&=-\frac{\delta}{2}+\frac{1}{2}\sqrt{\delta^2+4\alpha^2-4i\omega\alpha}\end{aligned} \tag{109}$$

Then we can express u_2 and v_2 in terms of the unknown functions $A_j(\alpha)$ as $(j=1,...,4)$

$$\begin{aligned}u_2(x,y)&=\frac{1}{2\pi}\int_{-\infty}^{\infty}\sum_j^4 q_jA_j(\alpha)e^{p_jx}e^{-i\alpha y}d\alpha\\v_2(x,y)&=\frac{1}{2\pi}\int_{-\infty}^{\infty}\sum_j^4 A_j(\alpha)e^{p_jx}e^{-i\alpha y}d\alpha\end{aligned} \tag{110}$$

From Hooke's law, the stresses corresponding to u_2 and v_2 are

$$\sigma_x^{(3)} = \frac{\mu(x,y)}{2\pi(\kappa-1)} \int_{-\infty}^{\infty} \sum_j^4 [(1+k)p_j q_j + (\kappa-3)i\alpha] A_j(\alpha) e^{p_j x - i\alpha y} d\alpha$$

$$\sigma_y^{(3)} = \frac{\mu(x,y)}{2\pi(\kappa-1)} \int_{-\infty}^{\infty} \sum_j^4 [-(1+k)i\alpha + (3-\kappa)p_j q_j] A_j(\alpha) e^{p_j x - i\alpha y} d\alpha \qquad (111)$$

$$\tau_{xy}^{(3)} = \frac{\mu(x,y)}{2\pi} \int_{-\infty}^{\infty} \sum_j^4 [p_j - i\alpha q_j] A_j(\alpha) e^{p_j x - i\alpha y} d\alpha$$

3.2 The Integral Equations

At a given point in the medium, the stress state is the sum of the stresses given by equations (111) and (94) or (99), depending on the sign of y_1. The free boundary conditions in equation (73) then yield the following set of equations for the unknown functions $A_j(\alpha)$ $(j = 1,...,4)$ in terms of the auxiliary functions g_1 and g_2,

$$\begin{aligned}
\sum_j^4 [(1+k)p_j q_j + (\kappa-3)i\alpha] A_j(\alpha) &= \frac{1}{2\pi(1+\kappa)} \sum_{j=1}^2 \int_0^b F_{1j}(\alpha,t) g_j(t) dt \\
\sum_j^4 [p_j - i\alpha q_j] A_j(\alpha) &= \frac{1}{2\pi(1+\kappa)} \sum_{j=1}^2 \int_0^b F_{2j}(\alpha,t) g_j(t) dt \\
\sum_j^4 [(1+k)p_j q_j + (\kappa-3)i\alpha] A_j(\alpha) e^{p_j h} &= \frac{1}{2\pi(1+\kappa)} \sum_{j=1}^2 \int_0^b F_{3j}(\alpha,t) g_j(t) dt \\
\sum_j^4 [p_j - i\alpha q_j] A_j(\alpha) e^{p_j h} &= \frac{1}{2\pi(1+\kappa)} \sum_{j=1}^2 \int_0^b F_{4j}(\alpha,t) g_j(t) dt
\end{aligned} \qquad (112)$$

where

$$
\begin{aligned}
F_{1j}(\alpha,t) &= (1-\kappa)\sum_{i=1}^{2}\{\zeta_{1j}{}^{(i)}(\alpha,t)\cos^2\theta + \zeta_{2j}{}^{(i)}(\alpha,t)\sin^2\theta - 2\zeta_{3j}{}^{(i)}(\alpha,t)\cos\theta\sin\theta\} \\
F_{2j}(\alpha,t) &= -\sum_{i=1}^{2}\{(\cos^2\theta-\sin^2\theta)\zeta_{3j}{}^{(i)}(\alpha,t) - [\zeta_{2j}{}^{(i)}(\alpha,t) - \zeta_{1j}{}^{(i)}(\alpha,t)]\sin\theta\cos\theta\} \\
F_{3j}(\alpha,t) &= (1-\kappa)\sum_{i=1}^{2}\{\xi_{1j}{}^{(i)}(\alpha,t)\cos^2\theta + \xi_{2j}{}^{(i)}(\alpha,t)\sin^2\theta - 2\xi_{3j}{}^{(i)}(\alpha,t)\cos\theta\sin\theta\} \\
F_{4j}(\alpha,t) &= -\sum_{i=1}^{2}\{(\cos^2\theta-\sin^2\theta)\xi_{3j}{}^{(i)}(\alpha,t) - [\xi_{2j}{}^{(i)}(\alpha,t) - \xi_{1j}{}^{(i)}(\alpha,t)]\sin\theta\cos\theta\}
\end{aligned}
\tag{113}
$$

Functions $\zeta_{kj}{}^{(i)}(\alpha,t)$ and $\xi_{kj}{}^{(i)}(\alpha,t)$ $(k=1...3,\ j=1..3,\ i=1..2)$ are defined as

$$
\begin{aligned}
\zeta_{kj}{}^{(1)}(\alpha,t) &= \int_{-\infty}^{\infty}\int_{0}^{\infty} K_{kj}{}^{(1)}(y\cos\theta,\rho)e^{i\rho(t-y\sin\theta)+i\alpha y}\,dy\,d\rho \\
\zeta_{kj}{}^{(2)}(\alpha,t) &= \int_{-\infty}^{\infty}\int_{-\infty}^{0} K_{kj}{}^{(2)}(y\cos\theta,\rho)e^{i\rho(t-y\sin\theta)+i\alpha y}\,dy\,d\rho
\end{aligned}
\tag{114}
$$

$$
\begin{aligned}
\xi_{kj}{}^{(1)}(\alpha,t) &= \int_{-\infty}^{\infty}\int_{h\tan\theta}^{\infty} K_{kj}{}^{(1)}(y\cos\theta - h\sin\theta,\rho)e^{i\rho(t-y\sin\theta-h\cos\theta)+i\alpha y}\,dy\,d\rho \\
\xi_{kj}{}^{(2)}(\alpha,t) &= \int_{-\infty}^{\infty}\int_{-\infty}^{h\tan\theta} K_{kj}{}^{(2)}(y\cos\theta - h\sin\theta,\rho)e^{i\rho(t-y\sin\theta-h\cos\theta)+i\alpha y}\,dy\,d\rho
\end{aligned}
\tag{115}
$$

From equations (112), the $A_j(\alpha)$ are obtained as:

$$
A_j(\alpha) = \sum_{i=1}^{2}\int_{a}^{b} C_{ji}(\alpha,t)g_i(t)dt \tag{116}
$$

where

$$
C_{ji}(\alpha,t) = \sum_{k=1}^{4} b_{jk}(\alpha)F_{ki}(\alpha,t), \qquad (j=1...4, i=1...2) \tag{117}
$$

Here, the matrix (b_{jk}) is the inverse of (a_{jk}) given by

$$
\begin{aligned}
a_{1j}(\alpha) &= (1+k)p_j q_j + (\kappa - 3)i\alpha \\
a_{2j}(\alpha) &= p_j - i\alpha q_j \\
a_{3j}(\alpha) &= [(1+k)p_j q_j + (\kappa - 3)i\alpha]e^{p_j h} \\
a_{4j}(\alpha) &= [p_j - i\alpha q_j]e^{p_j h}
\end{aligned}
\tag{118}
$$

From the boundary conditions

$$
\sigma_{y_1}(x_1,+0) = p_1(x_1),\ \tau_{x_1 y_1}(x_1,+0) = p_2(x_1) \qquad (a < x < b) \tag{119}
$$

where $p_1(x_1)$ and $p_2(x_1)$ are crack surface tractions, we obtain:

$$
\begin{aligned}
&\sigma_{y_1}{}^{(1)}(x_1,0) + \sin^2\theta\,\sigma_x{}^{(3)}(x_1\cos\theta,\, x_1\sin\theta) + \cos^2\theta\,\sigma_y{}^{(3)}(x_1\cos\theta,\, x_1\sin\theta) \\
&- 2\sin\theta\cos\theta\,\tau_{xy}{}^{(3)}(x_1\cos\theta,\, x_1\sin\theta) = p_1(x_1)
\end{aligned}
\tag{120}
$$

$$
\begin{aligned}
&\tau_{x_1 y_1}{}^{(1)}(x_1,0) + \tau_{xy}{}^{(3)}(x_1\cos\theta,\, x_1\sin\theta)(\cos^2\theta - \sin^2\theta) \\
&+ \sin\theta\cos\theta[\sigma_y{}^{(3)}(x_1\cos\theta,\, x_1\sin\theta) - \sigma_x{}^{(3)}(x_1\cos\theta,\, x_1\sin\theta)] = p_2(x_1)
\end{aligned}
\tag{121}
$$

Substituting the expressions of stresses and extracting the singular parts of (120), noting that for $\alpha \to \infty$

$$
\begin{aligned}
K_{21}{}^{\infty} &= 0 \\
K_{22}{}^{\infty} &= -2i\frac{|\alpha|}{\alpha}e^{-|\alpha|y}
\end{aligned}
\tag{122}
$$

we obtain

$$
\frac{1}{\pi}\int_a^b \{\frac{g_2(t)}{t-x_1} + \sum_{j=1}^{2}[k_{1j}{}^{(1)}(x_1,t) + k_{2j}{}^{(1)}(x_1,t)]g_j(t)\}dt = \frac{(1+\kappa)}{2\mu(x_1,0)}p_1(x_1) \tag{123}
$$

where the kernels are

$$
\begin{aligned}
&k_{11}^{(1)}(x_1,t)=\frac{1}{4}h_{21}^{(1)}(x_1,0,t)\\
&k_{12}^{(1)}(x_1,t)=\frac{1}{4}\int_{-\infty}^{\infty}[K_{22}^{(1)}(0,\alpha)-\lim_{\alpha\to\infty}K_{22}^{(1)}(0,\alpha)]e^{i\alpha(t-x_1)}d\alpha\\
&k_{2j}^{(1)}(x_1,t)\\
&=\frac{(1+\kappa)}{4(\kappa-1)}\int_{-\infty}^{\infty}\sum_{i}^{4}\{[(1+k)p_iq_i+(\kappa-3)i\alpha]\sin^2\theta\\
&+[-(1+k)i\alpha+(3-\kappa)p_iq_i]\cos^2\theta\\
&-2\sin\theta\cos\theta(\kappa-1)[p_i-i\alpha q_i]\}C_{ij}(\alpha,t)e^{p_ix_1\cos\theta-i\alpha x_1\sin\theta}d\alpha
\end{aligned}
\tag{124}
$$

Similarly, equation (121) yields:

$$
\frac{1}{\pi}\int_a^b\{\frac{g_1(t)}{t-x_1}+\sum_{j=1}^{2}[k_{1j}^{(2)}(x_1,t)+k_{2j}^{(2)}(x_1,t)]g_j(t)\}dt=\frac{(1+\kappa)}{2\mu(x_1,0)}p_2(x_1)
\tag{125}
$$

with

$$
\begin{aligned}
&k_{12}^{(2)}(x_1,t)=\frac{1}{4}h_{32}^{(1)}(x_1,0,t)\\
&k_{11}^{(2)}(x_1,t)=\frac{1}{4}\int_{-\infty}^{\infty}[K_{31}^{(1)}(0,\alpha)-\lim_{\alpha\to\infty}K_{31}^{(1)}(0,\alpha)]e^{i\alpha(t-x_1)}d\alpha\\
&k_{2i}^{(2)}(x_1,t)=\frac{(1+\kappa)}{4(\kappa-1)}\int_{-\infty}^{\infty}\sum_{j}^{4}\{(\cos^2\theta-\sin^2\theta)(\kappa-1)[p_j-i\alpha q_j]\\
&+2\sin\theta\cos\theta(1-\kappa)[i\alpha+p_jq_j]\}C_{ji}(\alpha,t)e^{p_jx_1\cos\theta-i\alpha x_1\sin\theta}d\alpha
\end{aligned}
\tag{126}
$$

The single valuedness conditions (88) complete the formulation of the problem

$$
\int_a^b g_j(t)dt=0,\quad j=1,2
\tag{127}
$$

3.3 The Numerical Solution

The Cauchy-type singular integral equations obtained above can be solved numerically, using one of the techniques outlined above. Here we use the collocation method used in [38,39].

First, to normalize the integral interval $a < x, t < b$ to $-1 < r, s < 1$, we define

$$
\begin{aligned}
&t = \frac{b-a}{2} r + \frac{b+a}{2} \\
&x_1 = \frac{b-a}{2} s + \frac{b+a}{2} \\
&g_1(t) = \phi_1(r) \quad g_2(t) = \phi_2(r) \\
&p_1(x_1) = f_1(s) \;\; p_2(x_1) = f_2(s) \\
&\mu(x_1,0) = m(s,0) \\
&q_{ij}^{(n)}(s,r) = \frac{b-a}{2} k_{ij}^{(n)}(x_1,t) \quad (i = 1,2,\ j = 1,2,\ n = 1,2)
\end{aligned}
\tag{128}
$$

Thus, the integral equations (123), (125) become:

$$
\frac{1}{\pi} \int_{-1}^{1} \{ \frac{\phi_2(r)}{r-s} + \sum_{j=1}^{2} [q_{1j}^{(1)}(s,r) + q_{2j}^{(1)}(s,r)] \phi_j(r) \} dr = \frac{(1+\kappa)}{2m(s,0)} f_1(s) \tag{129}
$$

$$
\frac{1}{\pi} \int_{-1}^{1} \{ \frac{\phi_1(r)}{r-s} + \sum_{j=1}^{2} [q_{1j}^{(2)}(s,r) + q_{2j}^{(2)}(s,r)] \phi_j(r) \} dr = \frac{(1+\kappa)}{2m(s,0)} f_2(s) \tag{130}
$$

The fundamental solution of these equations is ([42,80])

$$
w(r) = \frac{1}{\sqrt{1-r^2}} \tag{131}
$$

so the solution of (123) and (125) may be expressed as an expansion of Chebyshev polynomials of the first kind:

$$\begin{aligned}\phi_1(r) &= \frac{1}{\sqrt{1-r^2}}\sum_{n=0}^{N} c_n^{(1)} T_n(r) \quad -1<r<1 \\ \phi_2(r) &= \frac{1}{\sqrt{1-r^2}}\sum_{n=0}^{N} c_n^{(2)} T_n(r) \quad -1<r<1\end{aligned} \tag{132}$$

where $c_n^{(1)}$ and $c_n^{(2)}$ $(n = 0,1,2...)$ are unknown constants. From equation (127), considering the orthogonality conditions of $T_n(r)$, it can be shown that

$$\begin{aligned}c_0^{(1)} &= 0 \\ c_0^{(2)} &= 0\end{aligned} \tag{133}$$

Using the properties

$$\frac{1}{\pi}\int_{-1}^{1} \frac{T_n(r)dr}{(r-s)\sqrt{1-r^2}} = \begin{cases} U_{n-1}(s) & |s|<1 \quad (n=1,2,...) \\ -\dfrac{(s-|s|\sqrt{s^2-1}/s)^n}{|s|\sqrt{s^2-1}/s} & |s|>1 \quad (n=1,2,...)\end{cases} \tag{134}$$

where the $U_n(s)$ is the Chebyshev polynomial of the second kind [29], and substituting (132) into (129) and (130), we obtain:

$$\begin{aligned}
&\sum_{n=1}^{\infty} c_n^{(1)} U_{n-1}(s) + \frac{1}{\pi}\sum_{n=1}^{\infty}\int_{-1}^{1}\sum_{j=1}^{2}[q_{1j}^{(1)}(s,r)+q_{2j}^{(1)}(s,r)]c_n^{(j)}\frac{T_n(r)}{\sqrt{1-r^2}}dr \\
&= \frac{(1+\kappa)}{2m(s,0)} f_1(s) \qquad -1<s<1 \\
&\sum_{n=1}^{\infty} c_n^{(2)} U_{n-1}(s) + \frac{1}{\pi}\sum_{n=1}^{\infty}\int_{-1}^{1}\sum_{j=1}^{2}[q_{1j}^{(2)}(s,r)+q_{2j}^{(2)}(s,r)]c_n^{(j)}\frac{T_n(r)}{\sqrt{1-r^2}}dr \\
&= \frac{(1+\kappa)}{2m(s,0)} f_2(s) \qquad -1<s<1
\end{aligned} \tag{135}$$

Equation (135) can be solved by truncating the series and choosing the collocation points s_n as

$$T_N(s_n)=0 \qquad s_n = \cos((2n-1)\frac{\pi}{2N}) \qquad n=1,\ldots,N \tag{136}$$

After determining $c_n^{(1)}$ and $c_n^{(2)}$, we can express the stress intensity factors at the crack tips as ([59])

$$\begin{aligned}
k_1(a) &= \sqrt{\frac{b-a}{2}}\frac{2\mu(a,0)}{1+\kappa}\sum_{n=1}^{\infty}(-1)^n c_n^{(1)} \\
k_2(a) &= \sqrt{\frac{b-a}{2}}\frac{2\mu(a,0)}{1+\kappa}\sum_{n=1}^{\infty}(-1)^n c_n^{(2)} \\
k_1(b) &= -\sqrt{\frac{b-a}{2}}\frac{2\mu(b,0)}{1+\kappa}\sum_{n=1}^{\infty} c_n^{(1)} \\
k_2(b) &= -\sqrt{\frac{b-a}{2}}\frac{2\mu(b,0)}{1+\kappa}\sum_{n=1}^{\infty} c_n^{(2)}
\end{aligned} \tag{137}$$

and the crack surface openings as

$$u(x_1,+0)-u(x_1,-0)=-\sqrt{(a'^2-x'^2)}\sum_{n=1}^{\infty}\frac{1}{n}c_n^{(1)}U_{n-1}(x'/a')$$
$$v(x_1,+0)-v(x_1,-0)=-\sqrt{(a'^2-x'^2)}\sum_{n=1}^{\infty}\frac{1}{n}c_n^{(2)}U_{n-1}(x'/a') \quad (138)$$

where

$$a'=\frac{b-a}{2} \quad (139)$$

which is the half length of the crack and

$$x'=x-\frac{b+a}{2} \quad (140)$$

3.4 Results and Discussion

To compare the results obtained in this study with previous results, several special cases are studied. First, we let $h\to\infty$, in which case the geometry is that of a crack in an infinite plane that was studied by Konda and Erdogan [59]. Table 1. shows the comparison of the stress intensity factors obtained here with those from [59]. The crack is under uniform crack surface traction:

$$p_1(x_1,0)=\sigma_0$$
$$p_2(x_1,0)=0 \quad (141)$$

The stress intensity factors are normalized by a factor of K_0,

$$K_0=\sigma_0\sqrt{a'} \quad (142)$$

where

$$a' = \frac{b-a}{2} \tag{143}$$

$a'\delta$ \ θ		0^0		45^0		90^0	
		Ref. [59]	Current Study	Ref. [59]	Current Study	Ref. [59]	Current Study
0.10	$K_1(a)/K_0$	1.023	1.023	1.021	1.021	1.009	1.009
	$K_1(b)/K_0$	0.975	0.975	0.987	0.987	1.009	1.009
	$K_2(a)/K_0$	0.000	0.000	0.022	0.022	0.026	0.026
	$K_2(b)/K_0$	0.000	0.000	-0.015	-0.015	-0.026	-0.026
0.25	$K_1(a)/K_0$	1.055	1.055	1.061	1.061	1.036	1.036
	$K_1(b)/K_0$	0.936	0.936	0.974	0.975	1.036	1.036
	$K_2(a)/K_0$	0.000	0.000	0.061	0.061	0.065	0.065
	$K_2(b)/K_0$	0.000	0.000	-0.031	-0.032	-0.065	-0.065
0.50	$K_1(a)/K_0$	1.103	1.104	1.141	1.140	1.101	1.100
	$K_1(b)/K_0$	0.871	0.873	0.960	0.961	1.101	1.100
	$K_2(a)/K_0$	0.000	0.000	0.141	0.141	0.129	0.131
	$K_2(b)/K_0$	0.000	0.000	-0.048	-0.050	-0.129	-0.131
1.00	$K_1(a)/K_0$	1.189	1.194	1.327	1.328	1.258	1.254
	$K_1(b)/K_0$	0.757	0.762	0.938	0.941	1.258	1.254
	$K_2(a)/K_0$	0.000	0.000	0.339	0.337	0.263	0.265
	$K_2(b)/K_0$	0.000	0.000	-0.065	-0.071	-0.263	-0.265

Table 1. Comparison of stress intensity factors from current study with those from Ref. [59] for an inclined crack in an infinite FGM plate under uniform crack surface traction

Different combinations of crack length and nonhomogeneity factors are used, while the angle θ varies from 0^0 to 90^0, which means that the orientation of the crack changes from normal to the boundary to parallel to it.

From the table it can be observed that the data show excellent qualitative and quantitative agreement between previous and current results. The difference between the results is less than 3%, which can easily be explained by the different numerical procedures employed and the rounding of errors.

Another special case considered is that of a crack perpendicular to the boundary. This problem was studied by Erdogan and Wu [39] and Zhao in his Ph. D. Thesis [96].

The comparison between the two sets of results is given in Table 2.

The results shown in Table 2 are stress intensity factors for a crack at the center of the strip i.e. $(a+b)/2 = h/2$, perpendicular to the boundary. The loading is uniform strain

$$\varepsilon_y(x,\pm\infty) = \varepsilon_0 \tag{144}$$

and the stress intensity factors are normalized by K_0 which is defined as

$$K_0 = \frac{8\mu_1}{1+\kappa}\varepsilon_0\sqrt{a'} \tag{145}$$

Again the results compare well with those reported in [39] and calculated in chapter 2.

Results showing the effect of crack length and crack orientation on the stress intensity factors have also been obtained. The loading is uniform strain at infinity, with

$$\varepsilon_{yy}(x,\pm\infty) = \varepsilon_0 \tag{146}$$

a'/h		$K_1(a)/K_0$	$K_1(b)/K_0$	$K_2(a)/K_0$	$K_2(b)/K_0$
0.05	Results from Chapter 2	2.928	3.477	N/A	N/A
	Current results	2.930	3.470	0.000	0.000
0.10	Results from Chapter 2	2.772	3.884	N/A	N/A
	Current results	2.780	3.880	0.000	0.000
0.20	Results from Chapter 2	2.691	5.086	N/A	N/A
	Current results	2.698	5.081	0.000	0.000
0.25	Results from Chapter 2	2.784	5.967	N/A	N/A
	Current results	2.790	5.970	0.000	0.000
0.30	Results from Chapter 2	3.001	7.147	N/A	N/A
	Current results	3.010	7.150	0.000	0.000
0.35	Results from Chapter 2	3.417	8.806	N/A	N/A
	Current results	3.430	8.820	0.000	0.000

Table 2. Comparison of stress intensity factors from current study with results from chapter 2 for a FGM strip with an internal center crack under uniform strain loadings

The crack surface traction defined by (75) may be expressed as,

$$p_1(x_1,0) = -\frac{8\mu_1 e^{\delta x\cos\theta}}{1+\kappa}\varepsilon_0\cos^2\theta$$
$$p_2(x_1,0) = -\frac{8\mu_1 e^{\delta x\cos\theta}}{1+\kappa}\varepsilon_0\cos\theta\sin\theta \qquad (147)$$

We define the normalizing stress as

$$\sigma_0 = \frac{8\mu_1}{1+\kappa}\varepsilon_0 \qquad (148)$$

Calculations were carried out for various crack lengths, with the θ varying from 0^0 to near 90^0. Figs. 14 to 20 show the stress intensity factors for a crack with varying crack lengths, for $a'/h = 0.05, 0.10, 0.15, 0.20, 0.25, 0.30, 0.35$ respectively. The stress intensity factors are normalized by

$$K_0 = \sigma_0\sqrt{a'} \qquad (149)$$

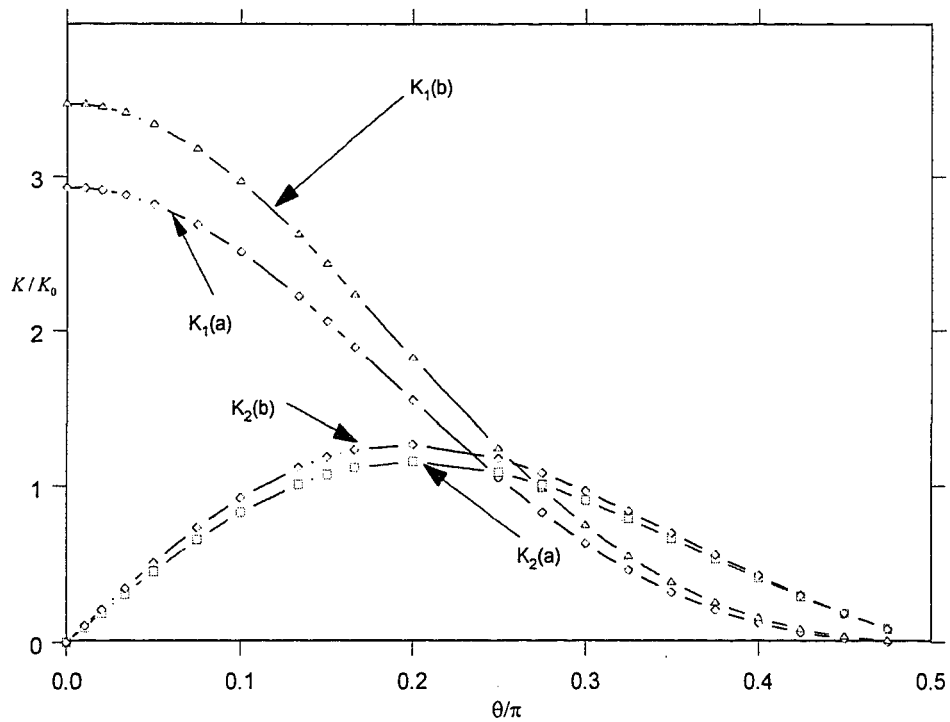

Fig 14. Variation of the normalized stress intensity factors K / K_0 with θ / π for an internal inclined crack in a FGM strip under uniform strain, $a' / h = 0.05$

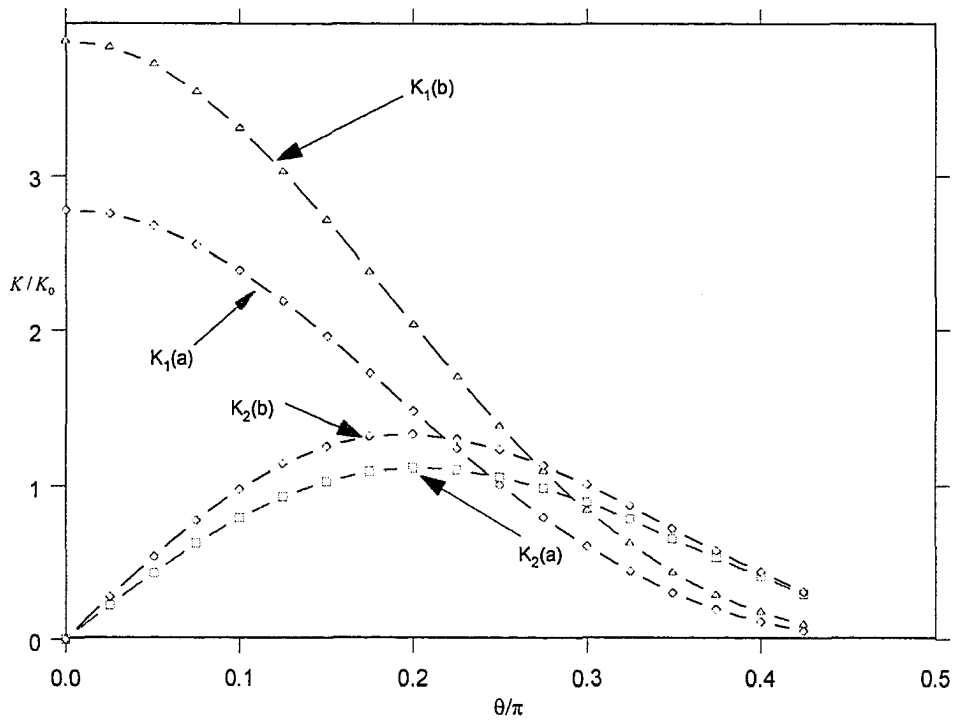

Fig. 15. Variation of the normalized stress intensity factors K / K_0 with θ / π for an internal inclined crack in a FGM strip under uniform strain, $a' / h = 0.10$

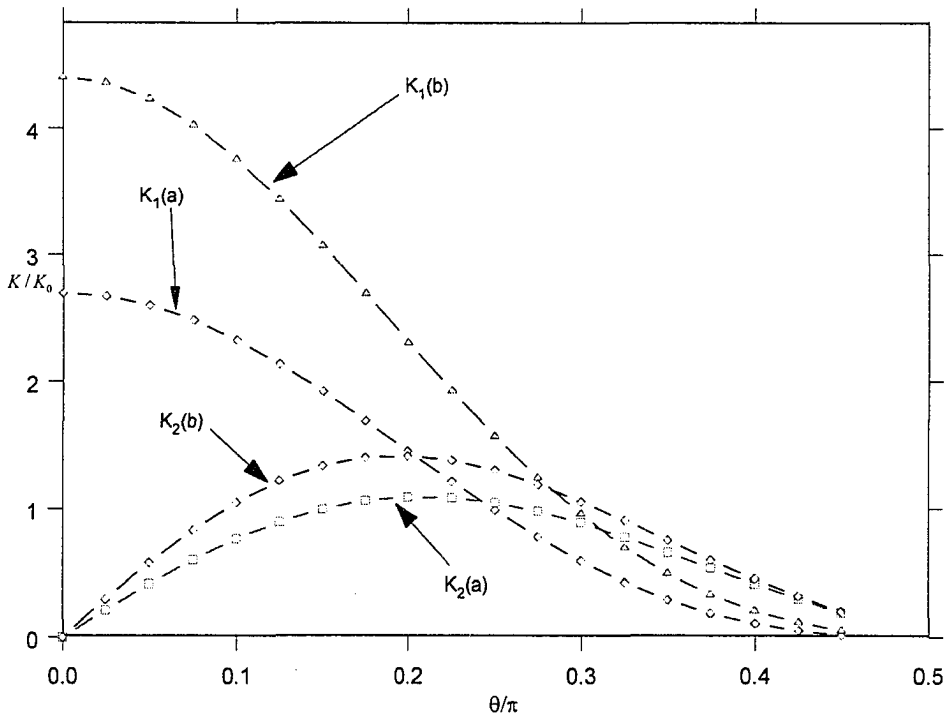

Fig. 16. Variation of the normalized stress intensity factors K / K_0 with θ / π for an internal inclined crack in a FGM strip under uniform strain, $a' / h = 0.15$

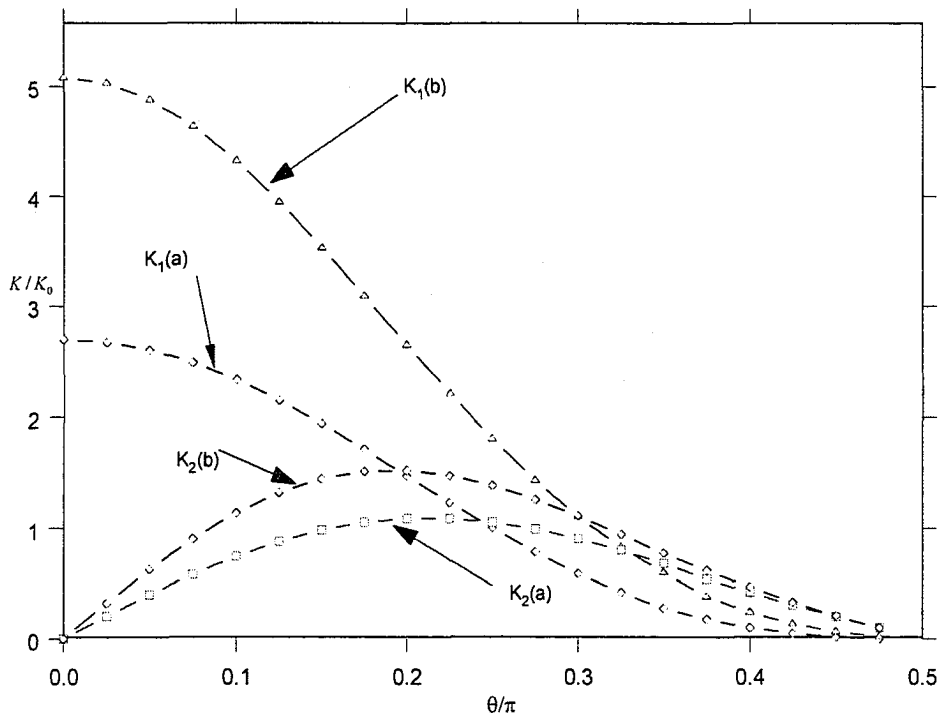

Fig. 17. Variation of the normalized stress intensity factors K / K_0 with θ / π for an internal inclined crack in a FGM strip under uniform strain, $a' / h = 0.20$

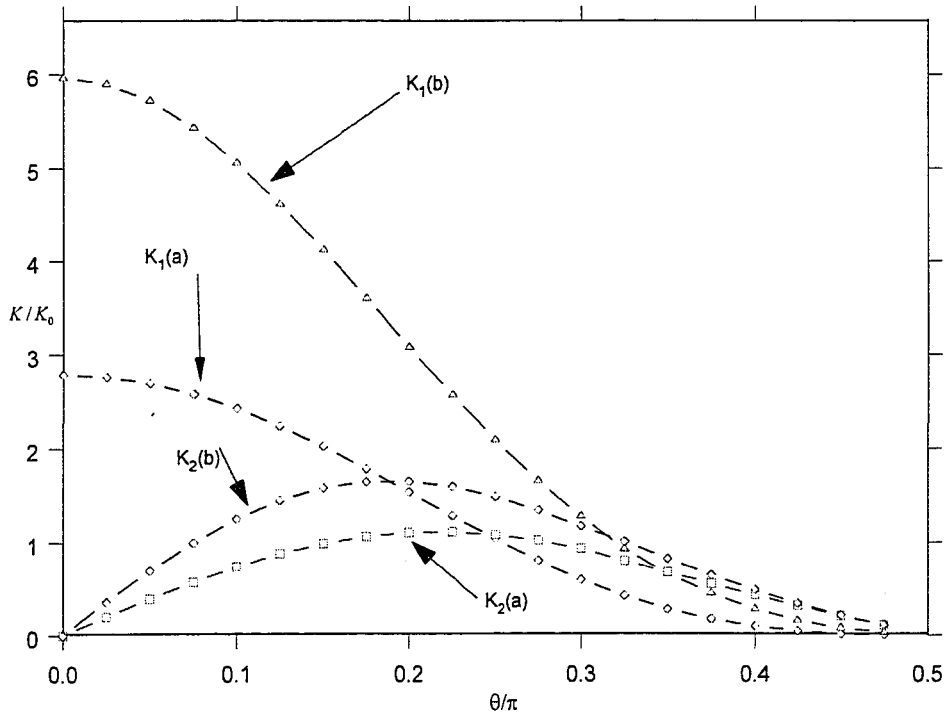

Fig. 18. Variation of the normalized stress intensity factors K / K_0 with θ / π for an internal inclined crack in a FGM strip under uniform strain, $a' / h = 0.25$

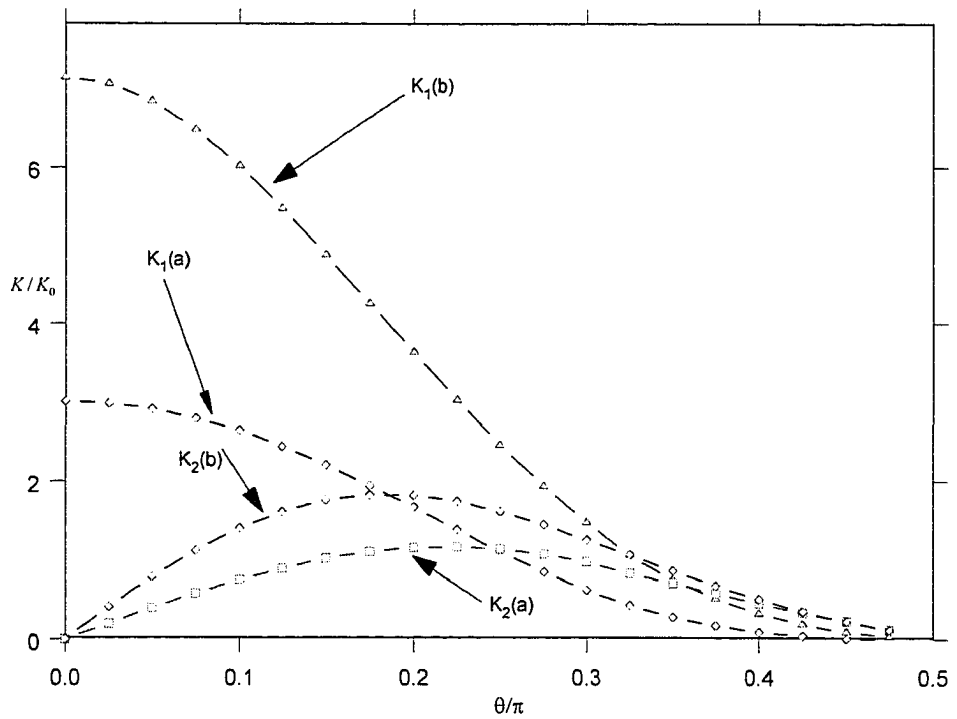

Fig. 19. Variation of the normalized stress intensity factors K / K_0 with θ / π for an internal inclined crack in a FGM strip under uniform strain, $a' / h = 0.30$

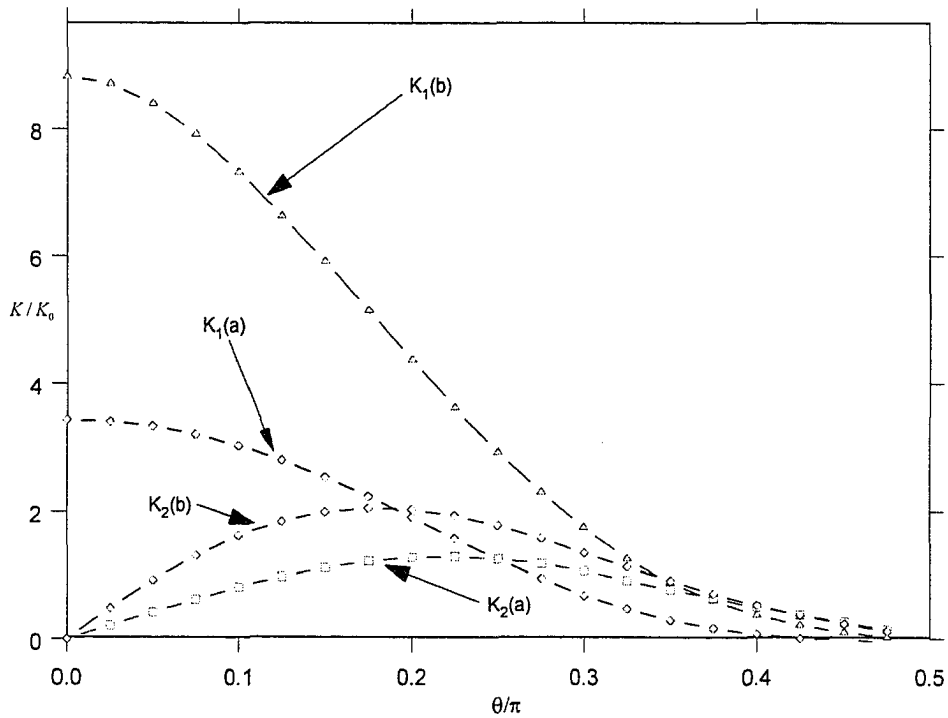

Fig. 20. Variation of the normalized stress intensity factors K / K_0 with θ / π for an internal inclined crack in a FGM strip under uniform strain, $a' / h = 0.35$

It can be observed that the stress intensity factors for mode *I* crack ($K_1(a)$ and $K_1(b)$) decrease when θ increase from 0^0 to near 90^0 while the stress intensity factors for mode *II* crack first increase then decrease as the crack angle increases. The stress intensity factors $(K_1)_s$ are always greater than $(K_2)_s$ in the beginning, when the problem is mostly under mode *I* deformation. After θ increases to a given point, $(K_1)_s$ become smaller than $(K_2)_s$, because mode *II* loading starts to dominate. This trend is not affected by the length of the crack, while the values of stress intensity factors are. Fig. 21

shows $K_1(b)$ for different crack lengths with the orientation of the crack changing from 0^0 to 90^0. Fig. 22 shows the stress intensity factors for different crack length when $\theta = 45^0$.

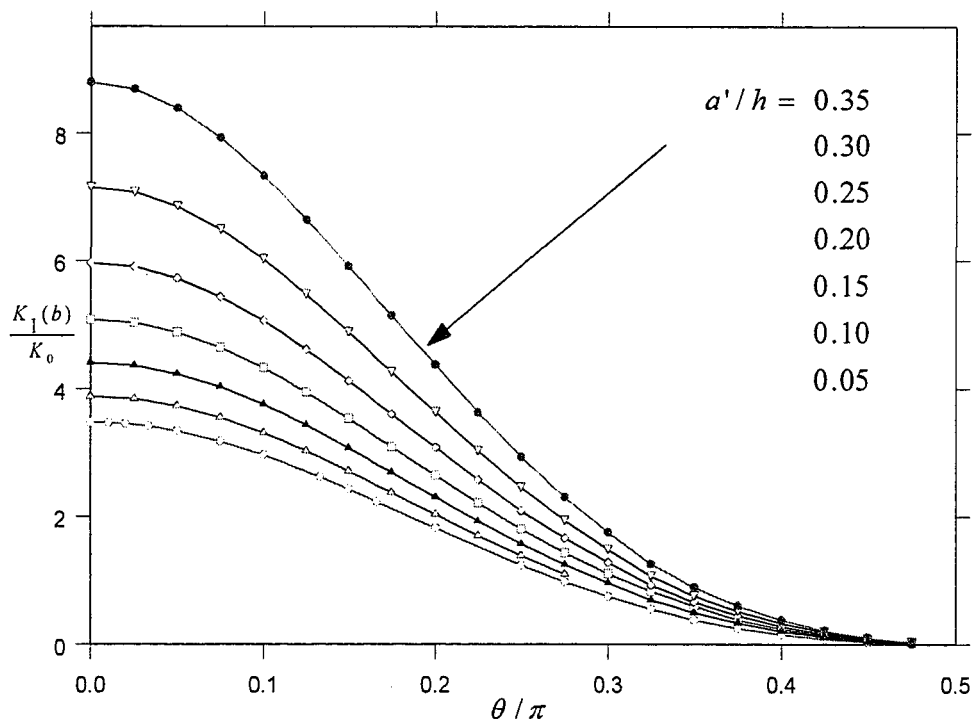

Fig. 21. Variation of the normalized stress intensity factors $K_1(b)/K_0$ with θ/π for an internal inclined crack in a FGM strip under uniform strain, for various a'/h ratios

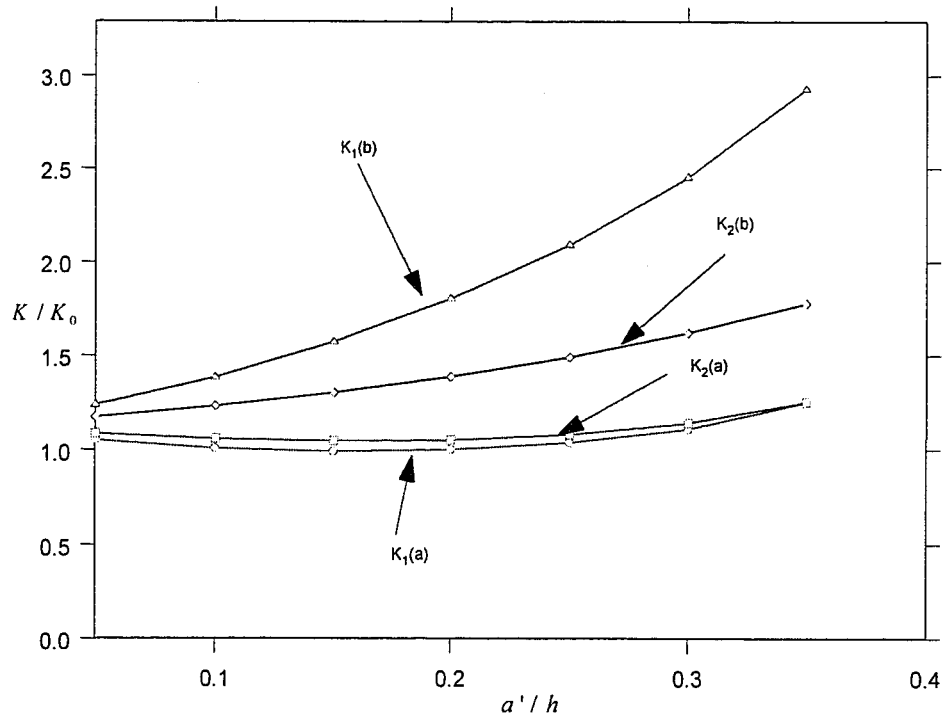

Fig. 22. Variation of the normalized stress intensity factors K / K_0 with a' / h for an internal inclined crack in a FGM strip under uniform strain, $\theta = \pi / 4$

The crack surface openings are displayed in Fig. 23 and Fig. 24. Fig. 23 depicts the crack surface opening in y_1 direction with the crack length $a' / h = 0.35$. Fig. 24 shows the corresponding opening in x_1 direction. For Fig. 24, since there is no crack displacement in x_1 direction, the orientations of the cracks are chosen as 4.5^0, 45^0 and 67.5^0 respectively. In Fig. 23, the orientations of the cracks are chosen as 0^0, 45^0 and 67.5^0.

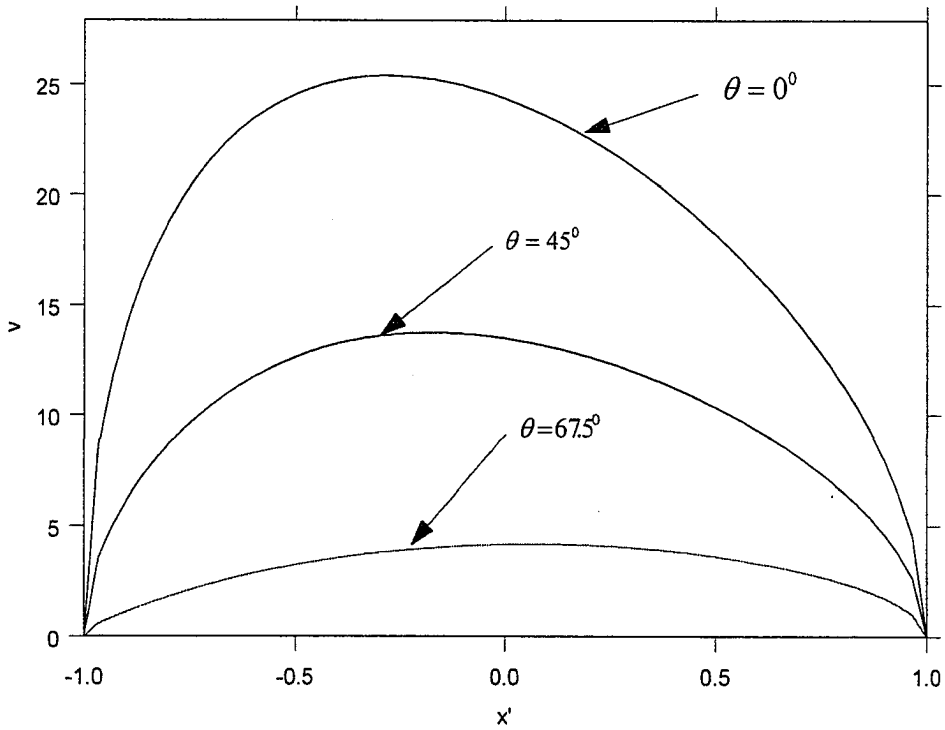

Fig. 23. Crack surface openings in the y_1 direction for $a'/h = 0.35$, $\theta = 0^0$, 45^0 and 67.5^0

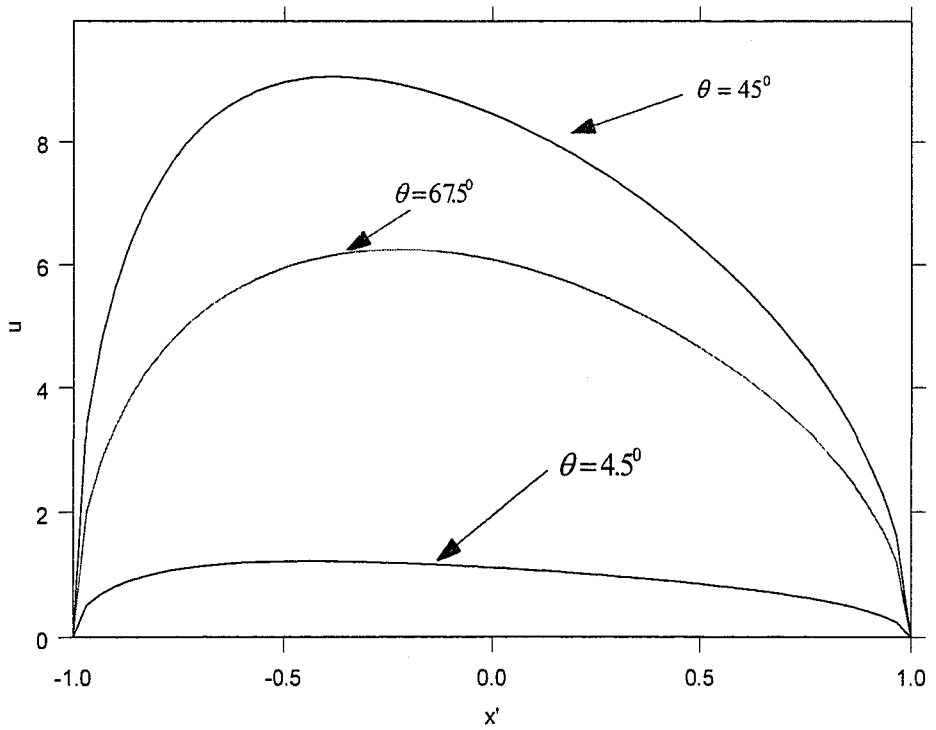

Fig. 24. Crack surface openings in the x_1 direction for $a'/h = 0.35$, $\theta = 4.5^0$, 45^0 and 67.5^0

Some preliminary numerical calculations have also been carried out for eccentric cracks, especially for cracks near interfaces. Fig. 25 shows the normalized stress intensity factors $K_1(b)/K_0$ for different eccentric cracks, where $a' = 0.5$ and ϑ is a factor depicting the eccentricity of the crack, defined as:

$$\vartheta = \frac{h-(a+b)}{h} \tag{150}$$

It can be observed that when the cracks move closer to the interface (in our model, the Young's modulus of the material decreases in this direction), the stress intensity factors decrease. It is also worth pointing out that when studying eccentric cracks, the convergence

speed of the numerical quadrature decreases significantly when the cracks are close to the boundary, thus, making it extremely difficult to obtain accurate results.

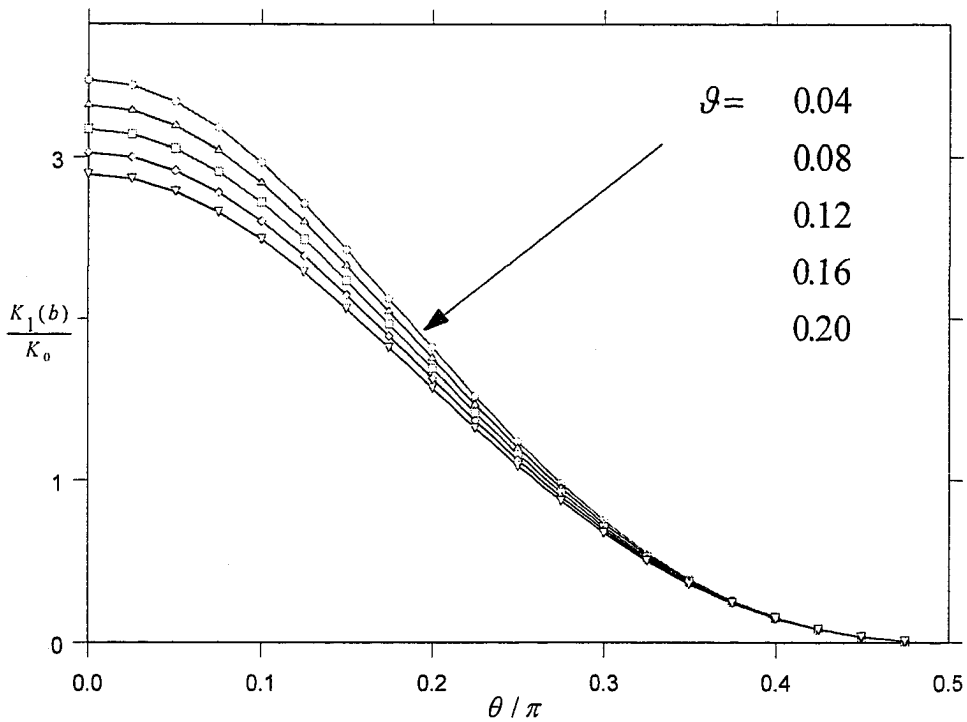

Fig. 25. Variation of the normalized stress intensity factors $K_1(b)/K_0$ with θ/π for an internal inclined eccentric crack in a FGM strip under uniform strain

Chapter 4 The Mixed Mode Crack Problem in a FGM Strip Bonded to a Homogeneous Half Plane

In this chapter, the general in-plane mixed mode problem for an arbitrarily oriented crack in a FGM strip bonded to a homogeneous half plane is considered (Fig. 26). As mentioned before, FGMs layers are widely used in high temperature applications as thermal barrier coatings. These layers usually are bonded to metal substrates, which have same mechanical properties of the bonding surface of the FGMs layers. Compared to FGMs layers, these substrates are generally much thicker. Thus, it is safe to model them as half-planes when studying fracture problems in FGMs layers. It is under these consideration that we model the general fracture problem as an arbitrarily oriented crack in a FGM layer bounded to a homogeneous half plane.

It appears that the general fracture problem has not been solved before. Some researchers have studied crack problems in bonded plates with at least one of them nonhomogeneous, such as [13,15,16,17,19,22,23,30,35,36,37,40,57,68,93,95], to name but a few. It should be noted that in most of these problems, the loadings are anti-plane shears, which are rather easy to deal with but their practical importance is very limited. For some mode *I* crack problems, the cracks are either interfacial or in aligned directions. The most noteworthy problems that are somewhat close to current research are the two studied by Choi ([15] and [17]). In [15], it is a mode *I* problem of a crack located in a homogeneous semi-infinite substrate that is bonded to a surface layer through a nonhomogeneous interfacial layer. The crack is perpendicular to the nominal interface (Fig. 10). In [17], Choi investigated the mode *I* crack in the same geometry but at an arbitrary angle to the graded

interfacial zone, instead of perpendicular to it. For both problems, the cracks are located in the homogeneous layers, which greatly simplified the mathematical analysis.

In this chapter, based on the study presented in the previous chapter, we provide an analytical solution for the problem of an arbitrarily oriented crack in a FGM layer bounded to a homogeneous half plane. Again, Fourier transforms are used to construct a system of Cauchy-type singular integral equations. These equations are then solved numerically to obtain the stress intensity factors at the crack tips.

4.1 The Formulation

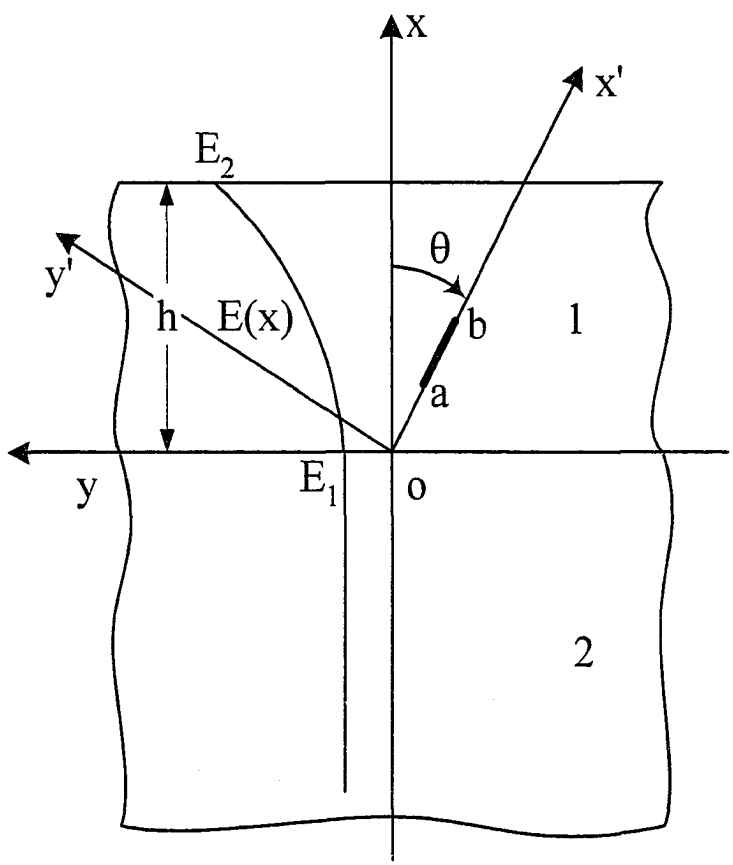

Fig.26. Geometry of the crack in a bonded strip

Here we consider a FGM strip (layer 1 in Fig. 26) containing an embedded finite crack on the $y'=0$ plane; the strip is bonded to a homogeneous half plane (layer 2 in Fig. 26).

In the FGM strip, the material properties vary in the direction perpendicular to the boundaries. The Poisson's ratio is assumed constant. The Young's modulus E and the shear modulus μ are defined by

$$E(x) = E_1 e^{\delta x} \tag{151}$$

or

$$E(x', y') = E_1 e^{\beta x' + \gamma y'} \tag{152}$$

with

$$\beta = \delta \cos\theta, \quad \gamma = -\delta \sin\theta, \tag{153}$$

and

$$\mu(x) = \mu_1 e^{\delta x} \tag{154}$$

$$\mu(x', y') = \mu_1 e^{\beta x' + \gamma y'} \tag{155}$$

and the Lame constant is:

$$\lambda(x, y) = \frac{3-\kappa}{\kappa-1} \mu_1 e^{\beta x' + \gamma y'} \tag{156}$$

δ is a constant that describes the nonhomogeneity of the FGM. The relationship between the two coordinates system is as below:

$$\begin{aligned} x' &= x\cos\theta + y\sin\theta \\ y' &= -x\sin\theta + y\cos\theta \end{aligned} \tag{157}$$

with $|\theta| \le \pi/2$.

To simplify the analysis, we assume $\delta \ge 0$.

For layer 2, which is homogeneous, the mechanical properties of the material are:

$$E(x) = E_1; \qquad \mu(x) = \mu_1 \tag{158}$$

This problem will be solved under plane elasticity conditions, with the following boundary and continuity conditions:

$$\begin{aligned} &\sigma_{y'}(x',+0) = \sigma_{y'}(x',-0) \\ &\tau_{x'y'}(x',+0) = \tau_{x'y'}(x',-0) \qquad 0 < x < h \end{aligned} \tag{159}$$

$$\begin{aligned} &\sigma_x(+0,y) = \sigma_x(-0,y) \\ &\tau_{xy}(+0,y) = \tau_{xy}(-0,y) \qquad -\infty < y < \infty \end{aligned} \tag{160}$$

$$\sigma_x(h,y) = \tau_{xy}(h,y) = 0 \qquad -\infty < y < \infty \tag{161}$$

$$\begin{aligned} &v(x',+0) = v(x',-0) \\ &u(x',+0) = u(x',-0) \qquad x' < a \text{ or } x' > b \text{ and } 0 < x < h \end{aligned} \tag{162}$$

$$\begin{aligned} &v(+0,y) = v(-0,y) \\ &u(+0,y) = u(-0,y) \qquad -\infty < y < \infty \end{aligned} \tag{163}$$

$$\sigma_{y'}(x',0) = p_1(x')$$
$$\tau_{x'y'}(x',0) = p_2(x') \qquad a < x' < b \tag{164}$$

where $p_1(x')$ and $p_2(x')$ are known crack surface tractions, which can be determined by solving the elasticity problem for the uncracked strip under the given external loads.

The solution of layer 1 is expressed as the sum of two states of strain as $u_{1'}(x', y')$, $v_{1'}(x', y')$ and $u_1(x, y)$ and $v_1(x, y)$ where the coordinates (x', y') and (x, y) are defined in Fig. 26.

With $\kappa = 3 - 4\nu$ for plane strain and $\kappa = (3-\nu)/(1+\nu)$ for plane stress, Navier's equations for the FGM layer may be expressed as:

$$(\kappa+1)\frac{\partial^2 u_{1'}}{\partial x'^2} + (\kappa-1)\frac{\partial^2 u_{1'}}{\partial y'^2} + 2\frac{\partial^2 v_{1'}}{\partial x'\partial y'} + \beta(\kappa+1)\frac{\partial u_{1'}}{\partial x'} + \gamma(\kappa-1)\left(\frac{\partial u_{1'}}{\partial y'} + \frac{\partial v_{1'}}{\partial x'}\right) + \beta(3-\kappa)\frac{\partial v_{1'}}{\partial y'} = 0$$
$$(\kappa-1)\frac{\partial^2 v_{1'}}{\partial x'^2} + (\kappa+1)\frac{\partial^2 v_{1'}}{\partial y'^2} + 2\frac{\partial^2 u_{1'}}{\partial x'\partial y'} + \gamma(3-\kappa)\frac{\partial u_{1'}}{\partial x'} + \beta(\kappa-1)\left(\frac{\partial u_{1'}}{\partial y'} + \frac{\partial v_{1'}}{\partial x'}\right) + \gamma(\kappa+1)\frac{\partial v_{1'}}{\partial y'} = 0 \tag{165}$$

Assuming, $u_{1'}(x', y')$ and $v_{1'}(x', y')$ as:

$$u_{1'}(x', y') = \frac{1}{2\pi}\int_{-\infty}^{\infty} U(y', \alpha)e^{-i\alpha x'}d\alpha$$
$$v_{1'}(x', y') = \frac{1}{2\pi}\int_{-\infty}^{\infty} V(y', \alpha)e^{-i\alpha x'}d\alpha \tag{166}$$

and repeating the procedure outlined in the previous chapter, we get:

$$U(y',\alpha)=\sum_{j=1}^{4} m_j F_j(\alpha) e^{n_j y'} \qquad V(y',\alpha)=\sum_{j=1}^{4} F_j(\alpha) e^{n_j y'} \tag{167}$$

where $F_j(\alpha)$ are unknown functions and m_j $(j=1,...,4)$ are given by

$$m_j=\frac{[2\alpha i+\beta(\kappa-3)]n_j+i\alpha\gamma(\kappa-1)}{(\kappa-1)n_j^{\,2}+(\kappa-1)\gamma n_j-(\kappa+1)(\alpha+i\beta)\alpha} \qquad j=1,...,4 \tag{168}$$

while n_j $(j=1,...,4)$ are the roots of

$$[n^2+\gamma n-\alpha(a+i\beta)]^2+\frac{3-\kappa}{\kappa+1}(\alpha\gamma-i\beta n)^2=0 \tag{169}$$

The value of n_j are:

$$\begin{aligned}
n_1&=-\frac{\Delta_1}{2}-\frac{\sqrt{\Delta_1^{\,2}+4(\alpha^2+i\alpha\Delta_2)}}{2} & n_2&=-\frac{\Delta_3}{2}-\frac{\sqrt{\Delta_3^{\,2}+4(\alpha^2+i\alpha\Delta_4)}}{2}\\
n_3&=-\frac{\Delta_1}{2}+\frac{\sqrt{\Delta_1^{\,2}+4(\alpha^2+i\alpha\Delta_2)}}{2} & n_4&=-\frac{\Delta_3}{2}+\frac{\sqrt{\Delta_3^{\,2}+4(\alpha^2+i\alpha\Delta_4)}}{2}\\
\Delta_1&=\gamma+\beta\sqrt{\frac{3-\kappa}{\kappa+1}} & \Delta_3&=\gamma-\beta\sqrt{\frac{3-\kappa}{\kappa+1}}\\
\Delta_2&=\beta-\gamma\sqrt{\frac{3-\kappa}{\kappa+1}} & \Delta_4&=\beta+\gamma\sqrt{\frac{3-\kappa}{\kappa+1}}
\end{aligned} \tag{170}$$

Since u and v must vanish for $x^2+y^2\to\infty$, we have:

$$\begin{aligned}
F_3(\alpha)=F_4(\alpha)&=0, \qquad y>0\\
F_1(\alpha)=F_2(\alpha)&=0, \qquad y<0
\end{aligned} \tag{171}$$

Using generalized Hooke's Law, we obtain:

$$\sigma_{x1'}(x',y') = \frac{\mu}{2\pi(\kappa-1)}\int_{-\infty}^{\infty}\sum_{j=l}^{l+1}[-i\alpha m_j(1+\kappa)+n_j(3-\kappa)]F_j(\alpha)e^{n_j y'-i\alpha x'}d\alpha$$
$$\sigma_{y1'}(x',y') = \frac{\mu}{2\pi(\kappa-1)}\int_{-\infty}^{\infty}\sum_{j=l}^{l+1}[-i\alpha m_j(3-\kappa)+n_j(1+\kappa)]F_j(\alpha)e^{n_j y'-i\alpha x'}d\alpha \qquad (172)$$
$$\tau_{x1'y1'}(x',y') = \frac{\mu}{2\pi}\int_{-\infty}^{\infty}\sum_{j=l}^{l+1}[n_j m_j - i\alpha]F_j(\alpha)e^{n_j y'-i\alpha x'}d\alpha$$

where $l=1$ for $y>0$ and $l=3$ for $y<0$.

From the continuity conditions (159) and equations (172), we find:

$$F_3(\alpha) = R_1(\alpha)F_1(\alpha)+R_2(\alpha)F_2(\alpha), \quad F_4(\alpha) = R_3(\alpha)F_1(\alpha)+R_4(\alpha)F_2(\alpha) \qquad (173)$$

The functions of $R_j(\alpha)$ are given by

$$\begin{aligned}
R_1(\alpha) &= \{(m_4-m_1)[(1+\kappa)n_1n_4+(3-\kappa)\alpha^2]+i\alpha(n_4-n_1)[1+\kappa-(3-\kappa)m_1m_4]\}/R_0\\
R_2(\alpha) &= \{(m_4-m_2)[(1+\kappa)n_2n_4+(3-\kappa)\alpha^2]+i\alpha(n_4-n_2)[1+\kappa-(3-\kappa)m_2m_4]\}/R_0\\
R_3(\alpha) &= -\{(m_3-m_1)[(1+\kappa)n_1n_3+(3-\kappa)\alpha^2]+i\alpha(n_3-n_1)[1+\kappa-(3-\kappa)m_1m_3]\}/R_0\\
R_4(\alpha) &= -\{(m_3-m_1)[(1+\kappa)n_1n_3+(3-\kappa)\alpha^2]+i\alpha(n_3-n_1)[1+\kappa-(3-\kappa)m_1m_3]\}/R_0\\
R_0(\alpha) &= (m_4-m_3)[(1+\kappa)n_3n_4+(3-\kappa)\alpha^2]+i\alpha(n_4-n_3)[1+\kappa-(3-\kappa)m_3m_4]
\end{aligned} \qquad (174)$$

We then introduce the following new unknown functions:

$$\begin{aligned}
g_1(x') &= \frac{\partial}{\partial x'}[u_{1'}(x',+0)-u_{1'}(x',-0)],\ a<|x'|<b\\
g_2(x') &= \frac{\partial}{\partial x'}[v_{1'}(x',+0)-v_{1'}(x',-0)],\ a<|x'|<b
\end{aligned} \qquad (175)$$

We can then express $F_j(j=1,...,4)$ as:

$$
\begin{aligned}
F_1 &= \int_{-\infty}^{\infty} \frac{[\alpha(3-\kappa)f_{22} + i(1+\kappa)f_{32}]g_1 + (if_{12} + \alpha f_{42})(1+\kappa)g_2}{(1+\kappa)\alpha\omega_0} e^{i\alpha t} dt \\
F_2 &= -\int_{-\infty}^{\infty} \frac{[\alpha(3-\kappa)f_{21} + i(1+\kappa)f_{31}]g_1 + (if_{11} + \alpha f_{41})(1+\kappa)g_2}{(1+\kappa)\alpha\omega_0} e^{i\alpha t} dt \\
F_3 &= \int_{-\infty}^{\infty} \frac{[\alpha(3-\kappa)f_{24} + i(1+\kappa)f_{34}]g_1 + (if_{14} + \alpha f_{44})(1+\kappa)g_2}{(1+\kappa)\alpha\omega_0} e^{i\alpha t} dt \\
F_4 &= -\int_{-\infty}^{\infty} \frac{[\alpha(3-\kappa)f_{23} + i(1+\kappa)f_{33}]g_1 + (if_{13} + \alpha f_{43})(1+\kappa)g_2}{(1+\kappa)\alpha\omega_0} e^{i\alpha t} dt
\end{aligned}
\tag{176}
$$

where

$$
\begin{aligned}
f_{1j} &= n_3 m_4 m_j (n_4 - n_j) + n_4 m_3 m_j (n_j - n_3) + n_j m_3 m_4 (n_3 - n_4) \\
f_{2j} &= m_4 m_j (n_4 - n_j) + m_3 m_j (n_j - n_3) + m_3 m_4 (n_3 - n_4) \\
f_{3j} &= n_3 m_3 (n_4 - n_j) + n_4 m_4 (n_j - n_3) + n_j m_j (n_3 - n_4) \\
f_{4j} &= m_3 (n_4 - n_j) + m_4 (n_j - n_3) + m_j (n_3 - n_4) \qquad j = 1,2
\end{aligned}
\tag{177}
$$

$$
\begin{aligned}
f_{1j} &= -[n_1 m_2 m_j (n_2 - n_j) + n_2 m_1 m_j (n_j - n_1) + n_j m_1 m_2 (n_1 - n_2)] \\
f_{2j} &= -[m_2 m_j (n_2 - n_j) + m_1 m_j (n_j - n_1) + m_1 m_2 (n_1 - n_2)] \\
f_{3j} &= -[n_1 m_1 (n_2 - n_j) + n_2 m_2 (n_j - n_1) + n_j m_j (n_1 - n_2)] \\
f_{4j} &= -[m_1 (n_2 - n_j) + m_2 (n_j - n_1) + m_j (n_1 - n_2)] \qquad j = 3,4
\end{aligned}
\tag{178}
$$

and

$$
\begin{aligned}
\omega_0 &= (m_1 - m_2)(m_3 - m_4)(n_1 n_2 + n_3 n_4) + (m_1 - m_4)(m_2 - m_3)(n_2 n_3 + n_1 n_4) \\
&- (m_1 - m_3)(m_2 - m_4)(n_1 n_3 + n_2 n_4)
\end{aligned}
\tag{179}
$$

Substituting them back into equation (172), we can express $\sigma_{x'}$, $\sigma_{y'}$ and $\tau_{x'y'}$ in terms of g_1 and g_2, for $y' > 0$, as:

$$\sigma_{x'}^{(1)}(x',y') = \frac{\mu(x',y')}{2\pi(1+\kappa)} \int_0^b \sum_{j=1}^{2} h_{1j}^{(1)}(x',y',t) g_j(t) dt$$

$$\sigma_{y'}^{(1)}(x',y') = \frac{\mu(x',y')}{2\pi(1+\kappa)} \int_0^b \sum_{j=1}^{2} h_{2j}^{(1)}(x',y',t) g_j(t) dt \qquad (180)$$

$$\tau_{x'y'}^{(1)}(x',y') = \frac{\mu(x',y')}{2\pi(1+\kappa)} \int_0^b \sum_{j=1}^{2} h_{3j}^{(1)}(x',y',t) g_j(t) dt$$

where

$$h_{kj}^{(1)}(x',y',t) = \int_{-\infty}^{\infty} K_{kj}^{(1)}(y',\alpha) e^{i\alpha(t-x')} d\alpha, \qquad k = 1,2; \qquad j = 1,2,$$

$$K_{11}^{(1)}(y',\alpha) = -\frac{i\alpha m_1(1+\kappa) - n_1(3-\kappa)}{\alpha\omega_0(\kappa-1)} [\alpha(3-\kappa) f_{22} + i(1+\kappa) f_{32}] e^{n_1 y'}$$
$$+ \frac{i\alpha m_2(1+\kappa) - n_2(3-\kappa)}{\alpha\omega_0(\kappa-1)} [\alpha(3-\kappa) f_{21} + i(1+\kappa) f_{31}] e^{n_2 y'}$$

$$K_{12}^{(1)}(y',\alpha) = -\frac{i\alpha m_1(1+\kappa) - n_1(3-\kappa)}{\alpha\omega_0(\kappa-1)} (if_{12} + \alpha f_{42})(1+\kappa) e^{n_1 y'}$$
$$+ \frac{i\alpha m_2(1+\kappa) - n_2(3-\kappa)}{\alpha\omega_0(\kappa-1)} (if_{11} + \alpha f_{41})(1+\kappa) e^{n_2 y'}$$

$$K_{21}^{(1)}(y',\alpha) = \frac{i\alpha m_1(\kappa-3) + n_1(1+\kappa)}{\alpha\omega_0(\kappa-1)} [\alpha(3-\kappa) f_{22} + i(1+\kappa) f_{32}] e^{n_1 y'}$$
$$- \frac{i\alpha m_2(\kappa-3) + n_2(1+\kappa)}{\alpha\omega_0(\kappa-1)} [\alpha(3-\kappa) f_{21} + i(1+\kappa) f_{31}] e^{n_2 y'} \qquad (181)$$

$$K_{22}^{(1)}(y',\alpha) = \frac{i\alpha m_1(\kappa-3) + n_1(1+\kappa)}{\alpha\omega_0(\kappa-1)} (if_{12} + \alpha f_{42})(1+\kappa) e^{n_1 y'}$$
$$- \frac{i\alpha m_2(\kappa-3) + n_2(1+\kappa)}{\alpha\omega_0(\kappa-1)} (if_{11} + \alpha f_{41})(1+\kappa) e^{n_2 y'}$$

$$K_{31}^{(1)}(y',\alpha)=\frac{(n_1m_1-i\alpha)}{\alpha\omega_0}[\alpha(3-\kappa)f_{22}+i(1+\kappa)f_{32}]e^{n_1y'}$$
$$-\frac{(n_2m_2-i\alpha)}{\alpha\omega_0}[\alpha(3-\kappa)f_{21}+i(1+\kappa)f_{31}]e^{n_2y'}$$
$$K_{32}^{(1)}(y',\alpha)=\frac{(n_1m_1-i\alpha)}{\alpha\omega_0}(if_{12}+\alpha f_{42})(1+\kappa)e^{n_1y'}$$
$$-\frac{(n_2m_2-i\alpha)}{\alpha\omega_0}(if_{11}+\alpha f_{41})(1+\kappa)e^{n_2y'}$$

Similarly, we obtain equations (182) for $\sigma_{x'}$, $\sigma_{y'}$ and $\tau_{x'y'}$ when $y'<0$, as:

$$\sigma_{x'}^{(2)}(x',y')=\frac{\mu(x',y')}{2\pi(1+\kappa)}\int_0^{\phi}\sum_{j=1}^{2}h_{1j}^{(2)}(x',y',t)g_j(t)dt$$
$$\sigma_{y'}^{(2)}(x',y')=\frac{\mu(x',y')}{2\pi(1+\kappa)}\int_0^{\phi}\sum_{j=1}^{2}h_{2j}^{(2)}(x',y',t)g_j(t)dt \qquad (182)$$
$$\tau_{x'y'}^{(2)}(x',y')=\frac{\mu(x',y')}{2\pi(1+\kappa)}\int_0^{\phi}\sum_{j=1}^{2}h_{3j}^{(2)}(x',y',t)g_j(t)dt$$

where

$$h_{kj}^{(2)}(x',y',t)=\int_{-\infty}^{\infty}K_{kj}^{(2)}(y',\alpha)e^{i\alpha(t-x')}d\alpha,\qquad k=1,2;\qquad j=1,2,$$

$$K_{11}^{(2)}(y',\alpha)=-\frac{i\alpha m_3(1+\kappa)-n_3(3-\kappa)}{\alpha\omega_0(\kappa-1)}[\alpha(3-\kappa)f_{24}+i(1+\kappa)f_{34}]e^{n_3y'}$$
$$+\frac{i\alpha m_4(1+\kappa)-n_4(3-\kappa)}{\alpha\omega_0(\kappa-1)}[\alpha(3-\kappa)f_{23}+i(1+\kappa)f_{33}]e^{n_4y'}$$
$$K_{12}^{(2)}(y',\alpha)=-\frac{i\alpha m_3(1+\kappa)-n_3(3-\kappa)}{\alpha\omega_0(\kappa-1)}(if_{14}+\alpha f_{44})(1+\kappa)e^{n_3y'}$$
$$+\frac{i\alpha m_4(1+\kappa)-n_4(3-\kappa)}{\alpha\omega_0(\kappa-1)}(if_{13}+\alpha f_{43})(1+\kappa)e^{n_4y'}$$

$$K_{21}^{(2)}(y',\alpha)=\frac{i\alpha m_3(\kappa-3)+n_3(1+\kappa)}{\alpha\omega_0(\kappa-1)}[\alpha(3-\kappa)f_{24}+i(1+\kappa)f_{34}]e^{n_3y'}$$
$$-\frac{i\alpha m_4(\kappa-3)+n_4(1+\kappa)}{\alpha\omega_0(\kappa-1)}[\alpha(3-\kappa)f_{23}+i(1+\kappa)f_{33}]e^{n_4y'}$$
$$K_{22}^{(2)}(y',\alpha)=\frac{i\alpha m_3(\kappa-3)+n_3(1+\kappa)}{\alpha\omega_0(\kappa-1)}(if_{14}+\alpha f_{44})(1+\kappa)e^{n_3y'} \quad (183)$$
$$-\frac{i\alpha m_4(\kappa-3)+n_4(1+\kappa)}{\alpha\omega_0(\kappa-1)}(if_{13}+\alpha f_{43})(1+\kappa)e^{n_4y'}$$

$$K_{31}^{(2)}(y',\alpha)=\frac{(n_3m_3-i\alpha)}{\alpha\omega_0}[\alpha(3-\kappa)f_{24}+i(1+\kappa)f_{34}]e^{n_3y'}$$
$$-\frac{(n_4m_4-i\alpha)}{\alpha\omega_0}[\alpha(3-\kappa)f_{23}+i(1+\kappa)f_{33}]e^{n_4y'}$$
$$K_{32}^{(2)}(y',\alpha)=\frac{(n_3m_3-i\alpha)}{\alpha\omega_0}(if_{14}+\alpha f_{44})(1+\kappa)e^{n_3y'}$$
$$-\frac{(n_4m_4-i\alpha)}{\alpha\omega_0}(if_{13}+\alpha f_{43})(1+\kappa)e^{n_4y'}$$

For the coordinate system of (x,y), the Navier's equations for layer 1 may be expressed as:

$$(\kappa+1)\frac{\partial^2u_1}{\partial x^2}+(\kappa-1)\frac{\partial^2u_1}{\partial y^2}+2\frac{\partial^2v_1}{\partial x\partial y}+\delta(\kappa+1)\frac{\partial u_1}{\partial x}+\delta(3-\kappa)\frac{\partial v_1}{\partial y}=0$$
$$(\kappa-1)\frac{\partial^2v_1}{\partial x^2}+(\kappa+1)\frac{\partial^2v_1}{\partial y^2}+2\frac{\partial^2u_1}{\partial x\partial y}+\delta(\kappa-1)(\frac{\partial v_1}{\partial x}+\frac{\partial u_1}{\partial y})=0 \quad (184)$$

Assuming,

$$u_1(x,y)=\frac{1}{2\pi}\int_{-\infty}^{\infty}qA(\alpha)e^{px}e^{-i\alpha y}d\alpha$$
$$v_1(x,y)=\frac{1}{2\pi}\int_{-\infty}^{\infty}A(\alpha)e^{px}e^{-i\alpha y}d\alpha \quad (185)$$

after some manipulation, we can find p_j and q_j as:

$$
\begin{aligned}
p_1 &= -\frac{\delta}{2} - \frac{1}{2}\sqrt{\delta^2 + 4\alpha^2 + 4i\omega\alpha} \\
p_2 &= -\frac{\delta}{2} - \frac{1}{2}\sqrt{\delta^2 + 4\alpha^2 - 4i\omega\alpha} \\
p_3 &= -\frac{\delta}{2} + \frac{1}{2}\sqrt{\delta^2 + 4\alpha^2 + 4i\omega\alpha} \\
p_4 &= -\frac{\delta}{2} + \frac{1}{2}\sqrt{\delta^2 + 4\alpha^2 - 4i\omega\alpha}
\end{aligned} \tag{186}
$$

$$
q_j = \frac{(\kappa-1)(p_j+\delta)p_j - (\kappa+1)\alpha^2}{\alpha i[2p_j + \delta(\kappa-1)]}, \quad j = 1..4 \tag{187}
$$

Thus we have:

$$
\begin{aligned}
u_1(x,y) &= \frac{1}{2\pi}\int_{-\infty}^{\infty}\sum_j^4 q_j A_j(\alpha) e^{p_j x} e^{-i\alpha y} d\alpha \\
v_1(x,y) &= \frac{1}{2\pi}\int_{-\infty}^{\infty}\sum_j^4 A_j(\alpha) e^{p_j x} e^{-i\alpha y} d\alpha
\end{aligned} \tag{188}
$$

$$
\begin{aligned}
\sigma_x^{(3)} &= \frac{\mu(x,y)}{2\pi(\kappa-1)}\int_{-\infty}^{\infty}\sum_j^4 [(1+k)p_j q_j + (\kappa-3)i\alpha] A_j(\alpha) e^{p_j x - i\alpha y} d\alpha \\
\sigma_y^{(3)} &= \frac{\mu(x,y)}{2\pi(\kappa-1)}\int_{-\infty}^{\infty}\sum_j^4 [-(1+k)i\alpha + (3-\kappa)p_j q_j] A_j(\alpha) e^{p_j x - i\alpha y} d\alpha \\
\tau_{xy}^{(3)} &= \frac{\mu(x,y)}{2\pi}\int_{-\infty}^{\infty}\sum_j^4 [p_j - i\alpha q_j] A_j(\alpha) e^{p_j x - i\alpha y} d\alpha
\end{aligned} \tag{189}
$$

4.2 The Integral Equations

At a given point in layer 1 shown in Fig. 26, the stress state can be expressed as the sum of the stresses given by equations (189) and equations (180) or (182), depending on the sign of y' at that point.

From the free boundary conditions (161) of the problem at $x = h$, we have:

$$\sum_{j}^{4}[(1+k)p_j q_j + (\kappa-3)i\alpha]A_j(\alpha)e^{p_j h} = \frac{1-\kappa}{2\pi(1+\kappa)}\sum_{j=1}^{2}\int_{b} Q_{1j}(\alpha,t)g_j(t)dt \tag{190}$$

where

$$Q_{1j}(\alpha,t) = \sum_{i=1}^{2}\{\xi_{1j}^{(i)}(\alpha,t)\cos^2\theta + \xi_{2j}^{(i)}(\alpha,t)\sin^2\theta - 2\xi_{3j}^{(i)}(\alpha,t)\cos\theta\sin\theta\} \tag{191}$$

$$\begin{aligned}\xi_{kj}^{(1)}(\alpha,t) &= \int_{-\infty}^{\infty}\int_{h\tan\theta}^{\infty} K_{kj}^{(1)}(y\cos\theta - h\sin\theta,\rho)e^{i\rho(t - y\sin\theta - h\cos\theta) + i\alpha y}\,dyd\rho \\ \xi_{kj}^{(2)}(\alpha,t) &= \int_{-\infty}^{\infty}\int_{-\infty}^{h\tan\theta} K_{kj}^{(2)}(y\cos\theta - h\sin\theta,\rho)e^{i\rho(t - y\sin\theta - h\cos\theta) + i\alpha y}\,dyd\rho\end{aligned} \tag{192}$$

and

$$\sum_{j}^{4}[p_j - i\alpha q_j]A_j(\alpha)e^{p_j h} = \frac{-1}{2\pi(1+\kappa)}\sum_{j=1}^{2}\int_{b} Q_{2j}(\alpha,t)g_j(t)dt \tag{193}$$

where

$$Q_{2j}(\alpha,t) = \sum_{i=1}^{2}\{(\cos^2\theta - \sin^2\theta)\xi_{3j}^{(i)}(\alpha,t) - [\xi_{2j}^{(i)}(\alpha,t) - \xi_{1j}^{(i)}(\alpha,t)]\sin\theta\cos\theta\} \tag{194}$$

For layer 2, the Navier's equations for the elastic medium may be expressed as:

$$\begin{aligned}(\kappa+1)\frac{\partial^2 u_2}{\partial x^2} + (\kappa-1)\frac{\partial^2 u_2}{\partial y^2} + 2\frac{\partial^2 v_2}{\partial x\partial y} &= 0 \\ (\kappa-1)\frac{\partial^2 v_2}{\partial x^2} + (\kappa+1)\frac{\partial^2 v_2}{\partial y^2} + 2\frac{\partial^2 u_2}{\partial x\partial y} &= 0\end{aligned} \tag{195}$$

expressing the solution of $u_2(x,y)$ and $v_2(x,y)$ for $y<0$ as:

$$u_2(x,y)=\frac{1}{2\pi}\int_{-\infty}^{\infty}H_1(x,\alpha)e^{-i\alpha y}d\alpha$$
$$v_2(x,y)=\frac{1}{2\pi}\int_{-\infty}^{\infty}H_2(x,\alpha)e^{-i\alpha y}d\alpha \tag{196}$$

after some manipulation, we get:

$$u_2(x,y)=\frac{i}{2\pi}\int_{-\infty}^{\infty}\frac{\alpha}{|\alpha|}[G_1(\alpha)+(x-\frac{\kappa}{|\alpha|})G_2(\alpha)]e^{|\alpha|x-i\alpha y}d\alpha$$
$$v_2(x,y)=\frac{1}{2\pi}\int_{-\infty}^{\infty}(G_1(\alpha)+xG_2(\alpha)e^{|\alpha|x-i\alpha y}d\alpha \tag{197}$$

From generalized Hooke's law, we obtain the stresses for layer 2 as:

$$\sigma_{2x}=\frac{\mu_1 i}{2\pi}\int_{-\infty}^{\infty}[2\alpha(G_1+xG_2)-\frac{\alpha}{|\alpha|}(1+\kappa)G_2]e^{|\alpha|x-i\alpha y}d\alpha$$
$$\sigma_{2y}=-\frac{\mu_1 i}{2\pi}\int_{-\infty}^{\infty}[2\alpha(G_1+xG_2)+\frac{\alpha}{|\alpha|}(3-\kappa)G_2]e^{|\alpha|x-i\alpha y}d\alpha \tag{198}$$
$$\tau_{2xy}=\frac{\mu_1}{2\pi}\int_{-\infty}^{\infty}[2|\alpha|(G_1+xG_2)+(1-\kappa)G_2]e^{|\alpha|x-i\alpha y}d\alpha$$

From the continuity conditions (160) and (163), we get following relations:

$$\sum_j^4[(1+k)p_jq_j+(\kappa-3)i\alpha]A_j(\alpha)-i[2\alpha G_1-\frac{\alpha}{|\alpha|}(1+\kappa)G_2](\kappa-1)$$
$$=\frac{1-\kappa}{2\pi(1+\kappa)}\sum_{j=1}^{2}\int_b Q_{3j}(\alpha,t)g_j(t)dt \tag{199}$$

where

$$Q_{31}(\alpha,t)$$
$$= -\int_{-\infty}^{\infty} \frac{-i\rho m_1[(1+\kappa)\cos^2\theta + (3-\kappa)\sin^2\theta] + n_1[(3-\kappa)\cos^2\theta + (1+\kappa)\sin^2\theta] - 2(n_1 m_1 - i\rho)(\kappa-1)\cos\theta\sin\theta}{\rho\omega_0(\kappa-1)(n_1\cos\theta - i\rho\sin\theta + i\alpha)}$$
$$[\rho(3-\kappa)f_{22} + i(1+\kappa)f_{32}]e^{i\rho t}d\rho$$
$$+ \int_{-\infty}^{\infty} \frac{-i\rho m_2[(1+\kappa)\cos^2\theta + (3-\kappa)\sin^2\theta] + n_2[(3-\kappa)\cos^2\theta + (1+\kappa)\sin^2\theta] - 2(n_2 m_2 - i\rho)(\kappa-1)\cos\theta\sin\theta}{\rho\omega_0(\kappa-1)(n_2\cos\theta - i\rho\sin\theta + i\alpha)}$$
$$[\rho(3-\kappa)f_{21} + i(1+\kappa)f_{31}]e^{i\rho t}d\rho$$
$$+ \int_{-\infty}^{\infty} \frac{-i\rho m_3[(1+\kappa)\cos^2\theta + (3-\kappa)\sin^2\theta] + n_3[(3-\kappa)\cos^2\theta + (1+\kappa)\sin^2\theta] - 2(n_3 m_3 - i\rho)(\kappa-1)\cos\theta\sin\theta}{\rho\omega_0(\kappa-1)(n_3\cos\theta - i\rho\sin\theta + i\alpha)}$$
$$[\rho(3-\kappa)f_{24} + i(1+\kappa)f_{34}]e^{i\rho t}d\rho$$
$$- \int_{-\infty}^{\infty} \frac{-i\rho m_4[(1+\kappa)\cos^2\theta + (3-\kappa)\sin^2\theta] + n_4[(3-\kappa)\cos^2\theta + (1+\kappa)\sin^2\theta] - 2(n_4 m_4 - i\rho)(\kappa-1)\cos\theta\sin\theta}{\rho\omega_0(\kappa-1)(n_4\cos\theta - i\rho\sin\theta + i\alpha)}$$
$$[\rho(3-\kappa)f_{23} + i(1+\kappa)f_{33}]e^{i\rho t}d\rho \qquad (200)$$

$$Q_{32}(\alpha,t)$$
$$= -\int_{-\infty}^{\infty} \frac{-i\rho m_1[(1+\kappa)\cos^2\theta + (3-\kappa)\sin^2\theta] + n_1[(3-\kappa)\cos^2\theta + (1+\kappa)\sin^2\theta] - 2(n_1 m_1 - i\rho)(\kappa-1)\cos\theta\sin\theta}{\rho\omega_0(\kappa-1)(n_1\cos\theta - i\rho\sin\theta + i\alpha)}$$
$$(if_{12} + \rho f_{42})(1+\kappa)e^{i\rho t}d\rho$$
$$+ \int_{-\infty}^{\infty} \frac{-i\rho m_2[(1+\kappa)\cos^2\theta + (3-\kappa)\sin^2\theta] + n_2[(3-\kappa)\cos^2\theta + (1+\kappa)\sin^2\theta] - 2(n_2 m_2 - i\rho)(\kappa-1)\cos\theta\sin\theta}{\rho\omega_0(\kappa-1)(n_2\cos\theta - i\rho\sin\theta + i\alpha)}$$
$$(if_{11} + \rho f_{41})(1+\kappa)e^{i\rho t}d\rho$$
$$+ \int_{-\infty}^{\infty} \frac{-i\rho m_3[(1+\kappa)\cos^2\theta + (3-\kappa)\sin^2\theta] + n_3[(3-\kappa)\cos^2\theta + (1+\kappa)\sin^2\theta] - 2(n_3 m_3 - i\rho)(\kappa-1)\cos\theta\sin\theta}{\rho\omega_0(\kappa-1)(n_3\cos\theta - i\rho\sin\theta + i\alpha)}$$
$$(if_{14} + \rho f_{44})(1+\kappa)e^{i\rho t}d\rho$$
$$- \int_{-\infty}^{\infty} \frac{-i\rho m_4[(1+\kappa)\cos^2\theta + (3-\kappa)\sin^2\theta] + n_4[(3-\kappa)\cos^2\theta + (1+\kappa)\sin^2\theta] - 2(n_4 m_4 - i\rho)(\kappa-1)\cos\theta\sin\theta}{\rho\omega_0(\kappa-1)(n_4\cos\theta - i\rho\sin\theta + i\alpha)}$$
$$(if_{13} + \rho f_{43})(1+\kappa)e^{i\rho t}d\rho \qquad (201)$$

$$\sum_{j}^{4}[p_j - i\alpha q_j]A_j(\alpha) - [2|\alpha|G_1 + (1-\kappa)G_2] = \frac{-1}{2\pi(1+\kappa)}\sum_{j=1}^{2}\int_0^b Q_{4j}g_j(t)dt \qquad (202)$$

where:

$$
\begin{aligned}
Q_{41} &= -\int_{-\infty}^{\infty} \frac{-\sin 2\theta(i\rho m_1 + n_1) + (n_1 m_1 - i\rho)\cos 2\theta}{\rho\omega_0(n_1\cos\theta - i\rho\sin\theta + i\alpha)}[\rho(3-\kappa)f_{22} + i(1+\kappa)f_{32}]e^{i\rho t}d\rho \\
&+ \int_{-\infty}^{\infty} \frac{-\sin 2\theta(i\rho m_2 + n_2) + (n_2 m_2 - i\rho)\cos 2\theta}{\rho\omega_0(n_2\cos\theta - i\rho\sin\theta + i\alpha)}[\rho(3-\kappa)f_{21} + i(1+\kappa)f_{31}]e^{i\rho t}d\rho \\
&+ \int_{-\infty}^{\infty} \frac{-\sin 2\theta(i\rho m_3 + n_3) + (n_3 m_3 - i\rho)\cos 2\theta}{\rho\omega_0(n_3\cos\theta - i\rho\sin\theta + i\alpha)}[\rho(3-\kappa)f_{24} + i(1+\kappa)f_{34}]e^{i\rho t}d\rho \\
&- \int_{-\infty}^{\infty} \frac{-\sin 2\theta(i\rho m_4 + n_4) + (n_4 m_4 - i\rho)\cos 2\theta}{\rho\omega_0(n_4\cos\theta - i\rho\sin\theta + i\alpha)}[\rho(3-\kappa)f_{23} + i(1+\kappa)f_{33}]e^{i\rho t}d\rho
\end{aligned} \tag{203}
$$

$$
\begin{aligned}
Q_{42} &= -\int_{-\infty}^{\infty} \frac{-\sin 2\theta(i\rho m_1 + n_1) + (n_1 m_1 - i\rho)\cos 2\theta}{\rho\omega_0(n_1\cos\theta - i\rho\sin\theta + i\alpha)}(if_{12} + \rho f_{42})(1+\kappa)e^{i\rho t}d\rho \\
&+ \int_{-\infty}^{\infty} \frac{-\sin 2\theta(i\rho m_2 + n_2) + (n_2 m_2 - i\rho)\cos 2\theta}{\rho\omega_0(n_2\cos\theta - i\rho\sin\theta + i\alpha)}(if_{11} + \rho f_{41})(1+\kappa)e^{i\rho t}d\rho \\
&\int_{-\infty}^{\infty} \frac{-\sin 2\theta(i\rho m_3 + n_3) + (n_3 m_3 - i\rho)\cos 2\theta}{\rho\omega_0(n_3\cos\theta - i\rho\sin\theta + i\alpha)}(if_{14} + \rho f_{44})(1+\kappa)e^{i\rho t}d\rho \\
&- \int_{-\infty}^{\infty} \frac{-\sin 2\theta(i\rho m_4 + n_4) + (n_4 m_4 - i\rho)\cos 2\theta}{\rho\omega_0(n_4\cos\theta - i\rho\sin\theta + i\alpha)}(if_{13} + \rho f_{43})(1+\kappa)e^{i\rho t}d\rho
\end{aligned} \tag{204}
$$

and:

$$
\sum_{j}^{4} q_j A_j(\alpha) - \frac{\alpha i}{|\alpha|}[G_1(\alpha) - \frac{\kappa}{|\alpha|}G_2(\alpha)] = \sum_{j=1}^{2}\int_0^{\phi} Q_{5j}(\alpha,t)g_j(t)dt \tag{205}
$$

where

$$
\begin{aligned}
Q_{51}(\alpha,t) &= \frac{1}{2\pi(1+\kappa)}\int_{-\infty}^{\infty}\{-\frac{(\sin\theta - m_1\cos\theta)[\rho(3-\kappa)f_{22} + i(1+\kappa)f_{32}]}{(n_1\cos\theta - i\rho\sin\theta + i\alpha)\rho\omega_0} \\
&+ \frac{(\sin\theta - m_2\cos\theta)[\rho(3-\kappa)f_{21} + i(1+\kappa)f_{31}]}{(n_2\cos\theta - i\rho\sin\theta + i\alpha)\rho\omega_0} \\
&+ \frac{(\sin\theta - m_3\cos\theta)[\rho(3-\kappa)f_{24} + i(1+\kappa)f_{34}]}{(n_3\cos\theta - i\rho\sin\theta + i\alpha)\rho\omega_0} \\
&- \frac{(\sin\theta - m_4\cos\theta)[\rho(3-\kappa)f_{23} + i(1+\kappa)f_{33}]}{(n_4\cos\theta - i\rho\sin\theta + i\alpha)\rho\omega_0}\}e^{i\rho t}d\rho
\end{aligned} \tag{206}
$$

$$Q_{52}(\alpha,t)=\frac{1}{2\pi(1+\kappa)}\int_{-\infty}^{\infty}\{-\frac{(\sin\theta-m_1\cos\theta)(if_{12}+\rho f_{42})(1+\kappa)}{(n_1\cos\theta-i\rho\sin\theta+i\alpha)\rho\omega_0}$$
$$+\frac{(\sin\theta-m_2\cos\theta)(if_{11}+\rho f_{41})(1+\kappa)}{(n_2\cos\theta-i\rho\sin\theta+i\alpha)\rho\omega_0}$$
$$+\frac{(\sin\theta-m_3\cos\theta)(if_{14}+\rho f_{44})(1+\kappa)}{(n_3\cos\theta-i\rho\sin\theta+i\alpha)\rho\omega_0} \quad (207)$$
$$-\frac{(\sin\theta-m_4\cos\theta)(if_{13}+\rho f_{43})(1+\kappa)}{(n_4\cos\theta-i\rho\sin\theta+i\alpha)\rho\omega_0}\}e^{i\rho t}d\rho$$

and:

$$\sum_{j}^{4}A_j(\alpha)e^{-i\alpha y}-G_1(\alpha)=\sum_{j=1}^{2}\int_0^b Q_{6j}(\alpha,t)g_j(t)dt \quad (208)$$

where

$$Q_{61}(\alpha,t)=\frac{1}{2\pi(1+\kappa)}\int_{-\infty}^{\infty}\{-\frac{(m_1\sin\theta+\cos\theta)[\rho(3-\kappa)f_{22}+i(1+\kappa)f_{32}]}{(n_1\cos\theta-i\rho\sin\theta+i\alpha)\rho\omega_0}$$
$$+\frac{(m_2\sin\theta+\cos\theta)[\rho(3-\kappa)f_{21}+i(1+\kappa)f_{31}]}{(n_2\cos\theta-i\rho\sin\theta+i\alpha)\rho\omega_0}$$
$$+\frac{(m_3\sin\theta+\cos\theta)[\rho(3-\kappa)f_{24}+i(1+\kappa)f_{34}]}{(n_3\cos\theta-i\rho\sin\theta+i\alpha)\rho\omega_0} \quad (209)$$
$$-\frac{(m_4\sin\theta+\cos\theta)[\rho(3-\kappa)f_{23}+i(1+\kappa)f_{33}]}{(n_4\cos\theta-i\rho\sin\theta+i\alpha)\rho\omega_0}\}e^{i\rho t}d\rho$$

$$Q_{62}(\alpha,t)=\frac{1}{2\pi(1+\kappa)}\int_{-\infty}^{\infty}\{-\frac{(m_1\sin\theta+\cos\theta)(if_{12}+\rho f_{42})(1+\kappa)}{(n_1\cos\theta-i\rho\sin\theta+i\alpha)\rho\omega_0}$$
$$+\frac{(m_2\sin\theta+\cos\theta)(if_{11}+\rho f_{41})(1+\kappa)}{(n_2\cos\theta-i\rho\sin\theta+i\alpha)\rho\omega_0}$$
$$+\frac{(m3_j\sin\theta+\cos\theta)(if_{14}+\rho f_{44})(1+\kappa)}{(n_3\cos\theta-i\rho\sin\theta+i\alpha)\rho\omega_0} \quad (210)$$
$$-\frac{(m_4\sin\theta+\cos\theta)(if_{13}+\rho f_{43})(1+\kappa)}{(n_4\cos\theta-i\rho\sin\theta+i\alpha)\rho\omega_0}\}e^{i\rho t}d\rho$$

With equations (190), (193), (199), (202), (205) and (208) we have 6 equations for the 6 unknowns A_j $(j=1,\ldots,4)$ and $G_j(j=1,2)$:

$$
\begin{aligned}
&\sum_j^4[(1+k)p_jq_j+(\kappa-3)i\alpha]A_j(\alpha)e^{p_jh}=\frac{1-\kappa}{2\pi(1+\kappa)}\sum_{j=1}^{2}\int_0^b Q_{1j}(\alpha,t)g_j(t)dt\\
&\sum_j^4[p_j-i\alpha q_j]A_j(\alpha)e^{p_jh}=\frac{-1}{2\pi(1+\kappa)}\sum_{j=1}^{2}\int_0^b Q_{2j}(\alpha,t)g_j(t)dt\\
&\sum_j^4[(1+k)p_jq_j+(\kappa-3)i\alpha]A_j(\alpha)-i[2\alpha G_1-\frac{\alpha}{|\alpha|}(1+\kappa)G_2](\kappa-1)\\
&=\frac{1-\kappa}{2\pi(1+\kappa)}\sum_{j=1}^{2}\int_0^b Q_{3j}(\alpha,t)g_j(t)dt\\
&\sum_j^4[p_j-i\alpha q_j]A_j(\alpha)-[2|\alpha|G_1+(1-\kappa)G_2]=\frac{-1}{2\pi(1+\kappa)}\sum_{j=1}^{2}\int_0^b Q_{4j}g_j(t)dt\\
&\sum_j^4 q_jA_j(\alpha)-\frac{\alpha i}{|\alpha|}[G_1(\alpha)-\frac{\kappa}{|\alpha|}G_2(\alpha)]=\sum_{j=1}^{2}\int_0^b Q_{5j}(\alpha,t)g_j(t)dt\\
&\sum_j^4 A_j(\alpha)e^{-i\alpha y}-G_1(\alpha)=\sum_{j=1}^{2}\int_0^b Q_{6j}(\alpha,t)g_j(t)dt
\end{aligned}
\tag{211}
$$

Solving equations (211) we can obtain $A_j(\alpha)$ $(j=1,\ldots,4)$ and $G_1(\alpha), G_2(\alpha)$.

From the boundary conditions

$$
\sigma_{y_1}(x_1,+0)=p_1(x_1),\ \tau_{x_1y_1}(x_1,+0)=p_2(x_1)\qquad (a<x<b)
\tag{212}
$$

where $p_1(x_1)$ and $p_2(x_1)$ are the crack surface tractions, we obtain:

$$
\begin{aligned}
&\sigma_{y_1}{}^{(1)}(x_1,0)+\sin^2\theta\sigma_x{}^{(3)}(x_1\cos\theta,x_1\sin\theta)+\cos^2\theta\sigma_y{}^{(3)}(x_1\cos\theta,x_1\sin\theta)\\
&-2\sin\theta\cos\theta\tau_{xy}{}^{(3)}(x_1\cos\theta,x_1\sin\theta)=p_1(x_1)\\
&\tau_{x_1y_1}{}^{(1)}(x_1,0)+\tau_{xy}{}^{(3)}(x_1\cos\theta,x_1\sin\theta)(\cos^2\theta-\sin^2\theta)\\
&+\sin\theta\cos\theta[\sigma_y{}^{(3)}(x_1\cos\theta,x_1\sin\theta)-\sigma_x{}^{(3)}(x_1\cos\theta,x_1\sin\theta)]=p_2(x_1)
\end{aligned}
\tag{213}
$$

To obtain the asymptotic behavior of the stresses, first we can rewrite the first equation of (213) as:

$$\frac{\mu(x_1,0)}{2\pi(1+\kappa)}\int_b^b \sum_{i=1}^{2} h_{2j}^{(1)}(x_1,t)g_i(t)dt$$
$$+\frac{\mu(x_1\cos\theta,x_1\sin\theta)}{2\pi(\kappa-1)}\int_{-\infty}^{\infty}\sum_{j}^{4}\{[(1+k)p_jq_j+(\kappa-3)i\alpha]\sin^2\theta$$
$$+[-(1+k)i\alpha+(3-\kappa)p_jq_j]\cos^2\theta-2\sin\theta\cos\theta(\kappa-1)[p_j-i\alpha q_j]\}A_j(\alpha)e^{p_jx_1\cos\theta-i\alpha x_1\sin\theta}d\alpha$$
$$=p_1(x_1) \tag{214}$$

Since the asymptotic value of K_{21} and K_{22} for $\alpha\to\infty$ are:

$$K_{21}^{\infty}=0$$
$$K_{22}^{\infty}=-2i\frac{|\alpha|}{\alpha}e^{-|\alpha|y} \tag{215}$$

equation (214) yields,

$$\frac{1}{\pi}\int_b^b\{\frac{g_2(t)}{t-x_1}+\sum_{j=1}^{2}[k_{1j}^{(1)}(x_1,t)+k_{2j}^{(1)}(x_1,t)]g_j(t)\}dt=\frac{(1+\kappa)}{2\mu(x_1,0)}p_1(x_1) \tag{216}$$

where the kernels are

$$k_{11}^{(1)}(x_1,t)=\frac{1}{4}h_{21}^{(1)}(x_1,0,t)$$
$$k_{12}^{(1)}(x_1,t)=\frac{1}{4}\int_{-\infty}^{\infty}[K_{22}^{(1)}(0,\alpha)-\lim_{\alpha\to\infty}K_{22}^{(1)}(0,\alpha)]e^{i\alpha(t-x_1)}d\alpha$$
$$k_{2j}^{(2)}(x_1,t)=\frac{(1+\kappa)}{4(\kappa-1)}\int_{-\infty}^{\infty}\sum_{i}^{4}\{[(1+k)p_iq_i+(\kappa-3)i\alpha]\sin^2\theta \tag{217}$$
$$+[-(1+k)i\alpha+(3-\kappa)p_iq_i]\cos^2\theta$$
$$-2\sin\theta\cos\theta(\kappa-1)[p_i-i\alpha q_i]\}C_{ij}(\alpha,t)e^{p_ix_1\cos\theta-i\alpha x_1\sin\theta}d\alpha$$

Similarly, the second equation of equation (213) becomes:

$$\frac{1}{\pi}\int_a^b \{\frac{g_1(t)}{t-x_1}+\sum_{j=1}^{2}[k_{1j}{}^{(2)}(x_1,t)+k_{2j}{}^{(2)}(x_1,t)]g_j(t)\}dt=\frac{(1+\kappa)}{2\mu(x_1,0)}p_2(x_1) \tag{218}$$

where

$$\begin{aligned}
&k_{12}{}^{(2)}(x_1,t)=\frac{1}{4}h_{32}{}^{(1)}(x_1,0,t)\\
&k_{11}{}^{(2)}(x_1,t)=\frac{1}{4}\int_{-\infty}^{\infty}[K_{31}{}^{(1)}(0,\alpha)-\lim_{\alpha\to\infty}K_{31}{}^{(1)}(0,\alpha)]e^{i\alpha(t-x_1)}d\alpha\\
&k_{2i}{}^{(2)}(x_1,t)=\frac{(1+\kappa)}{4(\kappa-1)}\int_{-\infty}^{\infty}\sum_{j}^{4}\{(\cos^2\theta-\sin^2\theta)(\kappa-1)[p_j-i\alpha q_j]\\
&+2\sin\theta\cos\theta(1-\kappa)[i\alpha+p_jq_j]\}C_{ji}(\alpha,t)e^{p_jx_1\cos\theta-i\alpha x_1\sin\theta}d\alpha
\end{aligned} \tag{219}$$

From equations (175), the definition of $g_j(t), j=1..2$, we obtain the single valuedness conditions to complete the formulation of the problem:

$$\int_a^b g_j(t)dt=0,\ \ j=1,2 \tag{220}$$

4.3 The Numerical Solution

To obtain stress intensity factors at the crack tips, we will solve the Cauchy-type singular integral equations obtained above numerically. The collocation method used to solve these equations was described in the previous chapter.

First, we define

$$
\begin{aligned}
&t = \frac{b-a}{2} r + \frac{b+a}{2} \\
&x_1 = \frac{b-a}{2} s + \frac{b+a}{2} \\
&g_1(t) = \phi_1(r) \quad g_2(t) = \phi_2(r) \\
&p_1(x_1) = f_1(s) \;\; p_2(x_1) = f_2(s) \\
&\mu(x_1,0) = m(s,0) \\
&q_{ij}^{(n)}(s,r) = \frac{b-a}{2} k_{ij}^{(n)}(x_1,t) \quad (i=1,2,\, j=1,2,\, n=1,2)
\end{aligned}
\tag{221}
$$

Thus, the integral equations (216) and (218) are normalized as:

$$
\frac{1}{\pi} \int_{-1}^{1} \{ \frac{\phi_2(r)}{r-s} + \sum_{j=1}^{2} [q_{1j}^{(1)}(s,r) + q_{2j}^{(1)}(s,r)] \phi_j(r) \} dr = \frac{(1+\kappa)}{2m(s,0)} f_1(s) \tag{222}
$$

$$
\frac{1}{\pi} \int_{-1}^{1} \{ \frac{\phi_1(r)}{r-s} + \sum_{j=1}^{2} [q_{1j}^{(2)}(s,r) + q_{2j}^{(2)}(s,r)] \phi_j(r) \} dr = \frac{(1+\kappa)}{2m(s,0)} f_2(s) \tag{223}
$$

The fundamental solution of these equations is ([42,80])

$$
w(r) = \frac{1}{\sqrt{1-r^2}}, \tag{224}
$$

thus the solution of (222) and (223) may be expressed in terms of Chebyshev polynomials of the first kind:

$$
\begin{aligned}
&\phi_1(r) = \frac{1}{\sqrt{1-r^2}} \sum_{n=0}^{N} c_n^{(1)} T_n(r) \quad -1 < r < 1 \\
&\phi_2(r) = \frac{1}{\sqrt{1-r^2}} \sum_{n=0}^{N} c_n^{(2)} T_n(r) \quad -1 < r < 1
\end{aligned}
\tag{225}
$$

where $c_n^{(1)}$ and $c_n^{(2)}$ $(n = 0,1,2...)$ are unknown constants. From the single valuedness condition (220), considering the orthogonality conditions of $T_n(r)$, it can be shown that

$$\begin{aligned} c_0^{(1)} &= 0 \\ c_0^{(2)} &= 0 \end{aligned} \tag{226}$$

Substituting (225) into (222) and (223), we obtain:

$$\begin{aligned} &\sum_{n=1}^{\infty} c_n^{(1)} U_{n-1}(s) + \frac{1}{\pi}\sum_{n=1}^{\infty}\int_{-1}^{1}\sum_{j=1}^{2}[q_{1j}^{(1)}(s,r) + q_{2j}^{(1)}(s,r)]c_n^{(j)}\frac{T_n(r)}{\sqrt{1-r^2}}dr \\ &= \frac{(1+\kappa)}{2m(s,0)} f_1(s) \qquad -1 < s < 1 \\ &\sum_{n=1}^{\infty} c_n^{(2)} U_{n-1}(s) + \frac{1}{\pi}\sum_{n=1}^{\infty}\int_{-1}^{1}\sum_{j=1}^{2}[q_{1j}^{(2)}(s,r) + q_{2j}^{(2)}(s,r)]c_n^{(j)}\frac{T_n(r)}{\sqrt{1-r^2}}dr \\ &= \frac{(1+\kappa)}{2m(s,0)} f_2(s) \qquad -1 < s < 1 \end{aligned} \tag{227}$$

Equation (227) can be solved by truncating the series and choosing the collocation points s_n as

$$T_N(s_n) = 0 \qquad s_n = \cos((2n-1)\frac{\pi}{2N}) \qquad n = 1,\ldots,N \tag{228}$$

After determining $c_n^{(1)}$ and $c_n^{(2)}$, we can express the stress intensity factors at the crack tips as ([59])

$$
\begin{aligned}
k_1(a) &= \sqrt{\frac{b-a}{2}}\,\frac{2\mu(a,0)}{1+\kappa}\sum_{n=1}^{\infty}(-1)^n c_n^{(1)} \\
k_2(a) &= \sqrt{\frac{b-a}{2}}\,\frac{2\mu(a,0)}{1+\kappa}\sum_{n=1}^{\infty}(-1)^n c_n^{(2)} \\
k_1(b) &= -\sqrt{\frac{b-a}{2}}\,\frac{2\mu(b,0)}{1+\kappa}\sum_{n=1}^{\infty} c_n^{(1)} \\
k_2(b) &= -\sqrt{\frac{b-a}{2}}\,\frac{2\mu(b,0)}{1+\kappa}\sum_{n=1}^{\infty} c_n^{(2)}
\end{aligned}
\tag{229}
$$

and the crack surface openings as

$$
\begin{aligned}
u(x_1,+0)-u(x_1,-0) &= -\sqrt{(a'^2-x'^2)}\sum_{n=1}^{\infty}\frac{1}{n}c_n^{(1)}U_{n-1}(x'/a') \\
v(x_1,+0)-v(x_1,-0) &= -\sqrt{(a'^2-x'^2)}\sum_{n=1}^{\infty}\frac{1}{n}c_n^{(2)}U_{n-1}(x'/a')
\end{aligned}
\tag{230}
$$

where

$$
a' = \frac{b-a}{2} \tag{231}
$$

which is the half length of the crack and

$$
x' = x - \frac{b+a}{2} \tag{232}
$$

4.4 Results and Discussion

The stress intensity factors at the crack tips were calculated numerically for different crack lengths and crack orientations. The loading is uniform strain at infinity, that is:

$$\varepsilon_{yy}(x,\pm\infty) = \varepsilon_0 \tag{233}$$

Thus, the crack surface tractions can be written as:

$$\begin{aligned} p_1(x_1,0) &= -\frac{8\mu_1 e^{\delta x\cos\theta}}{1+\kappa}\varepsilon_0\cos^2\theta \\ p_2(x_1,0) &= -\frac{8\mu_1 e^{\delta x\cos\theta}}{1+\kappa}\varepsilon_0\cos\theta\sin\theta \end{aligned} \tag{234}$$

The calculations were carried out for various crack lengths, with θ varying from 0^0 to near 90^0. All the stress intensity factors are normalized by

$$K_0 = \sigma_0\sqrt{a'} \tag{235}$$

where σ_0 is the normalizing stress which is defined as

$$\sigma_0 = \frac{8\mu_1}{1+\kappa}\varepsilon_0 \tag{236}$$

Fig. 27 shows the stress intensity factors for a crack with $a'/h = 0.05$. The dashed lines indicate the stress intensity factors for an inclined crack in a FGM strip bonded to a homogeneous half-plane, while the solid lines show the stress intensity factors for the crack in the same FGM strip. As it is shown, the difference between these two groups of intensity factors is very small, and nearly negligible. This is largely due to the fact that the crack length is very small compared to the thickness of the strip. Thus, the perturbation brought by the extra homogeneous half-plane is not distinctly reflected in the stress intensity factors at the crack tips.

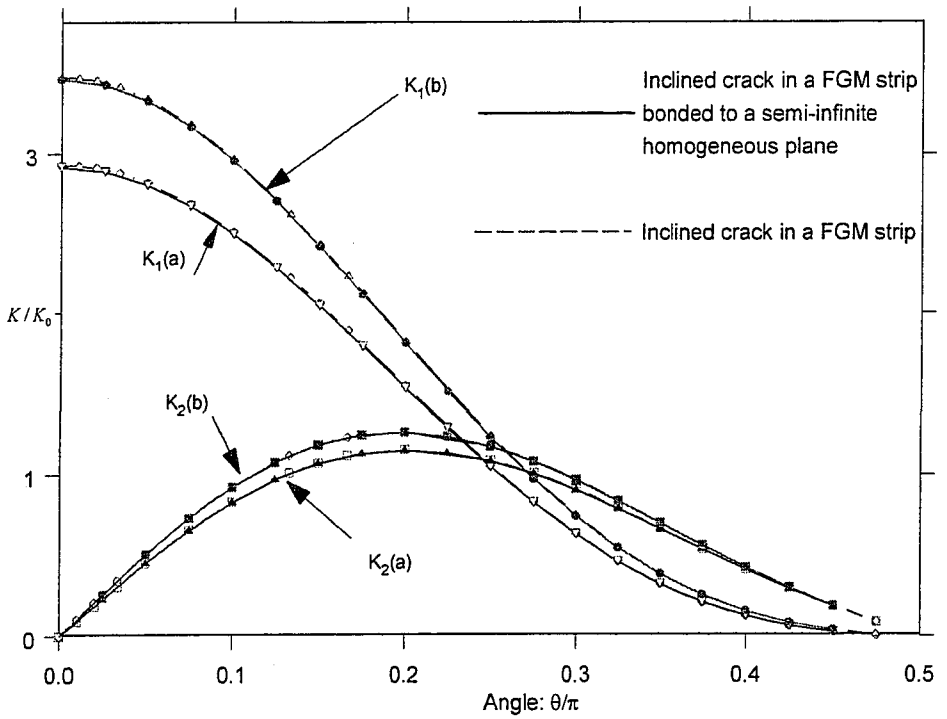

Fig. 27. Variation of the normalized stress intensity factors K / K_0 with θ / π for an internal inclined crack in a FGM strip and a FGM strip bounded to a homogeneous half-plane under uniform strain, $a' / h = 0.05$

Figs. 28 to 31 show the stress intensity factors for cracks with varying crack lengths, for $a' / h = 0.10, 0.15, 0.20$ respectively. It can be observed that as the crack length increases, the difference between the stress intensity factors for a FGM strip and a FGM strip bonded to a homogeneous half plane increases. But the trend of the variation of the intensity factors with respect to the crack angle remains the same.

Several important conclusions can be reached from these results:

1. The square-root stress singularity is still valid at the crack tips of cracks in an FGM layer for various lengths and orientation of the crack.

2. The non-homogeneity factor of the material greatly affects the intensity factors.

3. Due to the nonhomogeneous nature of the material, the difference between the stress intensity factors at the two crack tips increases significantly when the crack becomes longer, and the stress intensity factors at the crack tip of the stronger side of the material can be very large.

4. In most cases, Mode *I* fracture introduces larger stresses at the crack tips. When Mode *II* fracture dominates, the magnitude of the stresses is generally lower than that when Mode *I* fracture dominates.

5. Homogeneous substrate affects the loading pattern of the crack, and thus affects the stress intensity factors at crack tips. But its effect generally is negligible when the crack is small and away from interface, and it does not change the nature of the crack.

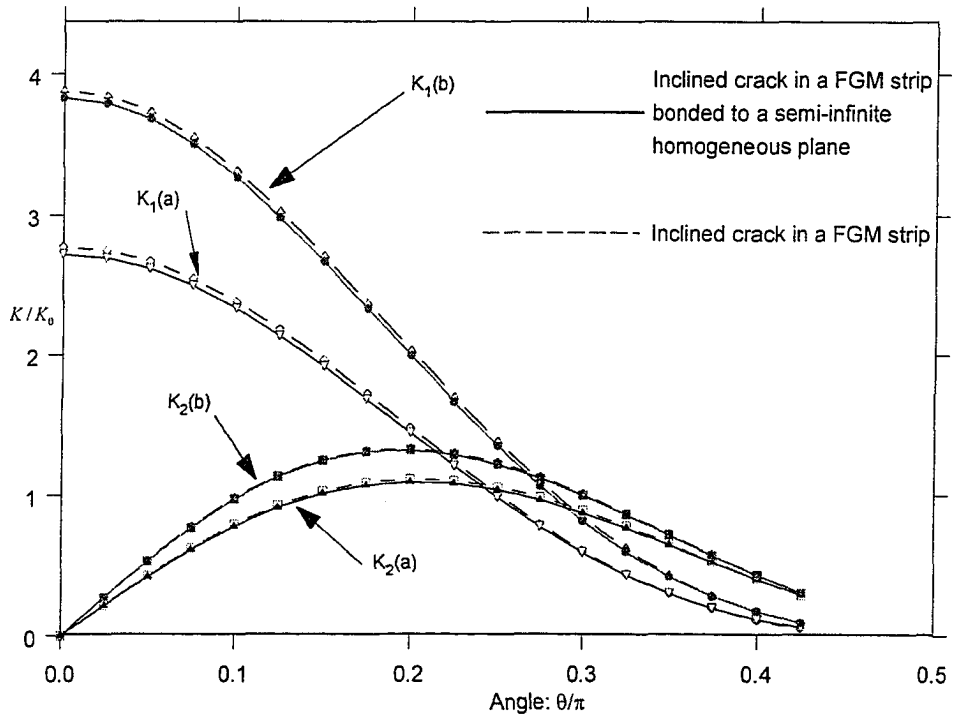

Fig. 28. Variation of the normalized stress intensity factors K / K_0 with θ / π for an internal inclined crack in a FGM strip and a FGM strip bounded to a homogeneous half-plane under uniform strain, $a' / h = 0.10$

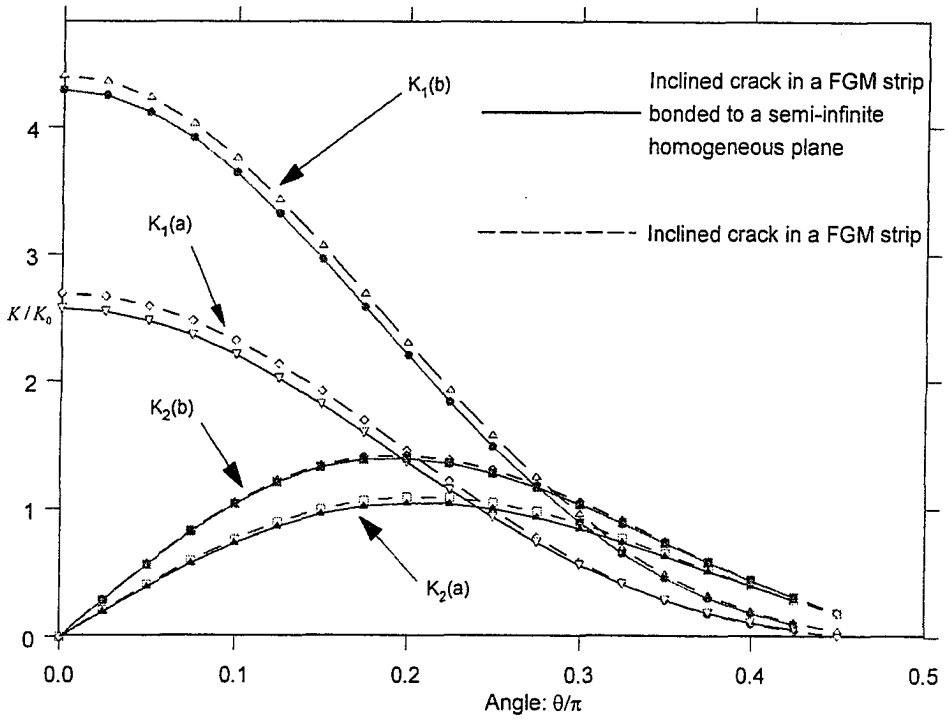

Fig. 29. Variation of the normalized stress intensity factors K / K_0 with θ / π for an internal inclined crack in a FGM strip and a FGM strip bounded to a homogeneous half-plane under uniform strain, $a' / h = 0.15$

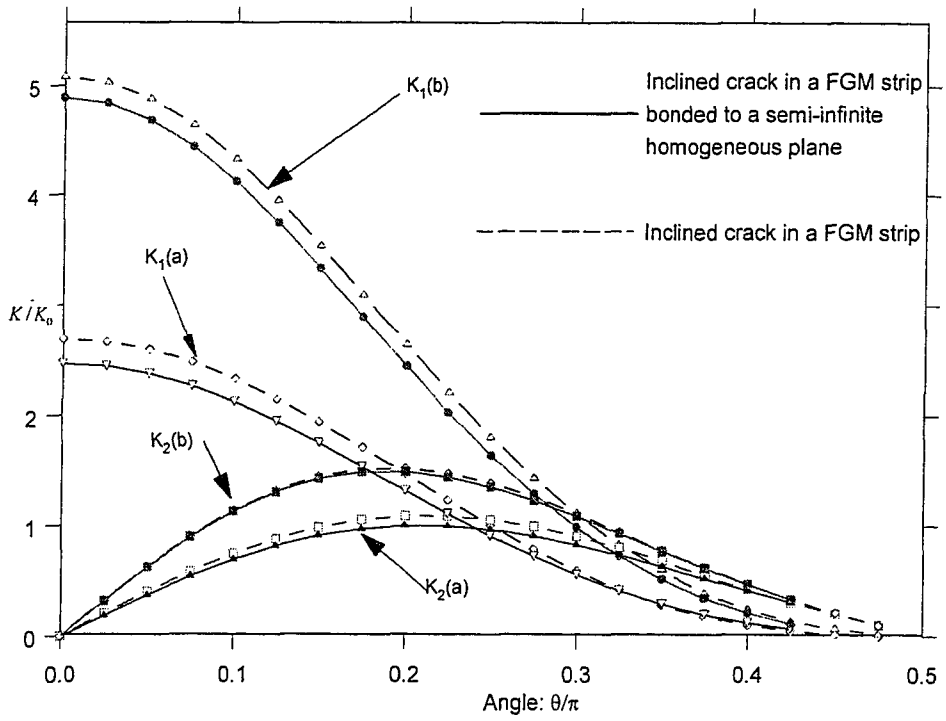

Fig. 30. Variation of the normalized stress intensity factors K / K_0 with θ / π for an internal inclined crack in a FGM strip and a FGM strip bounded to a homogeneous half-plane under uniform strain, $a' / h = 0.20$

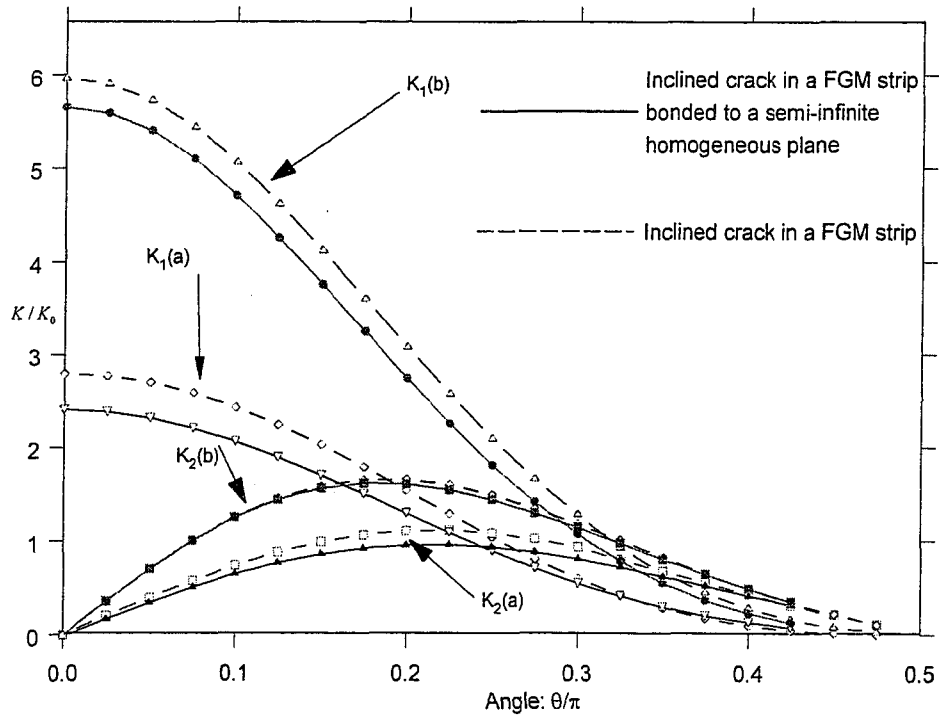

Fig. 31. Variation of the normalized stress intensity factors K/K_0 with θ/π for an internal inclined crack in a FGM strip and a FGM strip bounded to a homogeneous half-plane under uniform strain, $a'/h = 0.25$

The crack surface openings are shown in Figs. 32 and 33. Fig. 32 depicts the crack surface opening in y_1 direction for the crack length $a'/h = 0.20$. Fig. 33 shows the corresponding opening in x_1 direction. For Fig. 33, it should be noted that there is no crack displacement in x_1 direction when $\theta = 0^0$, thus, the orientations of the crack are chosen as 4.5^0, 45^0 and 67.5^0 respectively. In Fig. 32, the orientations of the crack are chosen as 0^0, 45^0 and 67.5^0. As expected, nonhomogeneity of the material results in larger openings on the softer side of the material.

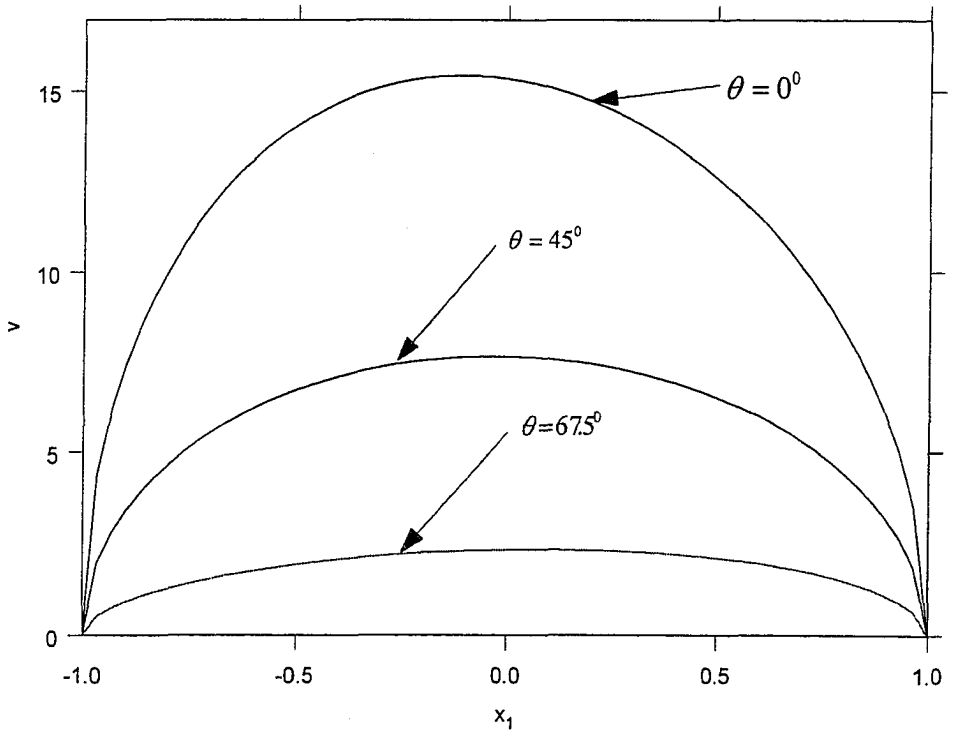

Fig. 32. Crack surface openings in the y_1 direction for $a'/h = 0.20$, $\theta = 0^0$, 45^0 and 67.5^0

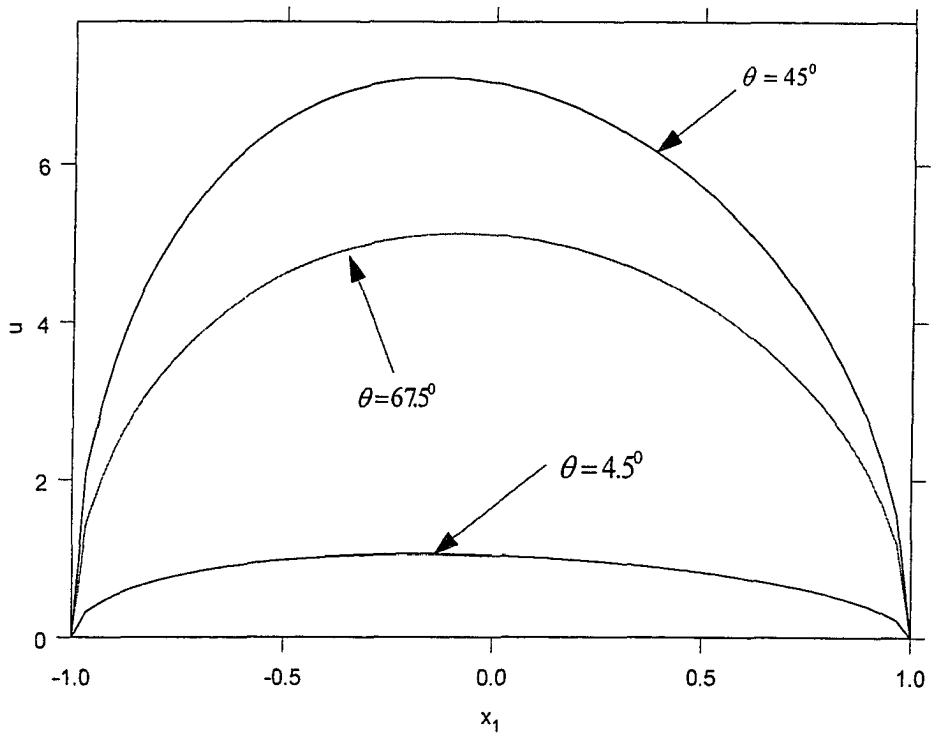

Fig. 33. Crack surface openings in the x_1 direction for $a'/h = 0.20$, $\theta = 4.5^0$, 45^0 and 67.5^0

Chapter 5 Proposed additional Studies

The mixed mode crack problem for an arbitrarily oriented crack in a FGM strip can be further investigated with more exhaustive parametric studies. These include more loadings and different geometries. Special emphasis should be placed on the eccentric crack, especially when the crack is moving near the boundary. It should be noted that all crack problems studied in this thesis are imbedded cracks. This is because edge crack problems, especially arbitrarily oriented edge crack problems have some intrinsic mathematical difficulties in solving them. For example, the integral equations for edge crack problems involve two singular terms instead of only one for imbedded cracks. This problem is not totally intractable, but significant work may be needed.

Another problem is the natural extension of the crack problem we solved in chapter 3. In addition to the arbitrarily oriented crack in the FGM layer, a crack may be introduced along the interface of the two layers (Fig. 34). This additional crack complicates the problem significantly, but it will be of great significance in studying the fracture of FGMs used as thermal barrier coating. At this stage, it is not clear whether this problem is analytically tractable but it should be an interesting and a challenging problem. Once this problem has been solved, most multi-layer problems studied previously can easily be treated as special cases of it.

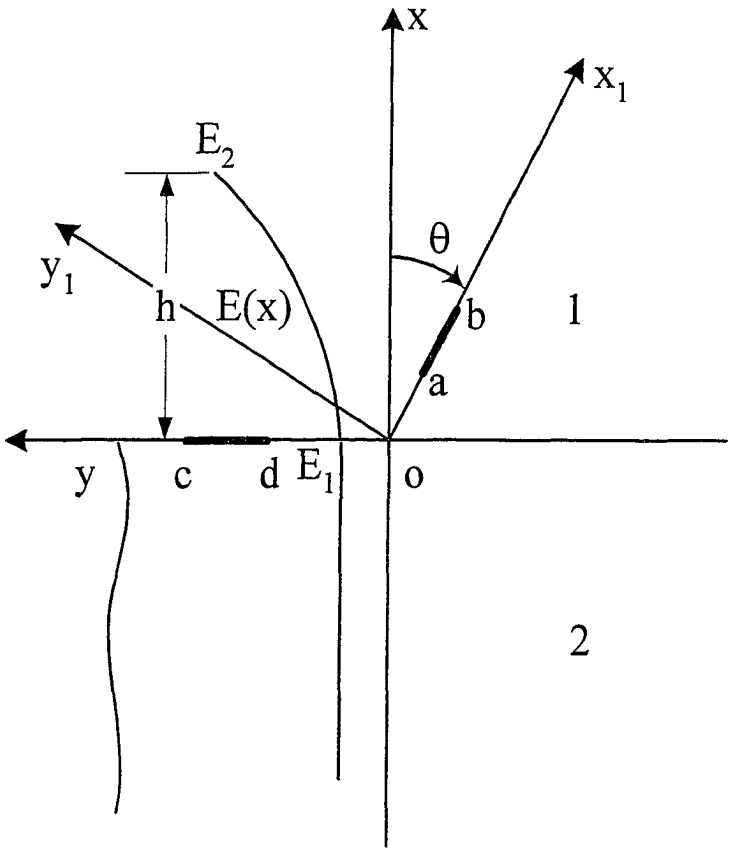

Fig. 34. Geometry of the problem for an arbitrarily oriented crack in a FGM layer bonded to a homogeneous substrate, with another crack along the interface.

The mixed mode crack problem should also be extended to include thermal stresses. Jin and Noda have extended many pure elasticity fracture problems to include thermal stresses ([52,54,55,72,73,74,75,76,77]). Those problems are of great technical interest, but it appears no mixed-mode crack problems have been studied under thermal loadings. This is due to the extreme difficulties involved in finding solutions that satisfy both the Navier's equations and the heat conduction equations, especially for FGMs, where the material properties vary spatially. As it was stated in [38] "... if the heat conduction is two-dimensional, in solving the diffusion equation one must account for partial insulation

introduced by the crack. This would complicate the thermal stress and the crack problem quite considerably... in the two-dimensional heat flow problems, because of the flux singularities at the end points of partially insulated cuts, particularly in FGMs, neither the diffusion problem nor the thermal stress problem would be analytically tractable."

It is a great challenge to solve the mixed mode crack problem in a FGM strip under thermal loads. The author has tried fruitlessly to tackle this problem. Though it is too early to state that this problem is not analytically tractable, it is safe to say that for now these problems must be solved numerically.

References

1. Aboudi, J., S. M. Arnold, et al. (1994). "Response of functionally graded composites to thermal gradients." Composites Engineering **14**(1): 1-18.

2. Aboudi, J., M.-J. Pindera, et al. (1994). "Elastic response of metal matrix composites with tailored microstructures to thermal gradients." International Journal of Solids and Structures **31**(10): 1393-1428.

3. Aboudi, J., M.-J. Pindera, et al. (1995). "Thermo-inelastic response of functionally graded composites." International Journal of Solids and Structures **32**(12): 1675-1710.

4. Aboudi, J., M.-J. Pindera, et al. (1996). "Thermoelastic theory for the response of materials functionally graded in two directions." International Journal of Solids and Structures **33**(7): 931-966.

5. Aboudi, J., M.-J. Pindera, et al. (1996). "Thermoplasticity theory for bidirectionally functionally graded materials." Journal of Thermal Stresses **19**(9): 809-861.

6. Aboudi, J., M.-J. Pindera, et al. (1997). "Microstructural optimization of functionally graded composites subjected to a thermal gradient via the coupled higher-order theory." Composites Part B: Engineering **28**(1-2): 93-108.

7. Aboudi, J., M.-J. Pindera, et al. (1999). "Higher-order theory for functionally graded materials." Composites Part B: Engineering **30**(8): 777-832.

8. Anlas, G., M. H. Santare, et al. (2000). "Numerical calculation of stress intensity fractors in functionally graded materials." International Journal of Fracture **104**: 131-143.

9. Bao, G. and H. Cai (1997). "Delamination cracking in functionally graded coating/metal substrate systems." Acta Materialia **45**(3): 1055-1066.

10. Bao, G. and L. Wang (1995). "Multiple cracking in functionally graded ceramic/metal coatings." International Journal of Solids and Structures **32**(19): 2853-2871.

11. Bunk, W. G. J. (1990). Advanced Aerospace Materials. Proceedings of the First International Symposium on Functionally Gradient Materials, Sendai, Japan.

12. Butcher, R. J., C.-E. Rousseau, et al. (1998). "A functionally graded particulate composite: preparation, measurements and failure analysis." Acta Materialia **47**(1): 259-268.

13. Chen, Y. F. and F. Erdogan (1996). "The interface crack problem for a nonhomogeneous coating bonded to a homogeneous substrate." Journal of the Mechanics and Physics of Solids **44**: 771-87.

14. Chen, Y. Z. (1995). "A Survey of new integral equations in plane elasticity crack problem." Engineering Fracture Mechanics **51**(1): 97-134.

15. Choi, H. J. (1996). "An analysis of cracking in a layered medium with a functionally graded nonhomogeneous interface." Journal of Applied Mechanics **63**: 479-86.

16. Choi, H. J. (1996). "Bonded dissimilar strips with a crack perpendicular to the functionally graded interface." International Journal of Solids and Structures **33**(28): 4101-4117.

17. Choi, H. J. (2001). "The problem for bonded half-planes containing a crack at an arbitrary angle to the graded interfacial zone." International Journal of Solids and Structures **38**(36): 6559-6588.

18. Clements, D. L., C. Atkinson, et al. (1978). "Antiplane crack problems for an inhomogeneous elastic material." Acta Mechanica **29**(1-4): 199-211.

19. Delale, F. (1985). "Mode-III fracture of bonded non-homogeneous materials." Engineering Fracture Mechanics **22**(2): 213-226.

20. Delale, F. and F. Erdogan (1979). "Bonded orthotropic strips with cracks." International Journal of Fracture **15**(4): 343-364.

21. Delale, F. and F. Erdogan (1983). "The crack problem for a nonhomogeneous plane." Journal of Applied Mechanics **50**(3): 609-614.

22. Delale, F. and F. Erdogan (1988). "Interface crack in a nonhomogeneous elastic medium." International Journal of Engineering Science **26**(6): 559-568.

23. Delale, F. and F. Erdogan (1988). "On the mechanical modeling of the interfacial region in bonded half-planes." Journal of Applied Mechanics **55**(2): 317-324.

24. Dhaliwal, R. S. and B. M. Singh (1978). "On the theory of elasticity of a nonhomogeneous medium." Journal of Elasticity **8**(2): 211-219.

25. Dolbow, J., N. Moes, et al. (2000). "Modeling fracture in Mindlin-Reissner plates with the extended finite element method." International Journal of Solids and Structures **37**(48-50): 7161-7183.

26. Dolbow, J. E. and M. Gosz (2002). "On the computation of mixed-mode stress intensity factors in functionally graded materials." International Journal of Solids and Structures **39**(9): 2557-2574.

27. Eischen, J. W. (1987). "Fracture of nonhomogeneous materials." International Journal of Fracture **34**(1): 3-22.

28. El-Borgi, S., L. Hidri, et al. (2000). "Stress intensity factors for a crack arbitrarily oriented in a functionally graded layer". Ceramic Transactions. **114:** 723-730.

29. Erdogan, F. (1978). "Mixed Boundary-value Problems in Mechanics." Mechanics Today **4**: 1-86.

30. Erdogan, F. (1985). "The crack problem for bonded nonhomogeneous materials under antiplane shear loading." Journal of Applied Mechanics **52**: 823-8.

31. Erdogan, F. (1995). "Fracture mechanics of functionally graded materials." Composites Engineering **5**(7): 753-770.

32. Erdogan, F. and K. Arink (1975). "A half plane and a strip with an arbitrarily located crack." International Journal of Fracture **11**: 191-204.

33. Erdogan, F. and G. D. Gupta (1972). "On the numerical solution of singular integral equations." Quarterly of Applied Mathematics **30**(1): 525-534.

34. Erdogan, F., G. D. Gupta, et al. (1973). "Numerical Solution of Singular Integral Equation." Mechanics of Fracture **1**: 368-425.

35. Erdogan, F., A. C. Kaya, et al. (1991). "The crack problem in bonded nonhomogeneous materials." Journal of Applied Mechanics **58**(2): 410-418.

36. Erdogan, F., A. C. Kaya, et al. (1991). "The mode III crack problem in bonded materials with a nonhomogeneous interfacial zone." Journal of Applied Mechanics **58**: 419-27.

37. Erdogan, F. and M. Ozturk (1992). "Diffusion problems in bonded nonhomogeneous materials with an interface cut." International Journal of Engineering Science **30**: 1507-1523.

38. Erdogan, F. and B. H. Wu (1996). "Crack problems in FGM layers under thermal stresses." Journal of Thermal Stresses **19**(3): 237.

39. Erdogan, F. and B. H. Wu (1997). "The surface crack problem for a plate with functionally graded properties." Journal of Applied Mechanics **64**(3): 449 (8 pages).

40. Gao, X. and Z.-B. Kuang (1992). "Mode I fracture in two dissimilar functional non-homogeneous planes." Engineering Fracture Mechanics **42**(1): 33-44.

41. Gerasoulis, A. and R. P. Srivastav (1980). "A Griffith crack problem for a nonhomogeneous medium." International Journal of Engineering Science **18**(1): 239-247.

42. Golberg, M. A. (1990). Numerical Solution of Integral Equations. New York, Plenum Press.

43. Gosz, M., J. Dolbow, et al. (1998). "Domain integral formulation for stress intensity factor computation along curved three-dimensional interface cracks." International Journal of Solids and Structures **35**(15): 1763-1783.

44. Gu, P., M. Dao, et al. (1999). "A simplified method for calculating the crack-tip field of functionally graded materials using the domain integral." Journal of Applied Mechanics **66**(1): 101-8.

45. Gupta, G. D. and F. Erdogan (1974). "The problem of edge cracks in an infinite strip." Journal of Applied Mechanics **41**(4): 1001-1006.

46. Hill, M. R., R. D. Carpenter, et al. (2002). Fracture testing of a layered functionally graded material. Fracture Resistance Testing of Monolithic and Composite Brittle Materials, ASTM STP 1409. J. A. Salem, G. D. Quinn and M. G. Jenkins. West Conshohocken, PA, American Society for Testing and Materials.

47. Honein, T. and G. Herrmann (1997). "Conservation laws in nonhomogeneous plane elastostatics." Journal of the Mechanics and Physics of Solids **45**(5): 789-805.

48. Ioakimidis, N. I. (1980). "Numerical solution of crack problems in plane elasticity in the case of loading discontinuities." Engineering Fracture Mechanics **13**(4): 709-716.

49. Ioakimidis, N. I. (1984). "A modification of the quadrature method for the direct numerical solution of singular integral equations." Computer Methods in Applied Mechanics and Engineering **46**: 1-13.

50. Ioakimidis, N. I. and M. S. Pitta (1988). "Remarks on the Gaussian quadrature rule for finite-part integrals with a second-order singularity." Computer Methods in Applied Mechanics and Engineering **69**: 325-43.

51. Ioakimidis, N. I. and P. S. Theocaris (1979). "Remark on the numerical evaluation of stress intensity factors by the method of singular integral equations." International Journal for Numerical Methods in Engineering **14**(11): 1710-1714.

52. Jin, Z.-H. and N. Noda (1993). "An internal crack parallel to the boundary of a nonhomogeneous half plane under thermal loading." International Journal of Engineering Science **31**(5): 793-806.

53. Jin, Z.-H. and N. Noda (1994). "Crack-tip singular fields in nonhomogeneous materials." Journal of Applied Mechanics **61**: 738-40.

54. Jin, Z.-H. and N. Noda (1994). "Edge crack in a nonhomogeneous half plane under thermal loading." Journal of Thermal Stresses **17**(4): 591-599.

55. Jin, Z.-h. and N. Noda (1994). "Transient thermal stress intensity factors for a crack in a semi-infinite plate of a functional gradient material." International Journal of Solids and Structures **31**(2): 203-218.

56. Jin, Z.-H., G. H. Paulino, et al. (2002). "Finite element investigation of quasi-static crack growth in functionally graded materials using a novel cohesive zone fracture model." Journal of Applied Mechanics **69**: 370-379.

57. Kim, H. K. and B. L. S. (1996). "Stress intensity factors of an oblique edge crack subjected to normal and shear tractions." Theoretical and Applied Fracture Mechanics **25**(2): 147-154.

58. Kim, J.-H. and G. H. Paulino (2002). "Finite element evaluation of mixed mode stress intensity factors in functionally graded materials." International Journal for Numerical Methods in Engineering **53**(8): 1903-1935.

59. Konda, N. and F. Erdogan (1994). "The mixed mode crack problem in a nonhomogeneous elastic medium". Engineering Fracture Mechanics. **47:** 533-546.

60. Krenk, S. (1975). "On quadrature formulas for singular integral equations of the first and the second Kind." Quarterly of Applied Mathematics **33**(3): 225-232.

61. Krenk, S. (1975). "On the elastic strip with an internal crack." International Journal of Solids and Structures **11**(6): 693-708.

62. Krenk, S. (1975). "On the use of the interpolation polynomial for solutions of singular integral equations." Quarterly of Applied Mathematics **32**(1): 479-484.

63. Krenk, S. (1978). "Numerical quadrature of periodic singular integral-equations." Journal of the Institute of Mathematics and its Application **21**(2): 181-187.

64. Krenk, S. (1978). "Quadrature formulae of closed type for solution of singular integral equations." Journal of the Institute of Mathematics and its Application **22**(1): 99-107.

65. Lanutti, J. J. (1994). "Functionally graded materials: properties, potential and design guidelines." Composites Engineering **4**: 81-94.

66. Lee, Y. D. and F. Erdogan (1995). "Residual/thermal stresses in FGM and laminated thermal barrier coatings." International Journal of Fracture **69**(2): 145.

67. Li, H., J. Lambros, et al. (2000). "Experimental investigation of the quasi-static fracture of functionally graded materials." International Journal of Solids and Structures **37**(27): 3715-3732.

68. Martin, P. A. (1992). "Tip behaviour for cracks in bonded inhomogeneous materials." Journal of Engineering Mathematics **26**: 467-480.

69. Marur, P. R. and H. V. Tippur (2000). "Numerical analysis of crack-tip fields in functionally graded materials with a crack normal to the elastic gradient." International Journal of Solids and Structures **37**(38): 5353-5370.

70. Mortensen, A. and S. Suresh (1995). "Functionally graded metals and metal-ceramic composites. 1. Processing." International Materials Reviews **40**(6): 239-265.

71. Niino, M. and S. Maeda (1990). "Recent development status of functionally graded materials." I.S.I.J. International **30**(9): 699-703.

72. Noda, N. (1997). "Thermal stress intensity factor for functionally gradient plate with an edge crack." Journal of Thermal Stresses **20**: 373-387.

73. Noda, N. (1999). "Thermal stresses in functionally graded materials." Journal of Thermal Stresses **22**(4): 477-512.

74. Noda, N. and Z.-H. Jin (1993). "Steady thermal stresses in an infinite nonhomogeneous elastic solid containing a crack." Journal of Thermal Stresses **16**: 181-196.

75. Noda, N. and Z.-H. Jin (1993). "Thermal stress intensity factors for a crack in a strip of a functionally gradient material." International Journal of Solids and Structures **30**(8): 1039-1056.

76. Noda, N. and Z.-H. Jin (1995). "Crack-tip singularity fields in nonhomogeneous body under thermal stress fields." JSME International Journal, Series A: Mechanics and Material Engineering **38**(3): 364-369.

77. Noda, N. and T. Tsuji (1990). Steady thermal stresses in a plate of functionally gradient material. Proceedings of the First International Symposium on Functionally Gradient Materials, Sendai, Japan.

78. Noda, N. A., K. Araki, et al. (1992). "Stress intensity factors in two bonded elastic layers with a single edge crack under various loading conditions." International Journal of Fracture **57**(2): 101.

79. Nogata, F. (1997). "Learning about design concepts from natural functionally graded materials." American Society of Mechanical Engineers, Materials Division (Publication) MD **80**: 11-18.

80. Peters, A. S. (1963). "A note on the integral equation of the first kind with a Cauchy kernel." Communications on Pure and Applied Mathematics **16**: 57-61.

81. Pindera, M.-J., J. Aboudi, et al. (1994). Thermo-inelastic analysis of functionally graded materials: inapplicability of the classical micromechanics approach. 12th US National Congress on Applied Mechanics. Inelasticity and Micromechanics of Metal Matrix Composites, Seattle, WA, USA, Amsterdam, Netherlands : Elsevier, 1994.

82. Pindera, M.-J., J. Aboudi, et al. (1995). "Limitations of the uncoupled, RVE-based micromechanical approach in the analysis of functionally graded composites." Mechanics of Materials **20**: 77-94.

83. Pindera, M.-J., J. Aboudi, et al. (1996). Microstructural effects in functionally graded thermal barrier coatings. Fourth International Symposium on Functionally Graded Materials, Tsukuba, Japan, Amsterdam, Netherlands : Elsevier, 1997.

84. Pindera, M.-J., J. Aboudi, et al. (1998). "Thermomechanical analysis of functionally graded thermal barrier coatings with different microstructural scales." Journal of the American Ceramic Society **81**(6): 1525-1536.

85. Pindera, M.-J. and P. Dunn (1997). "Evaluation of the higher-order theory for functionally graded materials via the finite-element method." Composites Part B: Engineering **28**(1-2): 109-119.

86. Porter, D. and D. S. G. Stirling (1990). Integral equations: a practical treatment, from spectral theory to applications. New York, Cambridge University Press.

87. Rabin, B. H. and I. Shiota (1995). "Functionally graded materials." Materials Research Society Bulletin **20**(1): 14-18.

88. Rogers, C. and D. L. Clements (1978). "Bergman's integral operator method in inhomogeneous elasticity." Quarterly of Applied Mathematics **36**(3): 315-321.

89. Rousseau, C.-E. and H. V. Tippur (2000). "Compositionally graded materials with cracks normal to the elastic gradient." Acta Materialia **48**(16): 4021-4033.

90. Ruys, A. J., E. B. Popov, et al. (2001). "Functionally graded electrical/thermal ceramic systems." Journal of the European Ceramic Society **21**(10-11): 2025-2029.

91. Schovanec, L. (1986). "Griffith crack problem for an inhomogeneous elastic material." Acta Mechanica **58**(1-2): 67-80.

92. Schovanec, L. and J. R. Walton (1988). "On the order of stress singularity for an antiplane shear crack at the interface of two bonded inhomogeneous elastic materials." Journal of Applied Mechanics **55**(234-236).

93. Shbeeb, N. I. and W. K. Binienda (1999). "Analysis of an interface crack for a functionally graded strip sandwiched between two homogeneous layers of finite thickness." Engineering Fracture Mechanics **64**(6): 693-720.

94. Theocaris, P. S. and N. I. Ioakimidis (1977). "Numerical integration methods for the solution of singular integral equations." Quarterly of Applied Mathematics **35**(1): 173-183.

95. Ueda, S. (2001). "The surface crack problem for a layered plate with a functionally graded nonhomogeneous interface." International Journal of Fracture **110**(2): 189-204.

96. Zhao, H. (1998). "Fracture and fatigue analysis of functionally graded and homogeneous materials using singular integral equation approach". Baltimore, Maryland, Johns Hopkins University.